

# **Stony Brook University**



OFFICIAL COPY

**The official electronic file of this thesis or dissertation is maintained by the University Libraries on behalf of The Graduate School at Stony Brook University.**

**© All Rights Reserved by Author.**

A Thesis Presented

by

**Sara Cernadas Martín**

to

The Graduate School

in Partial Fulfillment of the

Requirements

for the Degree of

**Master of Science**

in

**Marine and Atmospheric Science**

Stony Brook University

August 2012

Copyright by  
Sara Cernadas Martín  
2012

**Stony Brook University**

The Graduate School

**Sara Cernadas Martín**

We, the thesis committee for the above candidate for the  
Master of Science degree, hereby recommend  
acceptance of this thesis.

**Gordon T. Taylor – Thesis Advisor**  
**Professor, School of Marine and Atmospheric Science**

**Mary I. Scranton – Second Reader**  
**Professor, School of Marine and Atmospheric Science**

**Jackie L. Collier – Third Reader**  
**Associate Professor, School of Marine and Atmospheric Science**

This thesis is accepted by the Graduate School

Charles Taber  
Interim Dean of the Graduate School

Abstract of the Thesis

**Aerobic and anaerobic ammonia oxidizers in the Cariaco Basin: Identification,  
Quantification and Community Structure**

by

**Sara Cernadas Martín**

**Master of Science**

in

**Marine and Atmospheric Science**

Stony Brook University

**2012**

Fluorescence in situ hybridization (FISH) and quantitative PCR (q-PCR) analyses were performed to characterize the populations mediating ammonium oxidation processes in the oxic, suboxic and anoxic layers of the Cariaco Basin (Venezuela). To examine possible metabolic connections between nutrients and functional groups, distributions were compared to nutrient availability. Anaerobic ammonia-oxidizing bacteria (anammox), aerobic ammonia-oxidizing bacteria (AOB), and ammonia-oxidizing Archaea (AOA) were quantified within the water column. Two peaks in

abundance of anammox bacteria were consistently observed during the three cruises that took place on December 8, 2010; May 6, 2011 and November 9, 2011 (C-175, C-180 and C-186). One peak was within the suboxic zone (up to 11,000 cells mL<sup>-1</sup>) and the other just below the suboxic zone in anoxic waters (up to 4,700 cells mL<sup>-1</sup>). This vertical separation observed in the anammox bacteria populations might be due to two different nitrite sources. The anammox bacteria population within the suboxic zone would be using the nitrite originated in the nitrification process. Anammox bacteria populations within the anoxic zone would be using the nitrite originated in the denitrification process. Of the anammox bacteria detected, 97% ± 9% hybridized with the probe specific for the genus *Scalindua*. Aerobic ammonia-oxidizing bacteria and Archaea (*Nitrosopumilus maritimus*) exhibited abundance peaks in the lower oxic zone (up to 24,000 cells mL<sup>-1</sup>), at depths just above Anammox bacteria.

Lower NH<sub>4</sub><sup>+</sup> concentrations correlated with increases in AOA and AOB abundances. Higher NO<sub>2</sub><sup>-</sup> and NO<sub>3</sub><sup>-</sup> concentrations correlated with enrichments in AOA and AOB, and lower NO<sub>2</sub><sup>-</sup> concentrations covaried with enrichments in Anammox. Estimated vertical fluxes of NH<sub>4</sub><sup>+</sup> and NO<sub>3</sub><sup>-</sup> were related to inventories of ammonia oxidizers, where lower NH<sub>4</sub><sup>+</sup> upward fluxes coincided with higher anammox bacteria inventories and higher NO<sub>3</sub><sup>-</sup> downward fluxes coincided with larger anammox bacteria, AOA and AOB inventories. This investigation demonstrates the presence of both aerobic and anaerobic ammonium oxidizers in the Cariaco Basin, suggests a metabolic relationship between anammox bacteria and AOB and AOA and, for the first time, examines the possible relations between these functional groups and ammonium and nitrate vertical fluxes.

## Table of contents

List of Figures .....	viii
List of Tables .....	xiv
Acknowledgements.....	xvi
Introduction.....	1
Background .....	7
The Cariaco Basin.....	7
Aerobic Ammonia-Oxidizing $\beta$ - and $\gamma$ -proteobacteria (AOB) and Archaea (AOA).....	8
Anammox Bacteria.....	9
Methods.....	11
Sample collection and storage .....	11
FISH analysis .....	13
DNA extraction and Purification .....	15
DNA standards.....	15
Representative DNA samples. ....	155
PCR amplification of genes of interest.....	16
Gene ligation, cell transformation and plasmid extraction.....	17
Quantitative PCR optimization .....	199
Quantitative PCR .....	21
mRNA samples and Reverse Transcription quantitative PCR (RT q-PCR).....	21
Flux model.....	24
Anammox, AOA and AOB inventories.....	26
Statistical analyses.....	27
Results.....	28

Hydrography and Nutrient Profiles .....	28
Anammox Bacteria.....	28
Ammonia-Oxidizing Archaea (AOA).....	29
$\beta$ - Ammonia-Oxidizing Bacteria ( $\beta$ -AOB).....	30
$\gamma$ - Ammonia-Oxidizing Bacteria ( $\gamma$ -AOB).....	31
Comparison of ammonia-oxidizing Bacteria and Archaea inventories with vertical fluxes of Ammonium and Nitrate and Nitrite inventories .....	32
Probe and q-PCR intercomparisons .....	34
Amx368 and Sca1309.....	34
Cren679.....	35
Bet42a and Nso1225-190.....	35
Gam42a and Nscoc128.....	36
Discussion .....	37
Community structure and possible metabolic relations .....	37
q-PCR and FISH as quantification techniques for ammonia oxidizers .....	41
Summary of major findings and hypothesis .....	43
Future work .....	45
References .....	47
Appendix I: Figures.....	57
Appendix II: Tables.....	81
Appendix III: Creating a Standard Curve with Plasmid DNA.....	85
Appendix VI: Quantitative PCR for $\gamma$ -AOB.....	87
Appendix V: Numeric Data .....	89



## List of Figures

**Figure 1** Simplified nitrogen cycle. Main processes and the nutrients involved within the oxic and suboxic zone are represented. Atmospheric Nitrogen becomes fixed into biomass (PON) by nitrogen fixers like cyanobacteria. Through predation, excretion, fecal pellets and decaying biomass this PON becomes DON and is mineralized to ammonia/ammonium in the suboxic zone. Part of the PON reaches the bottom, where it becomes remineralized and transported upward. Ammonium can be directly assimilated, be aerobically oxidized as part of the nitrification process or be anaerobically oxidized by anammox bacteria. Nitrite in the oxic zone is rapidly oxidized to nitrate as the final step of the nitrification process. This nitrate, once in the suboxic zone becomes reduced back to nitrite and eventually to Nitrogen gas as part of the denitrification process. Nitrogen gas can be fixed again in surface waters or lost to the atmosphere. .... 57

**Figure 2** Map locating the Cariaco Basin and the sampling station. Courtesy of the CARIACO Project..... 58

**Figure 3** On board manifold set-up for filtration of DNA samples minimizing oxygen contamination. The compounder bags were filled directly from the Niskin bottles and attached to the filter holders with minimum contact with oxygen..... 59

**Figure 4** Photomicrograph of *Nitrosopumilus maritimus* cells stained with Acridine Orange observed under the epifluorescent microscope. Image captured with a MagnaFire® Digital Camera System (Optronics) and processed with the IPPWIN Image Pro Plus Version 7.0 (Media Cybernetics) for color resolution improvement..... 60

**Figure 5** *E. coli* colonies from cloning experiment after overnight incubation. Blue colonies are non-transformed cells and white colonies are the transformed cells..... 61

**Figure 6** Example of q-PCR Standard curve. Ten-fold dilutions of gene copies (*nirS*) from anammox bacteria, ranging from 1 to  $10^7$  copies were plotted against their Threshold cycles (Ct) and the linear regression for this data was calculated ..... 62

**Figure 7** Example of dissociation curve where the products of the PCR reaction went through a heating-cooling-heating cycle where the DNA products of the PCR reaction dissociate and later annealed again, the temperature at which DNA denatures reveals their the molecular weight. .... 63

**Figure 8** Example of data used to calculate the upward vertical flux of ammonium in C-175. Dashed lines mark the depth interval used in the calculations. Nutrient gradient and density gradient were estimated from the slope of the regression line of the data points within the dashed lines.....64

**Figure 9** Nutrient profiles for C-175, C-180 and C-186. The continuous lines represent the vertical profiles for  $\text{NH}_4^+$  concentration ( ● ),  $\text{NO}_2^-$  concentration ( ● ) and  $\text{NO}_3^-$  concentration ( ● ). The green area represents the CTD profile for oxygen concentration ( ■ ) and the triangles the oxygen measured in the lab from water samples ( ▲ ). The yellow area corresponds to  $\text{H}_2\text{S}$  concentration ( ■ ). The blue area represents the suboxic zone, separating the oxic zone from the anoxic zone ( ■ ).  $\text{NH}_4^+$ ,  $\text{NO}_2^-$  and  $\text{NO}_3^-$  data courtesy of Dr. Kent Fanning from University of South Florida.  $\text{H}_2\text{S}$  data courtesy of Lan T. Tong and Yrene Astor ..... 65

**Figure 10a** Nutrient profile for C-175; the continuous lines represent the vertical profiles for  $\text{NH}_4^+$  concentration (●),  $\text{NO}_2^-$  concentration (●) and  $\text{NO}_3^-$  concentration (●). The green area represents the CTD profile for oxygen concentration (■) and the triangles the oxygen measured in the lab from water samples (▲). The yellow area corresponds to  $\text{H}_2\text{S}$  concentration (■). The blue area represents the suboxic zone, separating the oxic zone from the anoxic zone (→).

**Figure 10b** FISH depth profile for anammox Bacteria (Amx368) and *Scalindua sp.* (Sca1309) positive cells.

**Figure 10c** FISH depth profile for AOA, *N. maritimus* (Cren67) positive cells.

**Figure 10d** FISH depth profile for  $\beta$ -Proteobacteria (Bet42a) and  $\beta$ -AOB (Nso1225-190) positive cells.

**Figure 10e** FISH depth profile for  $\gamma$ -Proteobacteria (Gam42a) and  $\gamma$ -AOB (Nscoc128) positive cells.....66

**Figure 11** Nutrient profile and DNA profiles obtained from the q-PCR analyses for C-175;

**Figure 11a** Nutrient profile for C-175. The continuous lines represent the vertical profiles for  $\text{NH}_4^+$  concentration (●),  $\text{NO}_2^-$  concentration (●) and  $\text{NO}_3^-$  concentration (●). The green area represents the CTD profile for oxygen concentration (■) and the triangles the oxygen measured in the lab from water samples (▲). The yellow area corresponds to  $\text{H}_2\text{S}$  concentration (■). The blue area represents the suboxic zone, separating the oxic zone from the anoxic zone (→).

**Figure 11b** Vertical profile of gene copies per mL of the gene *nirS*, specific for anammox bacteria of the genus *Scalindua*. Two peaks are observed at 250 and 292 meters.

**Figure 11c** Vertical profile of gene copies per mL of the gene *Arch-amoA*, specific for Archaeal aerobic ammonia oxidizers. One peak is observed at 192 meters.

**Figure 11d** Vertical profile of copies per mL of the gene *amoA* specific for  $\beta$ -bacterial ammonia oxidizers. One peak is observed at 192 meters.....67

**Figure 12a** Nutrient profile C-180; the continuous lines represent the vertical profiles for  $\text{NH}_4^+$  concentration ( ● ),  $\text{NO}_2^-$  concentration ( ● ) and  $\text{NO}_3^-$  concentration ( ● ). The green area represents the CTD profile for oxygen concentration ( ■ ) and the triangles the oxygen measured in the lab from water samples ( ▲ ). The yellow area corresponds to  $\text{H}_2\text{S}$  concentration ( ■ ). The blue area represents the suboxic zone, separating the oxic zone from the anoxic zone ( ■ ).

**Figure 12;** FISH depth profile for anammox bacteria (*Amx368*) and *Scalindua* (*Sca1309*)

**Figure 12c** FISH depth profile for AOA, *N. maritimus* (*Cren67*) positive cells.

**Figure 12d** FISH depth profile for  $\beta$ -Proteobacteria (*Bet42a*) and  $\beta$ -AOB (*Nso1225-190*) positive cells.

**Figure 12e** FISH depth profile for  $\gamma$ -Proteobacteria (*Gam42a*) and  $\gamma$ -AOB (*Nscoc128*) positive cells .....68

**Figure 13** Nutrient and DNA profiles obtained from the q-PCR analyses for C-180;

**Figure 13a** Nutrient profile; the continuous lines represent the vertical profiles for  $\text{NH}_4^+$  concentration ( ● ),  $\text{NO}_2^-$  concentration ( ● ) and  $\text{NO}_3^-$  concentration ( ● ). The green area represents the CTD profile for oxygen concentration ( ■ ) and the triangles the oxygen measured in the lab from water samples ( ▲ ). The yellow area corresponds to  $\text{H}_2\text{S}$  concentration ( ■ ). The blue area represents the suboxic zone, separating the oxic zone from the anoxic zone ( ■ ).

**Figure 13b** Vertical profile of gene copies per mL of the gene *nirS*, specific for anammox bacteria of the genus *Scalindua*. Two peaks are observed at 250 and 289 meters.

**Figure 13c** Vertical profile of gene copies per mL of the gene *Arch-amoA*, specific for Archaeal aerobic ammonia oxidizers. One peak is observed at 210 meters.

**Figure 13d** Vertical profile of gene copies per mL of the gene *amoA* specific for  $\beta$ -bacterial ammonia oxidizers. One peak is observed at 250 meters.....69

**Figure 14a** Nutrient profile C-186; the continuous lines represent the vertical profiles for  $\text{NH}_4^+$  concentration (●),  $\text{NO}_2^-$  concentration (●) and  $\text{NO}_3^-$  concentration (●). The green area represents the CTD profile for oxygen concentration (■) and the triangles the oxygen measured in the lab from water samples (▲). The yellow area corresponds to  $\text{H}_2\text{S}$  concentration (■). The blue area represents the suboxic zone, separating the oxic zone from the anoxic zone (■).

**Figure 14b** FISH depth profile for anammox bacteria (Amx368) and *Scalindua* (Sca1309) positive cells.

**Figure 14c** FISH depth profile for AOA, *N. maritimus* (Cren67) positive cells.

**Figure 14d** FISH depth profile for  $\beta$ -Proteobacteria (Bet42a) and  $\beta$ -AOB (Nso1225-190) positive cells.

**Figure 14e** FISH depth profile for  $\gamma$ -Proteobacteria (Gam42a) and  $\gamma$ -AOB (Nscoc128) positive cells.....70

**Figure 15** Nutrient and DNA profiles obtained from the q-PCR analyses for C-186;

**Figure 15a** Nutrient profile; the continuous lines represent the vertical profiles for  $\text{NH}_4^+$  concentration (●),  $\text{NO}_2^-$  concentration (●) and  $\text{NO}_3^-$  concentration (●). The green area represents the CTD profile for oxygen concentration (■) and the triangles the oxygen measured in the lab from water samples (▲). The yellow area corresponds to  $\text{H}_2\text{S}$  concentration (■). The blue area represents the suboxic zone, separating the oxic zone from the anoxic zone (■).

**Figure 15b** Vertical profile of gene copies per mL of the gene *nirS*, specific for anammox bacteria of the genus *Scalindua*. Two peaks are observed at 245 and 330 meters.

**Figure 15c** Vertical profile of gene copies per mL of the gene *Arch-amoA*, specific for Archaeal aerobic ammonia oxidizers. One peak is observed at 201 meters.

**Figure 15d** Vertical profile of gene copies per mL of the gene *amoA* specific for  $\beta$ -bacterial ammonia oxidizers. One major peak is observed at 226 meters.....71

**Figure 16** Upward flux of ammonium to the suboxic zone and downward flux of nitrate to the suboxic for the three cruises studied, where cruise to cruise variations can be observed.....72

**Figure 17** Inventories of  $\beta$ -ammonia oxidizers (a),  $\gamma$ -ammonia oxidizers (b) and Archaeal ammonia oxidizers (c) compared to downward flux of nitrate from the lower oxic zone to the suboxic zone, where higher bacterial concentrations coincide with higher nitrate fluxes.....73

**Figure 18** Inventories of anammox bacteria (a) and Total aerobic ammonia oxidizers (b) compared to downward flux of nitrate from the lower oxic zone to the suboxic zone, where higher bacterial concentrations coincide with higher nitrate fluxes.....74

**Figure 19** Inventories of  $\beta$ -ammonia oxidizers (a),  $\gamma$ -ammonia oxidizers (b) and Archaeal ammonia oxidizers and (c) compared to upward flux of ammonium from the anoxic zone to the suboxic zone and integrated nitrite, where higher bacterial concentrations coincide with lower nitrate fluxes and, in the case of  $\gamma$ -AOB, also with lower nitrite inventories.....75

**Figure 20** Inventories of anammox bacteria (a) and aerobic ammonia oxidizers (b) compared to upward flux of ammonium from the anoxic zone to the suboxic zone and integrated nitrite, where higher bacterial concentrations coincide with lower nitrate fluxes and lower nitrite inventories.....76

**Figure 21** Comparison of FISH data for anammox bacteria from the g. *Scalindua* (Sca1309) and all known anammox bacteria (Amx368) for all cruises. There is a

significant linear relation where 77% of the variance in the Sca1309 probe-positive cells is explained by variance in Amx368 abundances.....77

**Figure 22** Comparison of the q-PCR DNA data for archaeal ammonia-oxidizing bacteria to FISH data for Crenarchaeal *N. maritimus* (Cren679) for all cruises. There is a significant linear relation where 75% of the variance in the q-PCR probe-positive cells is explained by changes in Cren679 abundances.....78

**Figure 23** Comparison of FISH data for  $\beta$ -ammonia-oxidizing bacteria (Nso1225-190) and all  $\beta$ -Proteobacteria (Bet42a) for all cruises. There is a significant linear relation where 75% of the variance in the Nso1225-190 probe-positive cells is explained by changes in Bet42a abundances.....79

**Figure 24** Comparison of FISH data for  $\gamma$ -ammonia-oxidizing bacteria (Nscoc128) and all  $\gamma$ -Proteobacteria (Gam42a) for all cruises. There is a significant linear relation but only 29% of the variance in the Nscoc128 probe-positive cells is explained by changes in Gam42a abundances.....80

## List of Tables

<b>Table 1</b> Probes used for FISH analyses.....	81
<b>Table 2</b> Primer sets used for the PCR and q-PCR reactions. (T <sub>m</sub> = Melting temperature).....	82
<b>Table 3</b> PCR thermal profiles for each of the three functional groups studied; Anammox (nirS), $\beta$ -ammonia-oxidizing bacteria ( $\beta$ -AOB) and Archaeal ammonia oxidizers (AOA).....	83
<b>Table 4</b> Quantitative PCR detailed reaction chemistry for the three groups of ammonia oxidizers.....	84
<b>Table 5</b> Results and standard errors from the q-PCR analyses for C-175, C-180 and C-186. Values in red were below limits of detection and should be considered as zeros.....	89
<b>Table 6</b> C-175 FISH results for anammox bacteria (Amx368), anammox bacteria from the genus <i>Scalindua</i> (Sca1309) and Archaeal ammonia oxidizers from the species <i>Nitrosopumilus maritimus</i> (Cren679) with their respective standard errors.....	91
<b>Table 7</b> C-175 FISH results for $\beta$ -Proteobacteria (Bet42a), $\beta$ -ammonia-oxidizing bacteria (Nso1225-190), $\gamma$ -Proteobacteria (Gam42a) and $\gamma$ -ammonia-oxidizing bacteria (Nscoc128) with their respective standard errors.....	92
<b>Table 8</b> C-180 FISH results for anammox bacteria (Amx368), anammox bacteria from the genus <i>Scalindua</i> (Sca1309) and Archaeal ammonia oxidizers from the species <i>Nitrosopumilus maritimus</i> (Cren679) with their respective standard errors.....	93
<b>Table 9</b> C-180 FISH results for $\beta$ -Proteobacteria (Bet42a), $\beta$ -ammonia-oxidizing bacteria (Nso1225-190), $\gamma$ -Proteobacteria (Gam42a) and $\gamma$ -ammonia-oxidizing bacteria (Nscoc128) with their respective standard errors.....	94



**Table 10** C-186 FISH results for anammox bacteria (Amx368), anammox bacteria from the genus *Scalindua* (Sca1309) and Archaeal ammonia oxidizers from the species *Nitrosopumilus maritimus* (Cren679) with their respective standard errors.....95

**Table 11** C-186 FISH results for  $\beta$ -Proteobacteria (Bet42a),  $\beta$ -ammonia-oxidizing bacteria (Nso1225-190),  $\gamma$ -Proteobacteria (Gam42a) and  $\gamma$ -ammonia-oxidizing bacteria (Nscoc128) with their respective standard errors.....96

**Table 12** Spearman Rank Order Correlation. Cell content (Top to bottom): correlation coefficient, p-value and number of samples. The pairs of variables with p-values below 0.05 are considered significant. In pairs with P-values greater than 0.050 there is no significant relationship between the two variables.....97

## **Acknowledgments**

It is with the deepest gratitude that I want to thank my advisor Professor Gordon Taylor for giving me the opportunity and tools to become a better scientist. His advice and guidance have helped me mature as a researcher. I would also like to thank Professors Mary Scranton and Jackie Collier for their helpful comments on this thesis and for always having an open door to all my questions.

I would like to thank the crew of the B/O Hermano Ginés for their moral support and help during the cruises, especially for their encouraging words when sea sickness seemed unbearable. A big thanks also goes to the Edimar staff, for their help and friendship.

Special thanks go to my family, for their love and support. I'd like to thank my father for teaching me hard work and perseverance; to my mom, for teaching me to be passionate, imaginative, independent and optimistic; and to my sister Marta for always being ready to help, even from the distance. I'd like to specially thank my husband Douglas, for being by my side all the way, for your endless support, for never complaining for the late nights at the laboratory or having to spend a weekend processing samples, and simply, for being yourself.

Last but not least I'd like to thank all my friends for cheering me up and always supporting me. You are one of the most important discoveries I achieved during my research.

## Introduction

Nitrogen is an essential element for all organisms. Like carbon, nitrogen is a principal element of purines and pyrimidines, which are the structural units of DNA and RNA, and all amino acids. The biggest reservoir of nitrogen is the atmosphere, where approximately 78 % is nitrogen gas. Inert atmospheric nitrogen gas can be fixed biologically into the terrestrial and marine ecosystems and become reactive nitrogen (oxidized and reduced inorganic and organic nitrogen forms) (Bunt et al. 1970 and Duce et al. 2006). Reactive nitrogen from the oceans can be returned to the atmospheric form by denitrification, anaerobic ammonia oxidation or nitrous oxide emission (Carpenter and McCarthy, 1975, Capone and Carpenter, 1982 and Akiyama, 2006).

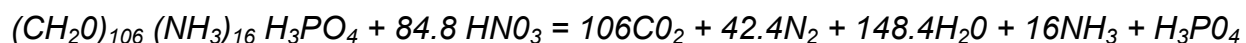
Nitrogen availability in the form of nutrients such as nitrate, nitrite or ammonium is a limiting factor for phytoplankton growth in non-eutrophic systems (Thomas, 1970). Atmospheric nitrogen is not usable by most phytoplanktonic species; it has to be fixed and assimilated into organic matter by diazotrophic microorganisms like cyanobacteria (Fay, 1981 and 1992; Berman-Frank et al. 2003 and Dyhrman, 2006). Through predation and cell decomposition, nitrogen becomes assimilated into organisms in surface waters, a portion of which eventually sinks to the deeper water as Particulate Organic Nitrogen (PON) in the form of fecal pellets and decaying biomass. During its trip through the water column part of the PON is decomposed to Dissolved Organic Nitrogen (DON) which can become mineralized to ammonium. A minor fraction of the PON gets buried in the sediments, decomposes and, eventually, is remineralized and released back into the water column.

In marine environments, surface waters are dominated by organisms whose metabolism depends directly on oxygen as their terminal electron acceptor (Wright, 2012). In areas where available oxygen in the water column becomes limiting, the community structure becomes dominated by microorganisms whose metabolisms are linked to other more abundant, but less energetically favorable oxidants, such as  $\text{NO}_3^-$ ,  $\text{NO}_2^-$  or  $\text{SO}_4^{2-}$  (Zhender and Stumm, 1988). Consequently, oxygen-dependent organisms are forced to inhabit shallower waters. The water layer which represents the transition zone between oxic and anoxic conditions is known as the redoxcline, which often contains a suboxic zone, where dissolved oxygen concentrations are below 2-3  $\mu\text{M}$  and hydrogen sulfide concentrations are less than 1  $\mu\text{M}$ . The suboxic zone represents a perfect niche for some chemoautotrophic bacteria dependent on reduced inorganic substrates (Santoro et al. 2011). It is within the redoxcline where the processes of nitrification and denitrification interact with the diffusion of substrates and products through concentration gradients (Ward, 1996).

The nitrification process is inhibited by light and usually takes place below the euphotic zone (Codispoti and Christensen, 1988). Nitrification consists of two basic steps; first ammonium is aerobically oxidized to  $\text{NO}_2^-$ . Second,  $\text{NO}_2^-$  is oxidized to  $\text{NO}_3^-$ , which might return to the euphotic zone by vertical mixing or upwelling and serve as a nutrient in shallower waters. If water becomes anoxic,  $\text{NO}_3^-$  undergoes denitrification, being reduced back to  $\text{NO}_2^-$ ,  $\text{N}_2\text{O}$ ,  $\text{NO}$  and, finally,  $\text{N}_2$  at the expense of organic matter. Part of this  $\text{N}_2$  might be biologically fixed back to PON in surface waters or escape to the atmosphere resulting in nitrogen loss (Figure 1) (Waksman et al. 1933

and Hayatsu et al. 2008). Originally, denitrification was thought to primarily occur in sediments and to be the only process leading to nitrogen loss from the oceans.

In 1972 deviations in N:P ratios from the expected Redfield ratio were discovered in oxygen deficient areas of the eastern Tropical North Pacific Ocean (Cline and Richards, 1972). Ammonium concentrations in the suboxic and anoxic layers were lower (<0.5 µg-atom/liter) than expected (2 µg-atom/liter) based on stoichiometric calculations from the following diagenetic reaction (Richards 1965):



Those same imbalances were found in many places through analysis of nutrient profiles including the Cariaco Basin, Venezuela (Walsh, 1996 and Walsh et al. 1999). This deficit in ammonium was assumed to be a consequence of the loss of nitrogen in the form of N<sub>2</sub> but no explanation of the process leading to it was found.

In 1977, the existence of the process of anaerobic ammonia oxidation was hypothesized based on thermodynamic calculations (Broda, 1977), but pure cultures of anaerobic ammonia-oxidizing bacteria were never obtained and the possibility of anaerobic ammonia oxidation being mediated by bacteria couldn't be proven following Koch's postulates. It wasn't until the first anammox bacteria were obtained in an enrichment culture from a sewage treatment plant, using Percoll density-gradient centrifugation (Strous et al. 1999) that biological anaerobic ammonia oxidation was

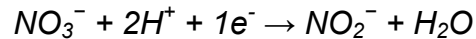
proven to be possible and present in the environment, and it became clear that the nitrogen cycle was even more complex than originally envisioned.

Within the last decade, numerous studies have focused on the nitrogen cycle and now provide a better understanding of the role of different microorganisms involved and their metabolic pathways. Anammox bacteria have been reported from several anoxic environments, such as arctic sediments and fjords (Rysgaard et al. 2004, Zhang et al. 2007, Schmid et al. 2007); the eastern tropical South Pacific Oxygen Minimum Zones (OMZs) (Galán et al. 2009, Lam et al. 2009, Stevens and Ulloa 2008); the Barent Sea, Black Sea and the Baltic Sea (Jensen et al. 2008, Lam et al. 2007, Hanning et al. 2007, Schmid et al. 2007); the Benguela (Namibia) upwelling (Kuypers et al. 2005); and in the Mid-Atlantic Ridge hydrothermal vents (Byrne et al. 2009). The presence of anammox bacterial cells has been recently reported within the Cariaco Basin by ladderane lipid biomarkers and FISH analyses (Wakeham et al. 2012). The main goal of my research is to extend previous research and provide a deeper understanding of the distribution of Anammox bacteria in the Cariaco Basin and the possible metabolic relations between them, Archaeal and bacterial aerobic ammonia oxidizers and nutrient enrichments and depletions.

Recent investigations have suggested that the metabolic pathways of Anammox bacteria, denitrifying bacteria and AOA as well as AOB might be linked (Lam et al. 2007 and 2009). The electron acceptor ( $\text{NO}_2^-$ ) for the Anammox reaction might be supplied by the chemoautotrophic nitrification process, where ammonium is oxidized into  $\text{NO}_2^-$  by AOA and AOB:



or from nitrate reduction in the chemoorganotrophic denitrification process, where nitrate is reduced to nitrite by denitrifying bacteria:



In this research I determined the distribution through the water column of aerobic ammonia-oxidizing bacteria and archaea and compared them with the distribution of anammox bacteria, expecting to find all three types of microorganisms living in close proximity near the oxic-anoxic interface considering previous research (Lam et al. 2007 and 2009).

Fluorescence In Situ Hybridization (FISH) and Quantitative PCR profiles of target organisms are common tools to describe the vertical distribution of microorganisms in the water column. Using general and genus/species-specific probes and primers targeting functional genes involved in the ammonia oxidation process carried out by bacteria (*amoA*) and archaea (*Arch-amoA*), as well as the gene specific for anammox bacteria from the genus *Scalindua* mediating in the process of nitrite reduction (*nirS*), I described the vertical distribution of anammox bacteria, AOB and AOA populations and studied the efficiency of those probes for characterizing ammonia-oxidizing populations. At the same time, the use of general and genus/species-specific probes allowed me to assess the diversity of those communities. As a final step, Reverse Transcription quantitative PCR (RT q-PCR) was attempted to quantify the levels of expression of the

functional genes (*nirS*, *amoA* and *Arch-amoA*) and to compare them to the q-PCR and FISH profiles. I also compared anammox, AOB and AOA depth distributions with nutrient concentration profiles and vertical flux estimates into the suboxic zone in order to examine relationships of AOB and AOA with  $\text{NH}_4^+$  and  $\text{NO}_3^-$  supplies and between Anammox inventories and depletions of  $\text{NO}_2^-$  and  $\text{NH}_4^+$ .



## **Background**

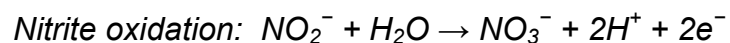
### **The Cariaco Basin**

The Cariaco Basin is a semi-enclosed, tectonically-formed depression located on the northern continental shelf of Venezuela (Figure 2). The basin is delimited by Margarita Island, Cubagua Island and the Araya Peninsula to the east; by Tortuga Island and the Tortuga Banks on the north; by Cape Codera and Farallón Centinela to the west; and by the central northern coast of Venezuela to the south. The basin is divided into two sub-basins by a saddle at a depth of 900 meters, each with a maximum depth of 1400 meters. The basin has two connections to the Caribbean Sea: the Centinela channel (Febres-Ortega and Herrera, 1975) and the Tortuga channel (Richards and Vaccaro, 1956), of 146 and 135 meters depth, respectively. Waters above about 100 meters exchange freely with the Caribbean Sea. The limited lateral exchange and slow vertical mixing caused by a prominent salinity maximum at 100 meters (Scranton et al. 2001) together with high productivity rates, supported by seasonal upwelling (Febres-Ortega and Herrera, 1975), result in oxygen depletion at depths below 100 meters and complete permanent anoxia from 250-350 meters to the bottom of the basin (Richards, 1975, Zhang and Millero, 1993 and Scranton et al. 2001). Study of the redoxcline (where  $O_2$  concentration decreases steeply and  $H_2S$  increases) has found a peak in chemoautotrophic production within the redoxcline (Tuttle and Jannasch 1973, 1977), in some cases, multiple peaks occurring immediately above and below the  $O_2$ - $H_2S$  interface (Taylor et al., 2001). These chemoautotrophic bacteria are thought to be dependent on upward fluxes of inorganic reductants such as  $NH_4^+$  and

reduced sulfur species and downward fluxes of oxidants ( $O_2$  and  $NO_3^-$ ) and to significantly contribute to the overall biological production of the Basin (Taylor et al. 2001).

### **Aerobic Ammonia-oxidizing $\beta$ - and $\gamma$ -proteobacteria (AOB) and Archaea (AOA)**

Aerobic ammonia-oxidizing  $\beta$ - and  $\gamma$ -proteobacteria (AOB) and Archaea (AOA) are the major players in the aerobic ammonium oxidation reaction within the nitrification zone, which is usually located in close relation to the redoxcline, where inorganic ammonium becomes oxidized to nitrite and subsequently to nitrate by nitrite-oxidizing bacteria (NOB), such as *Nitrobacter sp.* In areas where anammox bacteria are found, AOA and AOB are believed to act as substrate providers to the Anammox bacteria through production of  $NO_2^-$ , but at the same time they may act as competitors for  $NH_4^+$  (Lam et al. 2007).

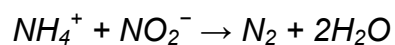


The isolation and genomic characterization of the marine Crenarchaea *Nitrosopumilus maritimus* (Könneke et al. 2005) led to the discovery of the presence of ammonium monooxygenase subunit A genes within the *N. maritimus* genome and their

distant relation with the  $\beta$ - and  $\gamma$ -proteobacteria (AOB) *amoA* genes (Francis et al. 2007). This finding was the starting point for a new series of investigations focused on assessing the relative importance of AOA versus AOB in the ammonia oxidation process (Agogu e et al. 2008, Beman et al. 2010, Coolen et al. 2007, Lam et al. 2007 and 2009, Martens-Habbena et al. 2009, Santoro et al. 2008 and 2010, Walker et al. 2010). Apparently AOA and AOB are equally important in the nitrification process in the studied OMZs, the mesopelagic and other anoxic basins and the differences in abundance (AOA>>AOB) might be balanced by the difference in the number of functional genes inside these two different microorganisms (AOA<AOB) (Lam et al. 2007 and Santoro et al. 2010).

### **Anammox Bacteria**

The Anammox reaction consists of the oxidation of inorganic ammonium into gaseous dinitrogen using nitrite as the electron acceptor:



$NH_4^+$  was thought to be biologically largely inert under anoxic conditions until  $NH_4^+$  was experimentally demonstrated to be removed in a denitrifying pilot plant for waste water treatment at Gist-Brocades, Netherlands (Mulder et al. 1995). It was not until 1999 that researchers were able to isolate “the missing lithotroph” (Broda, 1977),

the first Anammox bacterium isolated from an enrichment culture (Strous et al. 1999). Thanks to this discovery, the idea that all nitrogen loss in the oceans was due to denitrifying bacteria has been discarded, and an explanation for anomalous nitrogen losses in sediments and anoxic fjords emerged (Richards et al. 1965).

Anammox bacteria form an anaerobic monophyletic cluster, named Brocadiales, within the Order Planctomycetales (Jetten et al. 2008). They are capable of performing the anaerobic oxidation of ammonium into dinitrogen creating a sink for inorganic nitrogen. Because of the marginal energy yield of the anammox reaction, they are slow growing, observed to divide once every two weeks (Strous et al. 1999). They possess a unique structure, which differentiates them from all other known bacteria, called the anammoxosome. Anammoxosomes make up more than 30% of the cell's volume and the membrane that surrounds this organelle is comprised of unique ladderane lipids (Niftrik et al. 2004, Schouten et al. 2008). Five Anammox genera have been described in fresh water, marine and sediment environments since 1999: *Candidatus Kueneria*, *Candidatus Scalindua*, *Candidatus Brocadia*, *Candidatus Anammoxglobus* and *Candidatus Jettenia*, with the genus *Scalindua* appearing to dominate anammox bacteria in open sea (Schmid et al. 2003 and 2005, Strous et al. 2006 and Quan et al. 2008).

## Methods

### Sample collection and storage

Water samples were collected as part of the CARIACO Ocean Time Series onboard the B/O Hermano Ginés (Estación de Investigaciones Marinas, Fundación la Salle de Ciencias Naturales in Isla Margarita, Venezuela) during three cruises that took place on December 8, 2010; May 6, 2011 and November 9, 2011 (CAR-175, CAR-180 and CAR-186). Samples from 18 depths were collected with a SeaBird rosette equipped with 12 TFE (Teflon) coated 8 liter Niskin bottles. The Seabird rosette includes a CTD with conductivity, temperature and pressure probes; a Yellow Springs Instruments, Inc. (YSI) oxygen probe; a Chelsea Instruments fluorometer for estimating concentration of chlorophyll a and a Sea Tec beam c transmissometer (660 nm) (Muller-karger et al., 2001). Beam attenuation peaks were used as an indicator of the particle maxima close to the oxic-anoxic interface (Taylor et al., 2001). Water samples were collected at 10-20 meter intervals across the oxic-anoxic zone (redoxcline) and wider intervals were used for the shallower and deeper water samples. The Niskin bottles were slightly pressurized with argon gas to minimize chances of sample oxygenation. Nutrient profiles for  $\text{NH}_4^+$ ,  $\text{NO}_2^-$  and  $\text{NO}_3^-$  were provided by Dr. Kent Fanning from University of South Florida following the protocol developed by Gordon for autoanalyzers (Gordon et al. 1995).  $\text{H}_2\text{S}$  profiles were provided by Lan T. Tong and Yrene Astor using a spectrophotometric determination with N, N-di- methyl-p-phenylenediamine sulfate (modified from Cline, 1969).

For FISH analyses, samples of 45 ml of water were taken in duplicate for each depth, fixed with 5 ml of 20% filtered borate-buffered formaldehyde (final concentration 2%) on board and stored at -15°C. Back in the laboratory samples were thawed and filtered onto 47mm diameter, 0.2 µm pore size filters (GTTP type) using ≤ 300 mm Hg of vacuum pressure; washed with 10 ml of filter-sterilized ddH<sub>2</sub>O and stored at -15°C (Pernthaler et al. 2001).

For the DNA samples, 2-2.5 liters of water from each depth were directly collected from the Niskin bottles into sterile Secure™ EVA Compounder Bags (Capitol Medical Inc.). The compounder bags were attached to in-line filter holders containing 47mm diameter, 0.2 µm pore membranes (GTTP type) and attached to a filtration manifold (Figure 3). The enclosed system minimized sample exposure to the atmosphere and permitted filtration of 7 samples simultaneously. The filters were cut in four pieces and stored in 5 ml PowerWater® Bead Tubes (MO BIO Laboratories Inc., Carlsbad CA), submerged in 4mL of LifeGuard™ Soil Preservation Solution (MO BIO Laboratories Inc., Carlsbad CA) and stored at -15°C.

For transportation back to the U.S.A., FISH and DNA samples were placed in a polystyrene box surrounded by frozen ice packs. After arriving in the U.S.A. FISH samples were stored at -80°C (Pernthaler et al. 2001) until further analysis and DNA samples were stored at -20°C until DNA extraction.

## **FISH analysis**

FISH analysis for anammox bacteria and AOB were performed following Pernthaler's (2001) protocol. Briefly, small wedges were cut from the filters, submerged in hybridization buffer containing the oligonucleotide probes (Table 1) labeled with Cy3 (excitation: 550nm/ emission: 570nm) and incubated at 46°C for 2 hours at constant humidity in a hybridization oven (Boekel Scientific, Feasterville, PA). After hybridization, filters were washed and counter-stained with DAPI (4,6 diamidino-2-phenylindole, excitation: 358nm/ emission: 461nm), a general DNA stain. The probes Nso1225 and Nso190 were used for detection of  $\beta$ -ammonia oxidizers by successive hybridization (Wagner et al., 1994). The hybridization and washing steps (Pernthaler, 2001) for the probe with the highest stringency were followed by the hybridization and washing steps for the probe with the lowest stringency (first Nso1225 was processed with stringency of 55% followed by Nso190 with stringency of 35%).

Catalyzed Reporter Deposition FISH (CARD-FISH) analyses for AOA were performed following Pernthaler's (2002) protocol. Briefly, filter sections were embedded in 0.2% low-gelling-point agarose. Once dried, the filters were permeabilized by incubation with 1 mg mL<sup>-1</sup> of lysozyme. Possible peroxidase interference was inactivated by incubating the samples 15 min submerged in 0.01 M HCl and washing them with ethanol (96%). Filters were incubated overnight at 46°C submerged in hybridization buffer containing Horseradish Peroxidase (HRP) labeled Cren679 probe (Table 1). After hybridization the filters were incubated with Tyramide-Alexa Fluor<sup>®</sup> 555 for signal amplification using the Tyramide Signal Amplification Kit (Molecular Probes<sup>™</sup>,

Invitrogen™ Detection Technologies). After signal amplification the filters were counter-stained with DAPI.

All filters were mounted on glass slides using Citifluor anti-fading oil (Electron Microscopy Sciences) and visualized with an Axioskop epifluorescent microscope (Carl Zeiss). When necessary, images were captured with a MagnaFire® Digital Camera System (Optronics) and processed with the IPPWIN Image Pro Plus Version 7.0 (Media Cybernetics) for color resolution improvement.

Filter blanks (filtered ddH<sub>2</sub>O) were processed with the FISH samples as controls for reagent contamination. Concentrations of the targeted functional groups were compared to the total bacterial counts obtained with DAPI staining (20 grids per sample) and a ratio of target cell counts over total bacterial counts was calculated for each sample. To obtain the total concentration of the targeted functional groups for each depth, this ratio was multiplied by the corresponding number of total bacteria obtained by Acridine Orange (AO) staining and quantification, where 10 to 20 mL of water were filtered, stained with AO following Hobbie et al. (1977) and visualized with an Axioskop epifluorescent microscope (Carl Zeiss) for cell quantification (10 grids per filter).



## DNA extraction and purification

Before DNA extraction, the LifeGuard™ Soil Preservation Solution was removed from the samples by centrifuging the bead tubes containing the filters at 2,500 xg for 5 minutes and removing the supernatant according to manufacturer's instructions. DNA was captured in silica spin columns and eluted in 100 µL of PCR grade sterile water using the PowerWater® DNA Isolation kit (MO BIO Laboratories Inc., Carlsbad CA) following manufacturer instructions. Samples were stored at -80°C until further analysis.

## DNA standards

Production of the DNA standards required three main steps; obtaining representative DNA samples, PCR amplifying the genes of interest and obtaining plasmids containing those genes of interest through gene ligation into a plasmid, cell transformation of *E. coli* cells and plasmid extraction.

- **Representative DNA samples:** *Nitrosomonas europaea*, *Nitrosopumilus maritimus* and *candidatus Scalindua* were chosen as representative species for AOB, AOA and Anammox, respectively. Axenic cultures of *Nitrosomonas europaea* (ATCC® 25978™) and *Nitrosopumilus maritimus* (cell stock provided by Dr. Martin Könneke, Max-Planck Institute for Marine Microbiology in Bremen, Germany) were cultivated in Willm's modified synthetic Crenarchaeota medium for *Nitrosopumilus maritimus*, strain

SCM1, and their growth stage monitored every two days by staining 0.5-3 mL of the culture with Acridine Orange, a general nucleic acid stain, and quantified by epifluorescence microscopy (Hobbie et al., 1977) (Figure 4). In the *N. maritimus* culture, approximate concentrations of  $\text{NO}_3^-$  and  $\text{NO}_2^-$  were monitored with the  $\text{NO}_3^-$  and  $\text{NO}_2^-$  Profi Test kits (Salifert<sup>®</sup>, Holland) to document increases of those ammonia oxidation products. When the cultures reached exponential growth phase, DNA was extracted using the DNeasy Blood & Tissue kit (Invitrogen<sup>™</sup> Life Technologies<sup>™</sup>) and eluted in 100  $\mu\text{L}$  of PCR grade water (Roche Applied Science). Aliquots (10  $\mu\text{L}$ ) of the culture were cryopreserved in 20% sterile glycerol for future use. Anammox DNA from genus *Scalindua* was directly provided by Prof. Mike S.M. Jetten (Radboud University Nijmegen, Netherlands).

- **PCR amplification of genes of interest:** PCR protocols were developed for AOB, AOA and Anammox targeting the amplification of functional genes related to the nitrogen cycle which were unique to each group of microorganisms. Details of the genes targeted, primers names, sequences and melting temperatures ( $T_m$ ) are presented in Table 2. The PCR reaction mixes were as follows: 500 nM of forward and reverse primers, 100-500 ng of DNA, 0.5  $\mu\text{L}$  of Enzyme blend (Failsafe<sup>™</sup> PCR System, Epicentre<sup>®</sup> Biotechnologies), 25  $\mu\text{L}$  of premix 2X D/F (Failsafe<sup>™</sup> PCR System, Epicentre<sup>®</sup> Biotechnologies) and PCR grade water (Roche Applied Science) in a total reaction volume of 50  $\mu\text{L}$ . The thermal profiles used for amplification of each target gene are shown in Table 3. PCR products and specificity of the reactions were checked with gel electrophoresis (1% Agarose) stained with Ethidium Bromide (EtBr) and observed under U.V. light. Once the reactions were confirmed to work the PCR products were

purified using the QIAquick PCR Purification Kit (Qiagen Inc.) following manufacturer instructions and the purity of the amplicons was checked with a ND-1000 Spectrophotometer (Nanodrop®). According to manufacturer's instructions, acceptable purity levels are defined as  $\geq 1.8$  for the  $\lambda$  260/280 ratio and between 1.8 and 2.2 for the  $\lambda$  260/230 ratio.

- **Gene ligation, cell transformation and plasmid extraction:** Fresh PCR products of the bacterial *amoA*, Archaeal *amoA* and Anammox *nirS* genes were ligated to linearized plasmid vectors (pCR®2.1-TOPO®, Invitrogen™ Life Technologies™). Once the genes of interest were inserted into the plasmids, they were used to transform *E. coli* competent cells (One Shot® Mach1™-T1<sup>R</sup>, Invitrogen™ Life Technologies™) and incubated overnight at 37°C on LB plates containing 50  $\mu\text{g mL}^{-1}$  of Ampicillin (Fisher Bioagents, Fisher Scientific) and 40  $\mu\text{L}$  of 40  $\text{mg mL}^{-1}$  X-gal (Promega). Transformed cells were color-screened after incubation (white colonies-transformed cells / blue colonies-untransformed cells) (Figure 5). The TOPO TA Cloning® kit (Invitrogen™ Life Technologies™) was used for the ligation, transformation and growth of competent cells following manufacturer instructions. The following conditions were found to be optimal for the three genes of interest.

- TOPO® cloning reaction containing 3  $\mu\text{L}$  of PCR product, 1  $\mu\text{L}$  of diluted salt solution (200 mM NaCl, 10 mM MgCl<sub>2</sub>), 1  $\mu\text{L}$  PCR grade water (Roche Applied Science) and 1  $\mu\text{L}$  of pCR®2.1-TOPO® vector.

- The incubation times of the TOPO<sup>®</sup> Cloning Reaction and the Mach1<sup>™</sup>-T1<sup>®</sup> Chemical Transformation Reaction were increased from 5 to 20 minutes to increase colony yield.
- Optimal colony distribution on LB plates was achieved by spreading 50  $\mu\text{L}$  of the Mach1<sup>™</sup>-T1<sup>®</sup> chemical Transformation Reaction.

The plasmid extraction was performed using the PureLink<sup>™</sup> Quick Plasmid Miniprep kit (Invitrogen<sup>™</sup> Life Technologies<sup>™</sup>) following manufacturer instructions. The following steps produced optimal results:

- 10 white colonies were re-suspended in 10 mL of LB medium containing 50  $\mu\text{g mL}^{-1}$  of Ampicillin (Fisher Bioreagents, Fisher Scientific) and incubated overnight at 37°C.
- After the incubation, 2 mL of the cell cultures were transferred to a 2.5 mL Eppendorf tube and stored for 1 hour at -80°C for optimal membrane lysis.
- Extra centrifugation step of 4 minutes at 12000  $\times g$  (Eppendorf centrifuge 5417C) performed before transferring the supernatant containing the plasmid DNA into the extraction columns to increase Plasmid DNA purity.

- Plasmid DNA was eluted in 75  $\mu$ L of 10mM Tris (Mo Bio Laboratories, Inc.) instead of TE buffer to avoid possible PCR inhibition due to EDTA.

Successful extraction of the plasmids was checked by gel electrophoresis (1% Agarose) stained with EtBr. Gene insertion and correct orientation of the fragment was checked by performing a PCR for each one of the three different genes of interest with further checking of proper amplification of the genes as well as the purity and size of the amplified fragments.

Plasmid DNA concentrations were measured using the ND-1000 Spectrophotometer (Nanodrop®) and DNA standards were prepared from those plasmid extractions in a dilution range of 1 -  $10^7$  gene copies (Applied Biosystems™ by Life Technologies™, tutorials). All formulas and calculations used can be found in Appendix I.

### **Quantitative PCR optimization**

For q-PCR the same chemistry as for standard PCR reactions was used with the difference of the addition of SyBr Green (Lonza Group, Ltd.) as a nucleic acid stain and ROX (Stratagene-Agilent Technologies) as a reference dye. The same thermal profiles were used as for standard PCR reactions except that 40 cycles were run instead of 30

for better detection limit, and the final extension cycle of 15 minutes at 72°C was replaced by the melting analysis of one cycle with three stages: 1 minute at 95°C, 30 seconds at 55°C and 30 seconds at 95°C. Before performing the q-PCR assays the reactions had to be optimized for primer and nucleic acid stain concentrations. Three different concentrations of SyBr Green were tested 1:40,000, 1:50,000 and 1:66,666 (0.15X, 0.2X and 0.25X) and two different primer concentrations (500nM and 1µM). Primer concentrations of 500nM were found to be optimal for the PCR reactions, but because the volume for the q-PCR assays is reduced by half and the DNA load is higher, I decided to test higher primer concentrations to avoid possible primer limitation problems. Matrix reactions were run, for each gene, testing for a range of useful combinations of primer and SyBr Green concentrations from which the optimal results were selected. The criteria I followed for determining the optimal result were, in order of importance: amplification signal intensity, discard runs showing primer-dimer formation in the dissociation curve, select the combination with the highest normalized final fluorescence reading minus the normalized first fluorescence reading (dRn Last) and lowest Threshold cycle (Ct). In case of a tie, I chose the combination with the lowest primer concentration. If combinations are still tied, I chose the combination with the lowest dye concentration. Optimal q-PCR reactions chemistry for Anammox *nirS*, bacterial *amoA* and Archaeal *amoA* are shown in Table 4.

## **Quantitative PCR**

All q-PCR samples were run in triplicate and spiked with  $10^2$  copies of the target gene from the ligated plasmids acting as positive controls, in order to check for PCR inhibition and to avoid false negatives. No template controls (NTC) were run in triplicate as negative controls to check for reagent contamination and to avoid false positives.

Standard curve reactions ranging from 1 to  $10^7$  gene copies were run in triplicate with the samples. The standard curves showed efficiencies of 90-130% and  $r^2$  of 0.95-0.99 (example of optimal standard curve can be seen in Figure 6). Dissociation melting curves were performed with each run to test for primer-dimer formation. Small peaks below  $80^\circ\text{C}$  would be a signal of lower molecular weight products being amplified and creating a fluorescent signal not related to target gene amplification (example of optimal dissociation curve can be seen in Figure 7). After q-PCR amplification all samples were double tested for reaction specificity by examining their dissociation curves for possible primer-dimer formation and by gel electrophoresis (1% Agarose) stained with EtBr (visualized under U.V. light).

## **mRNA samples and Reverse Transcription quantitative PCR (RT q-PCR)**

mRNA samples were collected at the same time and using the same methods as DNA samples (see "Sample collection and storage" in Methods section). Before mRNA

extraction and processing, the LifeGuard™ Soil Preservation Solution was removed from the samples by centrifuging the bead tubes containing the filters at 2,500 xg for 5 minutes and removing the supernatant. mRNA was captured in silica spin columns using the PowerWater® RNA Isolation kit (MO BIO Laboratories Inc., Carlsbad CA Laboratories, Inc.) following manufacturer instructions. Briefly, samples were vortex at maximum speed (5 min) for bead beating with 990 µL of solution PWR1 and 10 µL of β-Mercaptoethanol (MP Biomedicals, LLC.), possible PCR inhibitors were removed with solution PWR2, mRNA was bound to the silica columns and DNA was removed by treatment with DNase I RNase free enzyme (incubation at room temperature for 15 min). DNase I was inactivated by a washing step with PWR7 solution. mRNA was eluted in 100 µL of solution PWR8 (DNA/RNA-free water). Samples were stored at -80°C until further analysis.

First-strand cDNA was synthesized from the mRNA samples using the SuperScript® VILO™ cDNA Synthesis Kit (Invitrogen™ Life Technologies™). Briefly, the extracted mRNA was combined with the kit's reaction mix (5X VILO), enzyme mix (10X SuperScript®) and DEPC-treated water. Samples were gently mixed and incubated at room temperature for 10 min, 42°C for 60 min and 85°C for 5 min. Synthesized cDNA was stored at -20°C until further use.

The same primer sets, chemistry and thermal profiles as for q-PCR were used for the RT q-PCR analyses (Tables 2, 3 and 4). All RT q-PCR cDNA samples were run in triplicate and spiked with  $10^2$  copies of the target gene from the ligated plasmids acting as positive controls, in order to check for PCR inhibition and to avoid false negatives.



No reverse transcription (NoRT) controls were run for each sample to check for DNA contamination in the mRNA samples. No template controls (NTC) were run in triplicate as negative controls to check for reagent contamination and to avoid false positives. Standard curve reactions ranging from 1 to  $10^7$  gene copies were run in triplicate with the samples.

It was not possible to collect any data from the RT q-PCR analyses due to failure of the amplification process. Reactions showed amplification levels below  $10^2$  gene copies  $\text{mL}^{-1}$  (below gene copies being spiked to sample) which mean that probably the PCR reaction was inhibited. In addition to possible inhibition, mRNA samples were checked for purity and concentration with a ND-1000 Spectrophotometer (Nanodrop<sup>®</sup>) and results did not meet the acceptable range for purity ( $\geq 2$  for the  $\lambda$  260/280 ratio and between 1.8 and 2.2 for the  $\lambda$  260/230 ratio) and concentrations were consistently low, ranging from 1 to 15  $\text{ng}/\mu\text{L}$ .

Low mRNA concentrations may be caused by inadequate preservation during collection and storage, even though the LifeGuard<sup>™</sup> Soil Preservation Solution (MO BIO Laboratories Inc., Carlsbad CA) is supposed to be optimal for mRNA preservation. Another explanation for the low concentrations and possible PCR inhibition would be the inadequate extraction of mRNA from the samples and inefficient removal of PCR inhibitors when using the PowerWater<sup>®</sup> RNA Isolation kit (MO BIO Laboratories Inc., Carlsbad CA Laboratories, Inc.).

Further RT q-PCR analyses were attempted with higher concentrations of cDNA (instead of 2µL, reactions with 3 and 4µL were tested) and increased number of amplification cycles in the thermal profile (50 cycles instead of 40) but the same low to non-detectable yields of mRNA were obtained. Due to time limitations no further optimization was possible, but in an attempt to avoid possible inhibition, for future work, I would recommend using a different preservation method for the mRNA samples and a different mRNA extraction method.

## **Flux model**

Vertical fluxes were estimated for  $\text{NH}_4^+$  and  $\text{NO}_3^-$  to examine their relationship to ammonia-oxidizing bacteria and Archaea within the suboxic zone during the three cruises. This flux model assumes that transport occurs exclusively by vertical eddy diffusion and ignores possible vertical or horizontal advection (Scranton, 1988 and Li et al., 2012). The vertical flux values (J) were obtained using Fick's first law:

$$J = -K_z \frac{\Delta C}{\Delta z}$$

where  $K_z$  is the vertical eddy diffusion coefficient and  $\Delta C/\Delta z$  is the concentration gradient.

The concentration gradient of ammonium was calculated at the base of the suboxic zone, where ammonium concentrations increase from close to detection limit to values up to 10-15  $\mu\text{M}$ . The concentration gradient was obtained from the slope of the linear regression obtained from plotting the concentrations of ammonium from the first value above 1  $\text{mmol/m}^3$  ( $=1 \mu\text{M}$ ) to the first value above 10  $\text{mmol/m}^3$  against their respective depths (Figure 8). For the nitrate concentration gradient, the slope of the linear regression was obtained plotting the values from the peak in nitrate concentration (lower oxic zone) to the first value below 1  $\text{mmol/m}^3$  against their respective depths.

The vertical eddy diffusion coefficient ( $K_z$ ) was estimated from the density gradient equations (Gargett, 1984 and Li, 2012):

$$K_z = a_0 \sqrt{\left(\frac{1}{N^2}\right)}$$

Where

$$N = \sqrt{\left(-\frac{g \delta \rho}{\rho \delta z}\right)}$$

The constant  $a_0$  is related to the input of energy to the basin via internal waves and other processes that cannot be directly measured, and has an estimated value for the Cariaco Basin of  $a_0 = 0.0004 \text{ cm}^2/\text{s}^2$  (Li et al. 2012). The constant  $g$  represents the gravitational acceleration constant which value is  $-9.8 \text{ m/s}^2$ ,  $\rho$  is the density at a given depth and  $\delta\rho/\delta z$  is the water density gradient over a depth interval. The water density

gradient was calculated from the slope of the fitted linear regression, always with a coefficient of determination ( $r^2$ ) higher than 0.98, resulting from plotting the same depth boundaries used to calculate the concentration gradients, against their respective water densities.

### **Anammox, AOA and AOB inventories**

Vertical fluxes of ammonium and nitrate were compared to integrated cell concentrations of ammonia-oxidizing bacteria using the data obtained from the FISH profiles of Anammox (Amx368), AOA (Cren679),  $\beta$ -AOB (Nso1225-190) and  $\gamma$ -AOB (Nscoc128). Inventories of cells per square meter were calculated as areas of the peaks observed within the suboxic zone in the vertical profiles of cell # versus depth, and the results of those peaks were added to find the total bacterial concentration per square meter. Those peak areas were obtained by the multiplication of the average concentration of cells between two consecutive depths by the depth interval between those same points. This single “trapezoid” is added to the next one until completing the area of the peak in the profile.

## **Statistical analyses**

Possible relations between nutrient concentration and ammonia-oxidizing bacteria and Archaea abundances were tested using the Spearman Rank Order correlation analysis. This test was selected because variables were not normally distributed (Shapiro-Wilk normality test).

Probe performance among probes targeting related functional groups of Bacteria or Archaea (Amx368-Sca1309, Bet42a-Nso1225-190 and Gam42a-Nscoc128) and the percentage of the general probe represented by the specific probe were tested by linear regression analyses.

## Results

### Hydrography and Nutrient Profiles

For each cruise,  $O_2$ ,  $H_2S$ ,  $NH_4^+$ ,  $NO_3^-$  and  $NO_2^-$  data were plotted together in vertical profiles (Figure 9). The suboxic zone, defined as the water layer where  $O_2$  concentrations are lower than 2-3  $\mu M$  and  $H_2S$  concentrations are less than 1  $\mu M$ , spanned from 210 to 255 meters (45 meters of thickness), from 240 to 280 meters (40 meters thickness) and from 245 to 295 meters (50 meters thickness) in C-175, C-180 and C-186 respectively. Vertical profiles show that  $NO_3^-$  accumulates in the oxic zone and reaches its maximum in the lower oxic zone (10-11  $\mu M$ ) where it starts declining and disappears in the mid-suboxic zone.  $NH_4^+$  concentrations are close to detection limits through the oxic zone and increase steeply in the lower suboxic-anoxic zone up to 30  $\mu M$ .  $NO_2^-$  values are low throughout the water column, with small enrichments within the suboxic zone only reaching 0.02  $\mu M$  at most.

### Anammox Bacteria

Anammox bacteria were quantified using FISH analyses targeting all known anammox bacteria (Amx368) and anammox bacteria from the genus *Scalindua* (Sca1309) and by q-PCR, targeting the functional gene nitrite reductase, specific for *Scalindua* (*nirS*). In all three cruises FISH profiles with the probe Amx368 and Sca1309

showed two peaks of anammox bacteria, the first one ranging from 7,000 to 11,000 cells mL<sup>-1</sup> always within the suboxic zone (C-175 lower suboxic, C-180 and C-186 upper suboxic) and the second one ranging from 3,000 to 4,700 cells mL<sup>-1</sup> in the upper anoxic zone (Figures 10b, 12b and 14b).

Vertical profiles obtained with q-PCR analyses featured peaks in abundances at the same depths as the FISH profiles, with the peaks within the suboxic zone ranging from 9.5 to 27.8 gene copies mL<sup>-1</sup> and the peaks in the anoxic zone ranging from 3.8 to 22.2 gene copies mL<sup>-1</sup> (Figures 11b, 13b and 15b).

Anammox bacteria hybridized with the probe Sca1309 and the probe Amx368 showed significant positive correlations with NO<sub>2</sub><sup>-</sup> concentrations over the 150 to 400 m depth interval (Sca1309: r=0.5, p=0.004, n=35; Amx368: r=0.4, p=0.024, n=35).

### **Ammonia-oxidizing Archaea (AOA)**

Ammonia-oxidizing archaea were quantified using a FISH probe specific for *N. maritimus* (Cren679) and a q-PCR with primer set targeting the Archaeal amoA gene (*Arch-amoA*). FISH vertical profiles for all three cruises showed a peak, ranging from 4,400 to 14,800 cells mL<sup>-1</sup>, in the lower oxic zone in close proximity to the suboxic zone (20-40 meters above) (Figures 10c, 12c and 14c).

Vertical profiles obtained with q-PCR analyses featured peaks in abundances at the same depths as the FISH profiles with the peaks in the lower oxic zone ranging from 5,800 to 18,900 gene copies mL<sup>-1</sup> (Figures 11c, 13c and 15c).

AOA data from the DNA and FISH profiles showed highly significant negative correlations with NH<sub>4</sub><sup>+</sup> concentrations (Arch-amoA:  $r=-0.7$ ,  $p<0.001$ ,  $n=35$ ; Cren679:  $r=-0.4$ ,  $p=0.001$ ,  $n=35$ ) and highly significant positive correlations with NO<sub>2</sub><sup>-</sup> (Arch-amoA:  $r=0.5$ ,  $p=0.006$ ,  $n=35$ ; Cren679:  $r=0.5$ ,  $p=0.007$ ,  $n=35$ ) and NO<sub>3</sub><sup>-</sup> concentrations (Arch-amoA:  $r=0.7$ ,  $p<0.001$ ,  $n=35$ ; Cren679:  $r=0.5$ ,  $p<0.001$ ,  $n=35$ ) over the 150 to 400 m depth interval.

### **β- Ammonia-oxidizing Bacteria (β-AOB)**

β-AOB were studied using profiles generated with FISH data from cells hybridized with the probe Bet42a (general probe for β-Proteobacteria) and Nso1225-190 (probe targeting β-AOB) and q-PCR analyses targeting the ammonia monooxygenase gene specific for β-AOB (*β-amoA*). FISH profiles showed peaks in β-AOB abundances, ranging from 8,100 to 13,700 cells mL<sup>-1</sup> in the lower oxic zone (C-175 and C-186) or the upper suboxic zone (C-180). Secondary smaller peaks, ranging from 2,600 to 9,600 cells mL<sup>-1</sup>, were detected in the upper anoxic zone in the cruises C-175 and C-180. Differences between Bet42a and the Nso1225-190 profiles are observed in C-180 within the oxic zone where only the general probe for β-



Proteobacteria peaks, probably due to the detection of non-ammonia-oxidizing  $\beta$ -Proteobacteria (Figures 10d, 12d and 14d).

Vertical profiles produced with q-PCR analyses featured a peak in abundances in the lower oxic zone (C-175 and C-186) or upper suboxic zone (C-186) ranging from 95.5 to 1006 gene copies mL<sup>-1</sup>. Secondary peaks were observed in the upper anoxic zone in C-180 and C-186 ranging from 38 to 290 gene copies mL<sup>-1</sup> (Figures 11d, 13d and 15d).

The vertical FISH profiles for general  $\beta$ -Proteobacteria showed a significant negative correlation with NH<sub>4</sub><sup>+</sup> concentrations ( $r = -0.6$ ,  $p < 0.001$ ,  $n = 35$ ) and significant positive correlations with NO<sub>2</sub><sup>-</sup> ( $r = 0.4$ ,  $p = 0.021$ ,  $n = 35$ ) and NO<sub>3</sub><sup>-</sup> concentrations ( $r = 0.6$ ,  $p < 0.001$ ,  $n = 35$ ) over the 150 to 400 m depth interval. The vertical FISH profiles for  $\beta$ -AOA showed a significant positive correlation with NO<sub>3</sub><sup>-</sup> concentrations ( $r = 0.4$ ,  $p = 0.04$ ,  $n = 35$ ) in the water layer from 150 to 400 meters.

### **$\gamma$ - Ammonia-oxidizing Bacteria ( $\gamma$ -AOB)**

$\gamma$ -AOB were studied using profiles generated with FISH data from cells hybridized with the probe Gam42a (general probe for  $\gamma$ -Proteobacteria) and FISH data from cells hybridized with the probe Nscoc128 (probe targeting  $\gamma$ -AOB). No q-PCR profiles were produced because a gene standard was not available for those

microorganisms (Appendix II). Profiles obtained with both probes showed similar results, where peaks in abundances, ranging from 3,350 to 24,000 cells mL<sup>-1</sup>, were observed in the lower oxic zone (C-175 and C-186) or the upper suboxic zone (C-180). Secondary smaller peaks were detected in the suboxic zone for C-175, (8,000 cells mL<sup>-1</sup>) and in the upper anoxic zone for C-180 and C-186 (3,000 to 4,000 cells mL<sup>-1</sup>) (Figures 10e, 12e and 14e).

The vertical FISH profiles for general  $\gamma$ -Proteobacteria did not show any significant correlation with NH<sub>4</sub><sup>+</sup>, NO<sub>2</sub><sup>-</sup> or NO<sub>3</sub><sup>-</sup> concentrations (p>0.05). However, vertical FISH profiles for  $\gamma$ -AOB showed a significant negative correlation with NH<sub>4</sub><sup>+</sup> concentrations (r= -0.5, p=0.001, n=35) and significant positive correlations with NO<sub>2</sub><sup>-</sup> (r=0.4, p=0.021, n=35) and NO<sub>3</sub><sup>-</sup> concentrations (r=0.6, p<0.001, n=35) in the water layer from 150 to 400 meters.

### **Comparison of ammonia-oxidizing Bacteria and Archaea inventories with vertical fluxes of ammonium and nitrate and nitrite**

Vertical fluxes of ammonium and nitrate in the suboxic zone are likely influenced by Bacterial and Archaeal populations. Aerobic ammonia-oxidizers (oxidize ammonium to nitrite), denitrifiers (reduce nitrate to nitrite) or anaerobic ammonia-oxidizers (oxidize ammonium, using nitrite as electron acceptor, to nitrogen gas) might control those nutrient fluxes. Vertical flux estimates for ammonium and nitrate for C-175, C-180 and

C-186 are presented in Figure 16, where cruise to cruise variations can be observed for ammonium upward flux and nitrate downward flux. The calculated upward flux of  $\text{NH}_4^+$  ranged from  $0.08 \text{ mmol N m}^{-2} \text{ d}^{-1}$  in C-175 to  $0.12 \text{ mmol N m}^{-2} \text{ d}^{-1}$  in C-186. Downward flux of  $\text{NO}_3^-$  to the suboxic zone ranged from  $0.08 \text{ mmol N m}^{-2} \text{ d}^{-1}$  in C-186 to  $0.14 \text{ mmol N m}^{-2} \text{ d}^{-1}$  in C-175.

Ammonium and nitrate fluxes were compared to anammox bacteria,  $\beta$ -AOB,  $\gamma$ -AOB and AOA inventories. No rigorous statistical analyses were possible due to the small number of data points ( $n=3$ ). However higher nitrate downward flux values corresponded to larger inventories of aerobic ammonia oxidizers and anammox bacteria ( $21 \cdot 10^{11} \text{ cells m}^{-2}$  and  $7.4 \cdot 10^{11} \text{ cells m}^{-2}$ ) (Figures 17 and 18). Higher ammonium upward flux values corresponded to smaller inventories of  $\gamma$ -AOB and anammox bacteria (Figures 19 and 20). Integrated nitrite inventories were also calculated for the suboxic zone of C-175, C-180 and C-186, and compared with the Anammox, AOA and AOB inventories. Lower integrated values of nitrite corresponded with bigger inventories of  $\gamma$ -AOB and anammox bacteria (Figures 19 and 20). Anammox bacteria and  $\gamma$ -AOB inventories follow a similar distribution, being larger for C-175, smaller for C-180 and even smaller for C-186. Taking into consideration their metabolic pathways, where anammox bacteria consume nitrite and  $\gamma$ -AOB produce nitrite, seems like the relation between lower nitrite inventories and higher  $\gamma$ -AOB was probably driven by anammox bacteria and denitrifying bacteria inventories which are being supported by the  $\gamma$ -AOB activity.

## Probe and q-PCR intercomparisons

One of the most important factors affecting reliable FISH quantification is the correct election of the probes to be used in the hybridization experiments. Here, I aimed to assess the performance of the specific probes by comparing data obtained from FISH quantifications with the general probes (Amx368, Bet42a and Gam42a) with data obtained from hybridization with the specific probes (Sca1309, Nso1225-190 and Nscoc128) and the q-PCR results for each functional group (Anammox,  $\beta$ -AOB and  $\gamma$ -AOB, respectively). Linear regressions between FISH and q-PCR data for anammox bacteria and  $\beta$ -AOB resulted in weak coefficients of determination ( $r^2$ ), probably due to under estimates provided by the q-PCR analyses (see “q-PCR and FISH as quantification techniques for ammonia oxidizers” in the Discussion section).

- **Amx368 and Sca1309:** The profiles of the two anammox probes were compared to the data provided by the q-PCR amplification of the *nirS* gene specific for the genus *Scalindua*. Only the probe Sca1309 showed a significant ( $p$ -value $<0.05$ ) correlation but only 15% of the variance in the profile created from q-PCR could be explained by changes in the Sca1309 probe. This low coefficient of determination might be caused by the low amplification efficiency of the q-PCR analyses that most probably led to underestimation of the number of gene copies in the samples.

When the two anammox probes were compared together, a highly significant ( $p$ -value $<0.001$ ) linear relation was found where 77% of the variance in the Sca1309 profile is explained by the probe Amx368. The regression slope ( $m$ ) was  $0.97\pm 0.09$ , which

means that practically 100% of the bacteria recognized with the general anammox probe Amx368 is recognized by the probe specific for the genus *Scalindua*, Sca1309 (Figure 21).

- **Cren679:** Ammonia-oxidizing Archaea FISH data obtained with the probe specific for *N. maritimus* (Cren679) was compared only to the q-PCR profiles of Archaeal-amoA gene copies mL<sup>-1</sup> due to the lack of a more general FISH probe for AOA to compare with. The specific probe (Cren679) showed a highly significant (p-value<0.001) linear relation with the data obtained from q-PCR quantification, where 75% of the variance in the q-PCR profile is explained by the FISH profile. The regression slope (*m*) was 1.08±0.12, which means that 92 to 100% of the ammonia-oxidizing Archaea detected in the q-PCR profile were represented in the profile generated with the specific probe Cren679 (Figure 22). Those direct comparisons between FISH profiles and gene copy number were possible considering that ammonia-oxidizing Crenarchaea have a maximum of 1 gene copy per cell (Hallam et al. 2006)

- **Bet42a and Nso1225-190:** The q-PCR data obtained from the amplification of the  $\beta$ -amoA gene was compared to the FISH profiles obtained with the general probe for  $\beta$ -Proteobacteria (Bet42a) and the specific probe for  $\beta$ -AOB (Nso1225-190) and significant linear relations (p-value<0.05) were found between both probes and the q-PCR data. The probe specific for  $\beta$ -AOB had a slightly higher coefficient of determination ( $r^2$ ) than the general probe for  $\beta$ -Proteobacteria (0.22 and 0.14, respectively) where 22% and 14% of the variance in the q-PCR profile is explained by changes in the Nso1225-190 and Bet42a profiles, respectively.

When the two probes were compared a highly significant ( $p$ -value $<0.001$ ) linear relation was found where 75% of the variance in the Nso1225-190 profile is explained by the probe Bet42a. The regression slope ( $m$ ) was  $0.55\pm 0.13$ , which means that in the order of 55% of the bacteria recognized with the general  $\beta$ -Proteobacteria probe, from 150 to 400 meters, are recognized by the specific probe for  $\beta$ -AOB (Figure 23).

- **Gam42a and Nscoc128:** The specific probe for  $\gamma$ -AOB (Nscoc128) was compared to the general probe for  $\gamma$ -Proteobacteria (Gam42a) and a highly significant ( $p$ -value=0.001) correlation was found, where 29% of the variance in the Nscoc128 profile is explained by the probe Gam42a. The regression slope ( $m$ ) was  $0.71\pm 0.18$ , which means in the order of 71% of the bacteria recognized with the general  $\gamma$ -Proteobacteria probe, from 150 to 400 meters, are recognized by the specific probe for  $\gamma$ -AOB (Figure 24).

## Discussion

### Community structure and possible metabolic relations

Anammox bacteria and aerobic ammonia-oxidizing bacteria and Archaea have been previously described to co-occur in the OMZs off Peru (Lam et al. 2009), off northern Chile (Galán et al. 2009) and in the Black Sea (Lam et al. 2007). In this investigation, they have been observed to co-occur within or near the suboxic zone of the Cariaco Basin. Peaks in abundance of aerobic ammonia oxidizers were detected in the lower oxic zone or in the upper suboxic zone and anammox bacteria were detected in close proximity within the suboxic zone.

The highest abundances detected for aerobic ammonia oxidizers were attributable to  $\gamma$ -AOB with peaks in the lower oxic zone up to 24,000 cells mL<sup>-1</sup>, followed by AOA with a maximum of 14,800 cells mL<sup>-1</sup> and then by  $\beta$ -AOB with a maximum of 13,700 cells mL<sup>-1</sup> which relate to previous studies in the Cariaco Basin where  $\gamma$ -Proteobacteria were found to be the most abundant group of microorganisms with increasing depths (Madrid et al. 2001).

Potential nitrification rates can be derived from laboratory incubation experiments with AOA and AOB which yielded 2-4 fmol N cell<sup>-1</sup> d<sup>-1</sup> and 7.2-1,272 fmol N cell<sup>-1</sup> d<sup>-1</sup>, respectively (Laanbroek and Gerards, 1993; Wuchter et al. 2006 and Magalhães et al. 2009). Considering the maximum peaks in abundance for  $\gamma$ -AOB,  $\beta$ -AOB and AOA (24,000 cells mL<sup>-1</sup>, 13,700 cells mL<sup>-1</sup> and 14,800 cells mL<sup>-1</sup>, respectively) which all were

detected during the same cruise (C-175), those organisms could, theoretically, support maximum nitrification rate of  $31 \mu\text{M d}^{-1}$ ,  $17 \mu\text{M d}^{-1}$  and  $59 \text{nM d}^{-1}$ , respectively. These results mean that  $\gamma$ -AOB would be the most important nitrifying group in the Cariaco Basin, potentially contributing to 64% of the community nitrification rate. In second place  $\beta$ -AOB potentially take care of 36% of the nitrification and finally, AOA with only 0.1% of the nitrification, even though they are more abundant than  $\beta$ -AOB.

The concentrations of AOA and AOB correlated with depletions in ammonium and enrichments in nitrite and nitrate as expected considering their role in the nitrification process. These organisms use ammonium as substrate and produce nitrite that becomes rapidly oxidized to nitrate in the final step of the nitrification process. High downward nitrate fluxes also corresponded to higher AOA and AOB concentrations, because their metabolic processes would be causing bigger nitrate accumulations in the lower oxic zone that will be either upwelled to surface waters or reduced to nitrite in the suboxic zone as part of the denitrification process. Secondary peaks in abundances of  $\beta$ - and  $\gamma$ -AOB were observed within the suboxic zone or in the upper anoxic zone. Those peaks might be caused by lateral intrusion of oxygenated water (Scranton et al. 2001) that promoted sporadic localized aerobic ammonia oxidation at those depths.

Ammonium concentrations at the depths where AOB and AOA peaked were close to detection limits, which would mean that uptake rate of this nutrient is balanced by upward or downward fluxes thereby preventing accumulation. One of the possible supply pathways for ammonium is likely to arrive from the surface, primarily in the form of sinking and suspended PN that is mineralized during transit. An estimate of potential



ammonium mineralized from sinking and suspended PN was calculated from monthly data of suspended PN decay and sediment trap data of sinking PON (225 meters to 410 meter) available for the Cariaco Basin (cruises C-163, November 2009 to C-173, October 2012). PON loss suggested  $\sim 0.41 \mu\text{mol L}^{-1}$  of potential mineralized  $\text{NH}_4^+$  from surface sinking and suspended PN.

Vertical diel migrations of fish and zooplankton excreting and defecating in the deeper oxic zone of the Cariaco Basin might also contribute to this supply of ammonium (Baird et al. 1975 and Love et al. 2003). The largest reservoir of ammonium resides in bottom waters where remineralized ammonium accumulates from PN diagenesis and is transported to the suboxic zone.

Two peaks in anammox bacteria abundances were consistently observed, the first within the suboxic zone and the second peak in the upper anoxic zone. This distribution divided in two groups might be related to nitrite sources. In the presence of oxygen (oxic and suboxic zones) the nitrification process takes place. Nitrification is divided into two steps, being the first one the aerobic oxidation of ammonia into nitrite. Therefore, the first step of the nitrification process could be considered as a nitrite source. Another source of nitrite would be located in oxygen depleted waters (anoxic zone) where the first step of the denitrification process takes place, reducing nitrate into nitrite. The presence of two peaks in anammox bacteria coinciding with the two depths where nitrite is being produced as part of the nitrification-denitrification processes is highly suggestive of a population vertical segregation based on these two different sources of nitrite.

Even though anammox bacteria are anaerobic microbes, previous research (Kalvelage et al. 2011 and Podlaska et al. 2012) has found peaks in abundance of anammox bacteria within the upper OMZs off Peru and off Costa Rica, respectively, where oxygen reached concentrations up to 15  $\mu\text{M}$ . Oxygen tolerance was tested in enrichment cultures of anammox bacteria for four different oxygen concentrations (0.25, 0.5, 1 and 18  $\mu\text{M}$ ) and the anammox reaction was reported to be reversibly inhibited by the concentrations of 0.25, 0.5 and 1  $\mu\text{M}$  and irreversibly inhibited by the oxygen concentration of 18  $\mu\text{M}$  (Egli, 2003). Therefore, a possible refuge from anammox inhibition in oxic waters might be within micro-oxic and anaerobic microenvironments where the anammox bacteria would be able to thrive (Paerl and Pinckney, 1996).

The anammox bacterial peaks within the suboxic zone correspond to oxygen concentrations of  $\sim 2$   $\mu\text{M}$ . Consistent with observations that anammox bacteria need micro-oxic to anoxic conditions to carry on their metabolic processes, living within the suboxic zone would mean living close to their limit of oxygen tolerance. This limitation may be offset by the continuous supply of nitrite from the aerobic ammonia oxidizers. The recurring presence of these two peaks of anammox bacteria from the genus *Scalindua* during the three cruises does not necessarily indicate activity, although it is highly suggestive and seems to support the hypothesis that anammox metabolism is linked to two different processes of the nitrogen cycle for nitrite supply, aerobic ammonia oxidation (nitrification) and nitrate reduction (denitrification).

Upward fluxes of remineralized ammonium from bottom waters were lower when anammox bacterial inventories were higher, which may mean that the major pathway for

ammonium supply to anammox bacteria would be ammonium remineralized in bottom waters and transported to the suboxic zone. Nitrite inventories were lower when anammox bacteria inventories were higher, which is what I expected to find, considering that, as part of the anammox reaction, nitrite is consumed as the electron acceptor for the oxidation of ammonia into hydroxylamine. Downward flux of nitrate to the suboxic zone was also seen to be related to anammox bacterial inventories, where higher downward fluxes of nitrate coincided with bigger anammox bacteria inventories.

### **q-PCR and FISH as quantification techniques for ammonia oxidizers**

Quantitative PCR and FISH are useful tools for the quantification of microorganisms, both possessing benefits and disadvantages. Quantitative PCR provides a quantification of the number of copies of the targeted gene, and, by applying Reverse Transcription q-PCR, the expression levels of those genes. The problem arises in the complexity of this technique, especially all those factors affecting the DNA/RNA extractions and reaction efficiencies, which can easily lead to over or underestimations of the studied samples.

In my research, ammonia-oxidizing archaea provided similar profiles when quantified with q-PCR and FISH techniques. Anammox bacteria and  $\beta$ -AOB, gene copy quantifications obtained with q-PCR assays provided vertical profiles featuring the same characteristics as the profiles obtained with the FISH analyses (peaks in abundance

featured at the same depths) but with quantifications one or two orders of magnitude lower.

Considering the *Arch-amoA* gene copy quantifications provided results similar to FISH quantification, that DNA extraction of all samples was performed following the same protocol and that same DNA stocks were used for q-PCR analyses targeting the different functional genes, I assumed that the differences observed among functional groups were not caused by inefficient extraction method, although the step where LifeGuard™ Soil Preservation Solution (MO BIO Laboratories Inc., Carlsbad CA) is removed from the samples might have led to some cell loss (in future work might be recommended to increase the centrifugation time from 5 min to 15 min). Therefore, the low q-PCR results might be caused by a q-PCR reaction mixture or thermal profile not properly optimized. In addition, a possible factor contributing to these differences might be different q-PCR efficiencies between the genomic DNA samples and the plasmid DNA standards.

Linear and circular plasmids sometimes can have different q-PCR efficiencies than environmental DNA samples (Hou et al. 2010). Plasmid standards consist of a short sequence of nucleotides with the gene of interest ligated in the middle (TOPO TA Cloning manual, Invitrogen™ Life Technologies™) whereas genomic DNA from the field samples consists mostly of complex DNA. During the PCR reaction, primers have to “find” and anneal to the target DNA sequences. Therefore, the annealing efficiency could be higher in plasmid standards, where there are only structures with the matching sequence than in environmental DNA samples which contain much more non-matching

genomic DNA that may interfere with the target region. Highly efficient plasmid DNA standards might under quantify the samples if those are not as efficient as they are. Another explanation for this difference between the FISH profiles and the q-PCR profiles would involve an overestimation in the FISH quantifications, but I doubt that being the case considering that the profiles generated with the general and the specific probes provided similar results and patterns.

The FISH technique is an easy and fast technique (compared to q-PCR) which provides abundances relative to the total number of bacteria present in samples. FISH quantifications provides information about the presence/absence of the targeted organism in samples which would prevent unnecessary wastes of time and resources employed in creating DNA standards and optimizing protocols for those organisms. FISH also provides a relative quantification of the concentration of the target organism; as long as the number of gene copies per cell is known, this information can be compared to profiles obtained with q-PCR analyses as a mean to control possible q-PCR efficiency issues leading to over or under quantifications.

### **Summary of major findings and hypothesis**

1. Anammox bacteria are present in the Cariaco Basin within the suboxic zone and in the anoxic zone in close proximity to bacterial and Archaeal aerobic ammonia oxidizers.

2. Anammox bacteria are spatially divided in two groups; the first one resides within the suboxic zone where nitrite for the anammox reaction could be supplied from aerobic ammonia oxidation (nitrification), and the second group resides in the anoxic zone where nitrite could be supplied by nitrate reduction (denitrification).
3. Potentially 64% of the nitrification occurring in the oxic-suboxic zone of the Cariaco Basin is performed by  $\gamma$ -AOB, 36% by  $\beta$ -AOB and only 0.1% by AOA.
4. Vertical distributions of aerobic ammonia oxidizers and anammox bacteria are consistent with the hypothesis that remineralized  $\text{NH}_4^+$  from sinking PON may be used as substrate mostly by AOA and AOB. Remineralized  $\text{NH}_4^+$  transported from depth would be used as substrate mostly by anammox bacteria.
5. FISH and q-PCR quantification techniques complement each other and FISH can help detect efficiency issues in q-PCR protocols.
6. In the depth range from the lower oxic zone (150-200 meters) to the upper anoxic zone (300-330 meters), an average of 97% of the Anammox bacteria community is represented by the genus *Scalindua*; 92% of the AOA community is represented by the species *Nitrosopumilus maritimus*;  $\beta$ -AOB represents the 82% of the  $\beta$ -Proteobacteria community and  $\gamma$ -AOB represents the 71% of the  $\gamma$ -Proteobacteria community.

## Future work

As long as human populations continue to increase, anthropogenic emissions of nitrogenous compounds will continue increasing at a proportional rate due to agriculture, waste, livestock and fossil fuel sources (Galloway et al. 2008 and Mosier, 2000). Eutrophication of coastal waters and open ocean deposition of anthropogenic nitrogen compounds are leading to changes in the natural nitrogen cycle (Duce et al. 2008, Jetten 2008) and could contribute to global climate change considering that  $N_2O$  has a strong greenhouse effect (Akiyama et al. 2006 and Wright et al. 2012). In order to assess the impact, possible consequences and future management of anthropogenic nitrogen inputs, a more thorough knowledge of the nitrogen cycle is imperative.

Future work should focus on the detection and quantification of other groups of bacteria that take part on the nitrogen cycle. Combined studies using q-PCR and FISH quantifications targeting the functional genes involved in each of the remaining steps of the nitrogen cycle could be used, focusing on the subunits specific for different groups of bacteria. Good examples would be the genes responsible for the synthesis of the nitrate reductase (NaR) or the nitrite reductase (NiR) enzymes, which mediate the reduction of  $NO_3^-$  to  $NO_2^-$  and the reduction of  $NO_2^-$  to  $NO$ , respectively, in order to quantify the denitrifying community in the water column (Braker et al., 1998, Michotey et al., 2000 and Philippot et al., 2002). Another good example would be the quantification of the gene responsible for the synthesis of the Nitrite oxidase enzyme (Faull et al., 1969 and Gieseke et al., 2003), responsible for the oxidation of  $NO_2^-$  to  $NO_3^-$  as part of the nitrification process.

In addition to quantification of genomic DNA (gene copies) for the functional genes involved in the nitrogen cycle, the quantification of the expression levels of those genes is recommended. Through Reverse Transcription quantitative PCR (RT q-PCR) it is possible to quantify not only the presence of those functional genes, but also if they are being expressed and how their levels of expression relate to the nutrient profiles. A study of the trophic relations of these organisms with their predators, and quantification of those, would also be a good method to assess a possible top-down control of the microorganisms taking part in the nitrogen cycle.



## References

- Agogu , H., Brink, M., Dinasquet, J., Herndl, G.J. (2008), Major gradients in putatively nitrifying and non-nitrifying Archaea in the deep North Atlantic, *Nature* vol. 456, pp.788–791.
- Akiyama, H., Yan, X. and Yagi, K. (2006), Estimations of emission factors for fertilizer-induced direct N<sub>2</sub>O emissions from agricultural soils in Japan: summary of available data. *Soil Sci. Plant Nutr.*, vol. 52, pp.774–787.
- Alzerreca, J.J., Norton, J.M. and Klotz, M.G. (1999), The amo operon in marine, ammonia-oxidizing  $\gamma$ -Proteobacteria. *FEMS Microbiol Lett.*, vol. 180, pp.21–29.
- Beman, J.M., Popp, B.N. and Francis, C.A. (2008), Molecular and biogeochemical evidence for ammonia oxidation by marine Crenarchaeota in the Gulf of California, *ISME J.*vol. 2, pp. 429–441.
- Beman, J.M., Sachdeva, R. and Furhman, J.A. (2010), Population ecology of nitrifying Archaea and Bacteria in the Southern California Bight, *Environmental Microbiology*. Vol.12, no.5, pp.1282-1292.
- Berman-Frank, I.,Lundgren, P. and Falkowski, P. (2003), Nitrogen fixation and photosynthetic oxygen evolution in cyanobacteria. *Research in Microbiology*, vol.154, pp.157–164.
- Braker, G., Fesefeldt, A. and Witzel, K-P. (1998), Development of PCR Primer Systems for Amplification of Nitrite Reductase Genes (nirK and nirS) To Detect Denitrifying Bacteria in Environmental Samples. *Applied and Environmental Microbiology*, Vol. 64, No. 10, pp. 3769–3775.
- Broda, E. (1977), Two kinds of lithotrophs missing in nature, *Z Allg Mikrobiol* vol. 17, pp. 491-493.
- Bunt, J.S., Cooksey, K.E., Heeb, M.A., Lee, C.C. and Taylor, B.F. (1970), Assay of algal nitrogen fixation in the marine subtropics by acetylene reduction. *Nature (Lond.)* vol. 227, pp. 1163-1164.
- Byrne, N., Strous, M., Cre peau, V., Kartal, B., Birrien, J-L., Schmid, M., Lesongeur, F., Schouten, S., Jaeschke, A. and Jetten, M. (2009), Presence and activity of anaerobic ammonium-oxidizing bacteria at deep-sea hydrothermal vents, *The ISME Journal*. Vol. 3, pp. 117-123.
- Capone, D.G. and Carpenter, E.J. (1982), Nitrogen Fixation in the Marine Environment. *Science, New Series*, Vol. 217, No. 4565, pp. 1140-1142.

- Carpenter, E.J. and McCarthy, J.J. (1975), Nitrogen Fixation and Uptake of Combined Nitrogenous Nutrients by Oscillatoria (*Trichodesmium*) *thiebautii* in the Western Sargasso. *Limnology and Oceanography*, Vol. 20, No. 3, pp. 389-401.
- Cline, J.D. (1969), Spectrophotometric Determination of Hydrogen Sulfide in Natural Waters, *Limnology and Oceanography*, Vol. 14, No. 3, pp. 454-458.
- Cline, J.D. and Richards, F.A. (1972), Oxygen Deficient Conditions and Nitrate Reduction in the Eastern Tropical North Pacific Ocean, *Limnology and Oceanography*, Vol. 17, No. 6, pp. 885-900.
- Codispoti, L.A. and Christensen, J.P. (1985), Nitrification, denitrification and nitrous oxide cycling in the eastern tropical South Pacific Ocean. *Marine Chem.* Vol. 16, pp. 277–300.
- Coolen, M.J.L, Abbas, B., van Bleijswijk, J., Hopmans, E.C., Kuypers, M.M.M., Wakeham, S.G. and Damsté, J.S.S. (2007), Putative ammonia-oxidizing Crenarchaeota in suboxic waters of the Black Sea: a basin-wide ecological study using 16S ribosomal and functional genes and membrane lipids, *Environmental Microbiology*, vol. 9, no.4, pp.1001-1016.
- Duce, R.A., LaRoche, J., Altieri, K., Arrigo, K.R., Baker, A.R., Capone, D.G., Cornell, S.S., Dentener, F., Galloway, J., Ganeshram, R.S., Geider, R.J., Jickells, T., Kuypers, M.M.M., Langlois, R., Liss, P.S., Liu, S.M., Middelburg, J.J., Moore, C.M., Nickovic, S., Oschlies, A., Pedersen, T., Prospero, J., Schlitzer, R., Seitzinger, S. and Sorensen, L.L. (2008), Impacts of atmospheric anthropogenic nitrogen on the open ocean, *Science* vol.320, pp.893–897.
- Dyhrman, S.T., Chappell, P.D., Haley, S.T., Moffett, J.W., Orchard, E.D., Waterbury, J.B. and Webb, E.A. (2006), Phosphonate utilization by the globally important marine diazotroph *Trichodesmium*. *Nature* vol.439, pp.68-71.
- Egli, K.R. (2003), On the use of anammox in treating ammonium-rich wastewater. A dissertation submitted to the Swiss Federal Institute of Technology Zurich for the degree of Doctor of Natural Sciences.
- Faull, K.F., Wallace, W. and Nicholas, D.J.D. (1969), Nitrite Oxidase and Nitrate Reductase in *Nitrobacter agilis*. *Biochem. J.* vol. 113, p.449.
- Fay, P. (1981), Photosynthetic microorganisms. Nitrogen fixation, vol. I. Ecology, pages 1-29. Ed. W.J. Broughton, Clarendon Press, Oxford.
- Fay, P. (1992), Oxygen relations of Nitrogen-Fixation in Cyanobacteria. *Microbiological Reviews*, Volume: 56, Issue: 2, pp. 340-373.
- Febres-Ortega, G., and L. E. Herrera (1975), Interpretacion dinamica de algunas de las características oceanograficas de la Fosa de Cariaco, Mar Caribe, Bol., Inst. Oceanogr. Univ. de Oriente, vol.14, pp. 3 –29.

- Francis, C.A., Roberts, K.J., Beman, J.M., Santoro, A.E. and Oakley, B.B. (2005), Ubiquity and diversity of ammonia-oxidizing archaea in water columns and sediments of the ocean, *Proc. Natl Acad. Sci. USA*, vol.102, pp. 14683–14688.
- Francis, C.A., Beman, J.M. and Kuypers, M.M.M. (2007), New processes and players in the nitrogen cycle: the microbial ecology of anaerobic and archaeal ammonia oxidation, *The ISME Journal* vol.1, pp. 19-27.
- Galán A., Molina, V., Thamdrup, B., Woebken, D., Lavik, G., Kuypers, M.M.M. and Ulloa, O. (2009), Anammox bacteria and the anaerobic oxidation of ammonium in the oxygen minimum zone off northern Chile, *Deep Sea Research Part II: Topical Studies in Oceanography*, vol. 56, pp.1021–1031.
- Gieseke, A., Bjerrum, L., Wagner, M. and Amann, R. (2003), Co-existence of nitrifying bacteria in biofilms. *Environmental Microbiology*, vol. 5, no.5, pp.355–369.
- Gordon, L.I., Jennings, J.C., Jr., Ross, A.A. and Krest, J.M. (1995), A Suggested Protocol for Continuous Flow Automated Analysis of Seawater Nutrients (Phosphate, Nitrate, Nitrite and Silicic Acid) in the WOCE Hydrographic Program and the Joint Global Ocean Fluxes Study, Operations and Methods, WHP Office Report, WHPO 91-1, WOCE Report No. 681091, Revision 1.
- Hallam, S.J., Mincer, T.J., Schleper, C., Preston, C.M., Roberts, K., Richardson, P.M. and DeLong, E.F. (2006), Pathways of Carbon Assimilation and Ammonia Oxidation Suggested by Environmental Genomic Analyses of Marine Crenarchaeota. *PLoS Biol* 4:e95.
- Hanning, M., Lavik, G., Kuypers, M.M.M., Woebken, D., Martens-Habbena, W. and Jürgens, K. (2007), Shift from denitrification to anammox after inflow events in the central Baltic Sea, *Limnol. Oceanogr.*, vol. 52, no.4, pp. 1336-1345.
- Hayatsu, M., Tago, K. and Saito, M. (2008). Various players in the nitrogen cycle: Diversity and functions of the microorganisms involved in nitrification and Denitrification. *Soil Science and Plant Nutrition*, vol. 54, pp.33–45.
- Hobbie, J.E., Daley, R.J., and Jasper, S. (1977), Use of Nuclepore Filters for Counting Bacteria by Fluorescence Microscopy. *Appl. Environ. Microbiol.*, vol. 33, no. 5 pp. 1225-1228.
- Hou, Y., Zhang, H., Miranda, L. and Lin, S. (2010), Serious Overestimation in Quantitative PCR by Circular (Supercoiled) Plasmid Standard: Microalgal *pcna* as the Model Gene. *PLoS ONE* 5(3): e9545
- Jensen, M.M., Kuypers, M.M.M., Lavik, G., Thamdrup, B. (2008), Rates and regulation of anammox in the Black Sea, *Limnol Oceanogr.*, vol. 53, pp.23–36.

- Jetten, M.S.M., Cirpus, I., Kartal, B. et al. (2005), 1994-2004: 10 years of research on the anaerobic oxidation of ammonium, *Biochemical Society Transactions*, Vol. 33, pp. 119-123.
- Jetten, M.S.M. (2008), The microbial nitrogen cycle, *Environmental Microbiology*, vol.10, no.11, pp. 2903-2909.
- Juretschko, S. (2000), Mikrobielle Populationsstruktur und -dynamik in einer nitrifizierenden/denitrifizierenden Belebtschlammanlage. Doctoral thesis (Technische Universität München).
- Kalvelage, T., Jensen, M.M., Contreras, S., Revsbech, N.P., Lam, P., Günter, M., LaRoche, J., Lavik, G. and Kuypers, M.M.M. (2011), Oxygen sensitivity of anammox and coupled N-cycle processes in oxygen minimum zones. *PLoS ONE* 6 (12) e29299.
- Koch, R. (1890), An Address on Bacteriological Research. *British medical journal*, Vol.2, Issue 1546, pp. 380-3.
- Könneke, M., Bernhard, A.E., de la Torre, J.R., Walker, C.B., Waterbury, J.B. and Stahl, D.A. (2005), Isolation of an autotrophic ammonia-oxidizing marine archaeon, *Nature*, vol. 437, pp. 543–546.
- Kuypers, M.M.M., Lavik, G., Woebken, D., Schmid, M., Fuchs, B.M., Amann, R., Jørgensen, B.B., Jetten, M.S.M. and Hayes, J.M. (2005), Massive nitrogen loss from the Benguela upwelling system through anaerobic ammonium oxidation, *Proc Natl Acad Sci USA*, vol.102, pp. 6478–6483.
- Laanbroek, H.J. and Gerards, S. (1993) Competition for limiting amounts of oxygen between *Nitrosomonas europaea* and *Nitrobacter winogradskyi* grown in mixed continuous cultures. *Arch Microbiol*, vol. 159, pp.453-459.
- Labrenz, M., Sintes, E., Toetzke, F., Zumsteg, A., Herndl, G.J., Seidler, M. and Jürgens, K. (2010), Relevance of a crenarchaeotal subcluster related to *Candidatus Nitrosopumilus maritimus* to ammonia oxidation in the suboxic zone of the central Baltic Sea. *The ISME Journal*, vol. 4, pp.1496–1508.
- Lam, P., Jensen, M.M., Lavik, G., McGinnis, D.F., Müller, B., Schubert, C.J., Amann, R., Thamdrup, B. and Kuypers, M.M.M. (2007), Linking crenarchaeal and bacterial nitrification to anammox in the Black Sea, *Proc. Natl Acad. Sci. USA*. Vol.104, pp. 7104–7109.
- Lam, P., Lavik, G., Jensen, M.M., van de Vossenberg, J., Schmid, M., Woebken, D., Gutiérrez, D., Amann, R., Jetten, M.S.M. and Kuypers, M.M.M. (2009), Revising the nitrogen cycle in the Peruvian oxygen minimum zone, *PNAS*, vol.106 no. 12, pp. 4752-4757.

- Li, X.N., Taylor, G.T., Astor, Y., Varela, R. and Scranton, M.I. (2012), The conundrum between chemoautotrophic production and reductant and oxidant supply: A case study from the Cariaco Basin. *Deep-Sea Research I*, vol. 61, pp.1–10.
- Lin, X., Scranton, M.I., Varela, R., Chistoserdov, A. and Taylor, G.T. (2007), Compositional responses of bacterial communities to redox gradients and grazing in the anoxic Cariaco Basin, *Aquatic Microbial Ecology*, Vol.47, pp.57-72.
- Madrid, V.M., Taylor, G.T., Scranton, M.I. and Chistoserdov, A.Y. (2001), Phylogenetic Diversity of Bacterial and Archaeal Communities in the Anoxic Zone of the Cariaco Basin. *Applied and Environmental Microbiology*, Vol. 67, No. 4, pp. 1663-1674.
- Magalhães, C.M., Machado, A. and Bordalo, A.A. (2009), Temporal variability in the abundance of ammonia oxidizing bacteria vs. archaea in sandy sediments of the Douro River estuary, Portugal. *Aquat. Microb. Ecol.*, Vol. 56, pp.13–23.
- Manz, W., Amann, R., Ludwig, W., Wagner, M. and Schleifer, K.H. (1992), Phylogenetic oligodeoxynucleotide probes for the major subclasses of Proteobacteria: problems and solutions. *Syst. Appl. Microbiol.* Vol.15, pp. 593 - 600.
- Martens-Habbena, W., Berube, P.M., Urakawa, H., de la Torre, J.R., Stahl, D.A. (2009), Ammonia oxidation kinetics determine niche separation of nitrifying Archaea and Bacteria, *Nature*, vol. 461, pp.976–979.
- Michotey, V., Mejean, V. and Bonin P (2000), Comparison of methods for quantification of cytochrome cd1-denitrifying bacteria in environmental marine samples. *Appl. Environ. Microbiol.*, vol.66, pp.1564–1571.
- Mobarry, B.K., Wagner, M., Urbain, V., Rittmann, B.E. and Stahl, D.A (1996), Phylogenetic Probes for Analyzing Abundance and Spatial Organization of Nitrifying Bacteria, *Applied and Environmental Microbiology*, Vol. 62, No. 6, pp.2156–2162.
- Mosier, A., Kroeze, C. (2000), Potential impact on the global atmospheric N<sub>2</sub>O budget of the increased nitrogen input required to meet future global food demands, Pergamon, *Chemosphere Global Change Science*, vol. 2, pp. 465-473.
- Mulder A., Graaf, A.A., Robertson, L.A. and Kuenen, J.G. (1995), Anaerobic ammonium oxidation discovered in a denitrifying fluidized bed reactor, *FEMS Microbiol Ecol.*, vol. 16, pp. 177–184.
- Muller-Karger, F., Varela, R., Thunell, R., Scranton, M., Bohrer, R., Taylor, G., Capelo, J., Astor, Y., Tappa, E., Ho, T-Y. and Walsh, J.J. (2001), Annual cycle of primary production in the Cariaco Basin: Response to upwelling and implications for vertical export. *Journal of Geophysical Research*, Vol. 106, No. C3, pp. 4527-4542.

- Niftrik, L.A., Fuerst, J.A., Damsté, J.S.S., Kuenen, J.G., Jetten, M.S.M. and Strous, M. (2004), The anammoxosome: an intracytoplasmic compartment in anammox bacteria, *El Sevier, FEMS Microbiology Letters*, vol. 233, pp. 7–13.
- Norton, J.M., Alzerreca, J.J., Suwa, Y. and Klotz, M.G. (2002), Diversity of ammonia monooxygenase operon in autotrophic ammonia-oxidizing bacteria. *Arch Microbiol.*, vol. 177, pp.139–149.
- Paerl, H.W. and Pinckney, J.L. (1996), A mini-Review of microbial consortia: their roles in aquatic production and biogeochemical cycling. *Microb. Ecol.*, vol.31, pp. 225-247.
- Pernthaler, A., Pernthaler, J. and Amann, R. (2002), Fluorescence In Situ Hybridization and Catalyzed Reporter Deposition for the Identification of Marine Bacteria. *Applied and Environmental Microbiology*, vol.68, no.6, pp.3094-3101.
- Pernthaler, J., Glöckner, F.O., Schönhuber, W., and Amann, R. (2001), Fluorescence in situ hybridization with rRNA-targeted oligonucleotide probes, *In J. Paul (ed.), Methods in Microbiology: Marine Microbiology*, vol. 30, Academic Press Ltd, London
- Philippot, L., Piutti, S., Martin-Laurent, F., Hallet, S., Germon, J.C. (2002), Molecular analysis of the nitrate-reducing community from unplanted and maize-planted soils. *Appl Environ Microbiol*, vol.68, pp. 6121–6128.
- Podlaska, A., Wakeham, S.G., Fanning, K.A. and Taylor, G.T. (2012), Microbial community structure and productivity in the oxygen minimum zone of the eastern tropical North Pacific. *Deep-Sea Research I*, vol.66, pp.77-89.
- Purkhold U., Pommerening-Röser, A., Juretschko, S., Schmid, M.C., Koops, H-P. and Wagner, M. (2000) Phylogeny of all recognized species of ammonia oxidizers based on comparative 16S rRNA and amoA sequence analysis: Implications for molecular diversity surveys. *Appl Environ Microbiol*. Vol. 66, pp.5368–5382.
- Quan, Z., Rhee, S-K., Zuo, J-E., Yang, Y., Bae, J-W., Park, J.R., Lee, S-T. and Park, Y-H. (2008), Diversity of ammonium-oxidizing bacteria in a granular sludge anaerobic ammonium-oxidizing (anammox) reactor, *Environmental Microbiology*, vol.10, no.11, pp.3130-3139.
- Richards, F. A., and R. F. Vaccaro (1956), The Cariaco Trench, an anaerobic basin in the Caribbean Sea, *Deep Sea Res.*, vol.3, pp. 214–228.
- Richards, F.A., Cline, J.D., Broenkow, W.W., Atkinson, L.P. (1965), Some Consequences of the Decomposition of Organic Matter in Lake Nitinat, an Anoxic Fjord, *Limnology and Oceanography*, Vol. 10, Supplement: Alfred C. Redfield 75<sup>th</sup> Anniversary Volume, pp. 185-201.

- Richards, F.A. (1975), Cariaco Basin (Trench), *Oceanography and Marine Biology Annual Reviews*, vol. 13, pp.11-67.
- Rotthauwe, J.H., Witzel, K.P. and Liesack, W. (1997) The ammonia monooxygenase structural gene *amoA* as a functional marker: Molecular fine-scale analysis of natural ammonia-oxidizing populations. *Appl Environ Microbiol*, vol.63, pp.4704–4712.
- Rysgaard, S., Glud, R.N., Risgaard-Petersen, N. and Dalsgaard, T. (2004), Denitrification and Anammox activity in Arctic marine sediments, *Limnol. Oceanogr.*, vol.49, no.5, pp. 1493-1502.
- Santoro, A.E., Francis, C.A., de Sieyes, N.R. and Boehm, A.B. (2008), Shifts in the relative abundance of ammonia-oxidizing bacteria and archaea across physicochemical gradients in a subterranean estuary, *Environmental Microbiology*, vol.10, no.4, pp.1068-1079.
- Santoro, A.E., Casciotti, K.L. and Francis, C.A. (2010), Activity, abundance and diversity of nitrifying archaea and bacteria in the central California Current, *Environmental Microbiology*, vol.12, no.7, pp.1989-2006.
- Santoro, A.E., Buchwald, C., McIlvin, M.R., and Casciotti, K.L. (2011), Isotopic signature of N<sub>2</sub>O produced by marine ammonia-oxidizing archaea. *Science*, vol. 333, pp.1282–1285.
- Schmid, M., Walsh, K., Webb, R., Rijpstra, I.C.W., Schonen van de pas K., Verbruggen, J.M., Hill, T., Moffet, B., Fuerst, J., Schouten, S., Damstè, S.S.J., Harris, J., Shaw P., Jetten, M. and Strous, M. (2003), Two new species of anaerobic ammonium-oxidizing bacteria. *Syst. Appl. Microbiol.*, vol. 26, pp. 529–538.
- Schmid, M.C., Maas, B., Dapena, A., van de Pas-Schoonen, K., van de Vossenberg, J., Kartal, B., van Niftrik, L., Schmidt, I., Cirpus, I., Kuenen, J.G., Wagner, M. Damstè, J.S.S., Kuypers, M., Revsbech, N.P., Mendez, R., Jetten, M.S.M. and Strous, M. (2005), Biomarkers for the in situ detection of anaerobic ammonium oxidizing (anammox) bacteria, *Appl Environ Microbiol.*, vol. 71, pp. 1677–1684.
- Schmid, M.C. Risgaard-Petersen, N., van de Vossenberg, J., Kuypers, M.M.M., Lavik, G., Petersen, J., Hulth, S., Thamdrup, B., Canfield, D., Dalsgaard, T., Rysgaard, S., Sejr, M.K. and Strous, M. (2007), Anaerobic ammonium-oxidizing bacteria in marine environments: widespread occurrence but low diversity, *Environ Microbiol.*, vol.9, pp. 1476–1484.
- Schouten, S., Hopmans, E.C., Baas, M., Boumann, H., Standfest, S., Könneke, M., Stahl, D.A. and Damstè, J.S.S. (2008), Intact Membrane Lipids of “*Candidatus Nitrosopumilus maritimus*” a Cultivated Representative of the Cosmopolitan

- Mesophilic Group I Crenarchaeota, *Applied and Environmental Microbiology*, vol. 74, no. 8, pp. 2433-2440.
- Scranton, M.I. (1988), Temporal variations in the methane content of the Cariaco Trench. *Deep-Sea Research*, Vol. 35, no.9, pp. 1511-1523.
- Scranton, M.I., Astor, Y., Bohrer, R., Ho, T-Y. and Muller-Karger, F. (2001), Controls on temporal variability of the geochemistry of the deep Cariaco Basin. *Deep-Sea Research I*, vol. 48, pp. 1605-1625.
- Stevens, H. and Ulloa, O. (2008), Bacterial diversity in the oxygen minimum zone of the eastern tropical South Pacific, *Environmental Microbiology*, vol.10, no.5, pp.1244-1259.
- Strous, M., Fuerst, J.A., Kramer, E.H.M., Logemann, S., Muyzer, G., van de Pas-Schoonen, K.T., Webb, R., Kuenen, J.G. and Jetten, M.S.M. (1999), Missing lithotroph identified as new planctomycete. *Nature*, vol.400, pp. 446–449.
- Strous, M., Pelletier, E., Mangenot, S., Rattei, T., Lehner, A., Taylor, M.W., Horn, M., Daims, H., Bartol-Mavel, D., Wincker, P., Barbe, V., Fonknechten, N., Vallenet, D., Segurens, B., Schenowitz-Truong, C., Médigue, C., Collingro, A., Snel, B., Dutilh, B.E., Op den Camp, H.J.M., van der Drift, C., Cirpus, I., van de Pas-Schoonen, K.T., Harhangi, H.R., van Niftrik, L., Schmid, M., Keltjens, J., van de Vossenberg, J., Kartal, B., Meier, H., Frishman, D., Huynen, M.A., Mewes, H-W., Weissenbach, J., Jetten, M.S.M., Wagner, M. and Le Paslier, D. (2006), Deciphering the evolution and metabolism of an Anammox bacterium from a community genome, *Nature*, vol. 440, pp.790–794.
- Taylor, G.T., Iabichella, M., Ho, T-Y, Scranton, M.I., Thunell, R.C., Muller-Karger, F. and Varela, R.. (2001), Chemoautotrophy in the redox transition zone of the Cariaco Basin: A significant midwater source of organic carbon production, *Limnol. Oceanogr.*, vol. 46, no.1, pp.148-163.
- Teira, E., Reinthaler, T., Pernthaler, A., Pernthaler, J. and Herndl, G.J. (2004), Combining Catalyzed Reporter Deposition-Fluorescence In Situ Hybridization and Microautoradiography To Detect Substrate Utilization by Bacteria and Archaea in the Deep Ocean, *Applied and Environmental Microbiology*, Vol. 70, pp. 4411–4414.
- Thomas, W.H. (1970), On Nitrogen Deficiency in Tropical Pacific Oceanic Phytoplankton: Photosynthetic Parameters in Poor and Rich Water. *Limnology and Oceanography*, Vol. 15, No. 3, pp. 380-385.
- Tuttle, J.H. and Jannasch, H.W. (1973), Sulfide- and thiosulfate-oxidizing bacteria in anoxic marine basins. *Mar. Biol.* Vol.20, pp.64–70.
- Tuttle, J.H. and Jannasch, H.W. (1977), Microbial dark assimilation of CO<sub>2</sub> in the Cariaco Trench. *Limnol. Oceanogr.*, vol. 24, pp.746–753.



- Wagner, M., Amann, R., Kampfer, P., Assmus, B., Hartmann, A., Hutzler, P., Springer, N. and Schleifer, K-H (1994), Identification and *in situ* Detection of Gram-negative Filamentous Bacteria in Activated Sludge. System. Appl. Microbiol. Vol 17, pp. 405-417.
- Wakeham, S.G., Turich, C., Schubotz, F., Podlaska, A., Li, X.N., Varela, R., Astor, Y., Sáenz, J.P., Rush, D., Damsté, J.S.S., Summons, R.E., Scranton, M.I., Taylor, G.T. and Hinrichs, K-U. (2012), Biomarkers, chemistry and microbiology show chemoautotrophy in a multilayer chemocline in the Cariaco Basin. Deep Sea Research, vol. 63, pp. 133–156.
- Waksman, S.A., Hotchkiss, M. and Carey, C.L. (1933), Marine bacteria and their role in the cycle of life in the sea II Bacteria concerned in the cycle of nitrogen in the sea. Biological Bulletin, vol.: 65, Issue: 2, pp.: 137-167
- Walker, C.B., de la Torre, C.B., Klotz, M.G., Urakawa, H., Pinel, N., Arp, D.J., Brochier-Armanet, C., Chain, P.S.G., Chan, P.P., Gollabgir, A., Hemp, J., Hügler, M., Karr, E.A., Könneke, M., Shin, M., Lawton, T.J., Lowe, T., Martens-Habbena, W., Sayavedra-Soto, L.A., Lang, D., Sievert, S.M., Rosenzweig, A.C., Manning, G. and Stahl, D.A.. (2010), *Nitrosopumilus maritimus* genome reveals unique mechanisms for nitrification and autotrophy in globally distributed marine crenarchaea, , PNAS, vol. 107 no.19, pp. 8818-8823.
- Walsh, J.J. (1996), Nitrogen fixation within a tropical upwelling ecosystem: Evidence for a Redfield budget of carbon/nitrogen cycling by the total phytoplankton community, Journal of Geophysical Research, vol. 101, No. C9, pp. 20,607-20,616.
- Walsh, J.J., Dieterie, D.A., Müller-Karger, F., Bohrer, R., Bissett, W.P., Varela, R.J., Aparicio, R., Diaz, R., Thunell, R., Taylor, G.T., Scranton, M.I., Fanning, K.A., and Peltzer, E.T. (1999), Simulation of carbon-nitrogen cycling during spring upwelling in the Cariaco Basin, Journal of Geophysical Research, vol. 104, No. C4, pp. 7807-7825.
- Ward, B.B. (1996), Nitrification and Denitrification: Probing the Nitrogen Cycle in Aquatic Environments. Microbial Ecology, vol. 32, pp.: 247-261.
- Wright, J.J., Konwar, K.M. and Hallam, S.J. (2012), Microbial ecology of expanding oxygen minimum zones. Nature Reviews, Microbiology, Volume 10, pp. 381-394.
- Wuchter, C., Abbas, B., Coolen, M.J.L., Herfort, L., van Bleijswijk, J., Timmers, P., Strous, M., Teira, E., Herndl, G.J., Middelburg, J.J., Schouten, S. and Damste, J.S.S. (2006), Archaeal nitrification in the ocean. PNAS, vol.103, no.33, pp.12317–12322.

Zehnder, A.J. and Stumm, W. (1988), *Biology of Anaerobic Microorganisms*. Ed. Zehnder, A. J. pp. 1–38. Wiley & Sons.

Zhang, Y., Ruan, X., Op den Camp, H.J.M., Smits, T.J.M., Jetten, M.S.M. and Schmid, M.C. (2007), Diversity and abundance of aerobic and anaerobic ammonium-oxidizing bacteria in freshwater sediments of the Xinyi River (China), *Environmental Microbiology*, vol. 9, no.9, pp.2375-2382.

## Appendix I: Figures

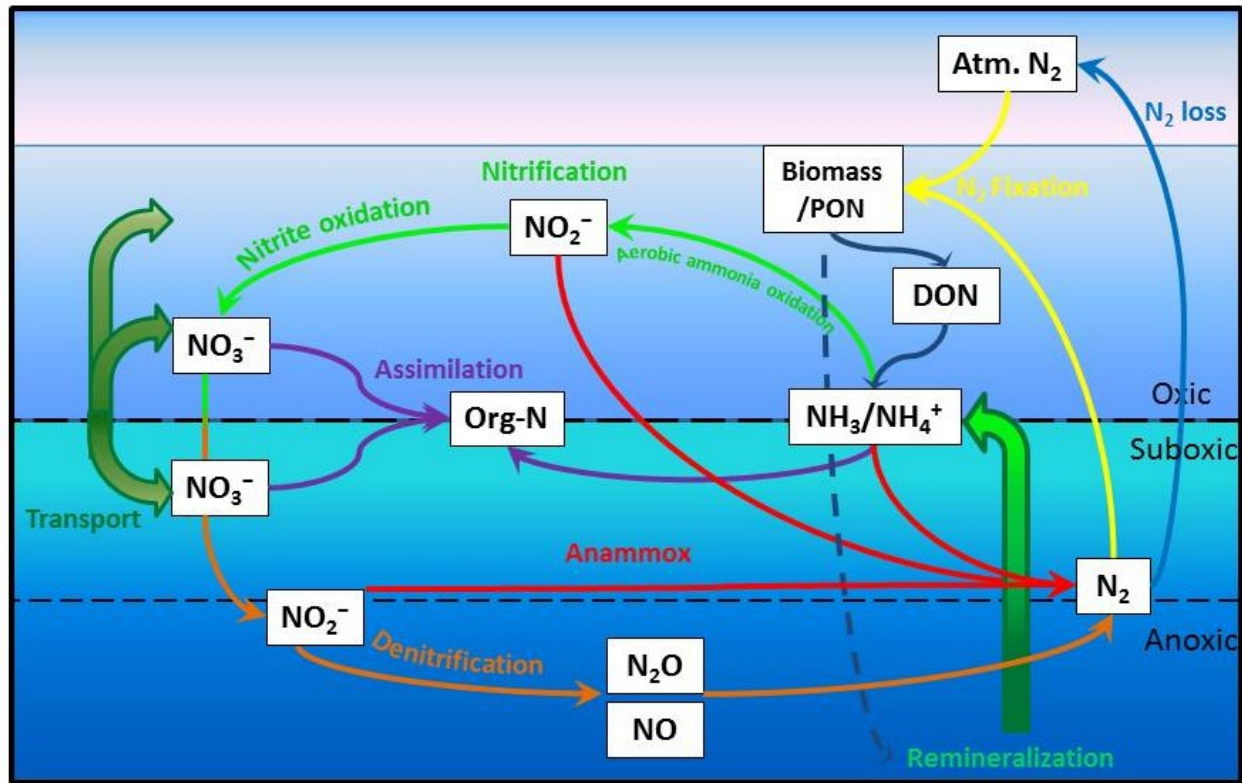


**Figure 1** Simplified nitrogen cycle. Main processes and the nutrients involved within the oxic, suboxic and anoxic zone are represented. Atmospheric Nitrogen becomes fixed into biomass (PON) by nitrogen fixers like cyanobacteria. Through predation, excretion, fecal pellets and decaying biomass this PON becomes DON and is mineralized to ammonia in the suboxic zone. Part of the PON reaches the bottom, where it becomes remineralized and transported upward. Ammonium can be directly assimilated, be aerobically oxidized as part of the nitrification process or be anaerobically oxidized by anammox bacteria. Nitrite in the oxic zone is rapidly oxidized to nitrate as the final step of the nitrification process. This nitrate, once in the suboxic zone becomes reduced back to nitrite and eventually to Nitrogen gas as part of the denitrification process. Nitrogen gas can be fixed again in surface waters or lost to the atmosphere.

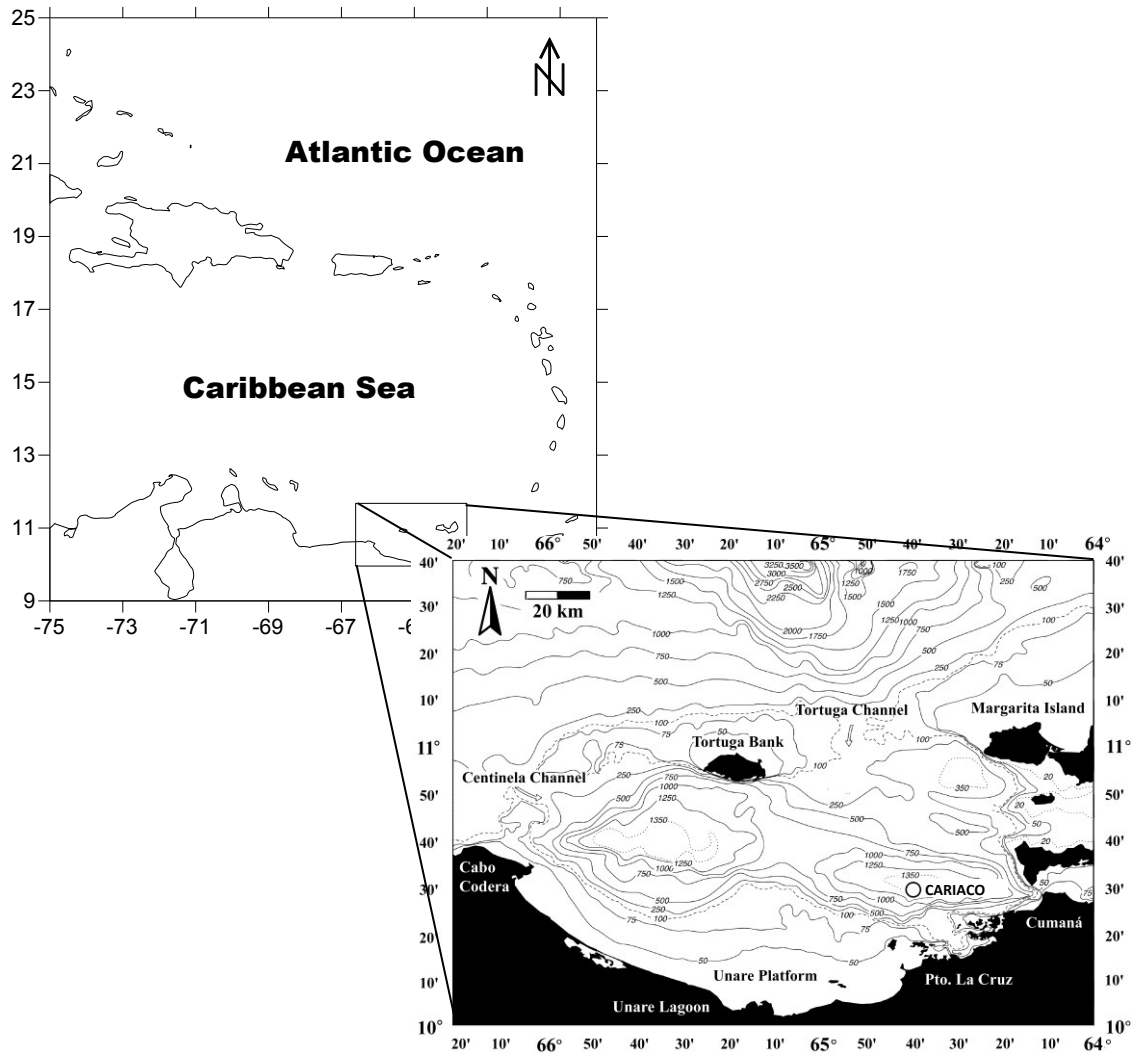


**Figure 2** Map locating the Cariaco Basin and the sampling station. Courtesy of the CARIACO Project.



**Figure 3** On board manifold set-up for filtration of DNA samples minimizing oxygen contamination. The compounder bags were filled directly from the Niskin bottles and attached to the filter holders with minimum contact with oxygen.

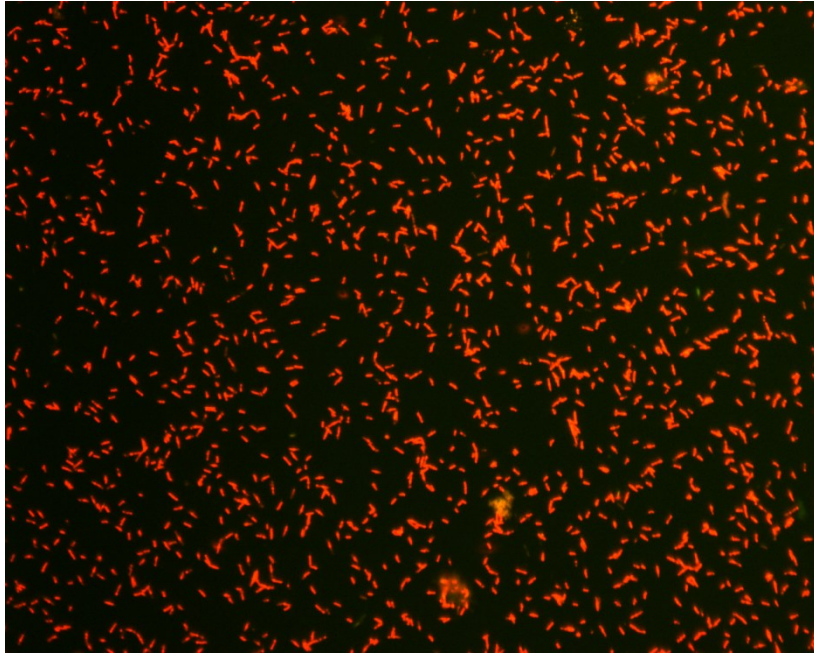


**Figure 4** Photomicrograph of *Nitrosopumilus maritimus* cells stained with Acridine Orange observed under the epifluorescent microscope. Image captured with a MagnaFire® Digital Camera System (Optronics) and processed with the IPPWIN Image Pro Plus Version 7.0 (Media Cybernetics) for color resolution improvement.

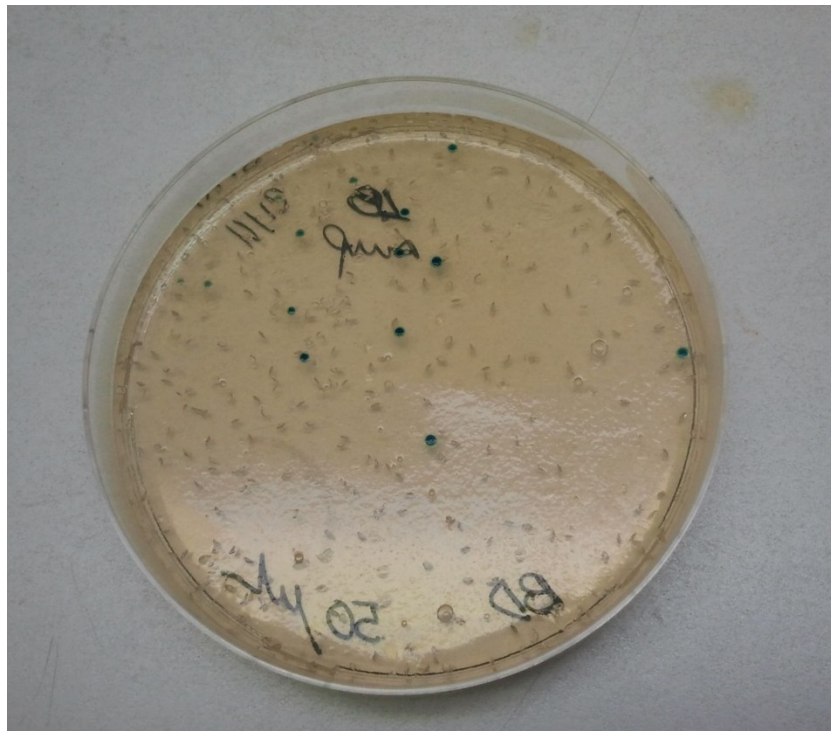


**Figure 5** *E. coli* colonies from cloning experiment after overnight incubation. Blue colonies are non-transformed cells and white colonies are the transformed cells.

## Standard Curve

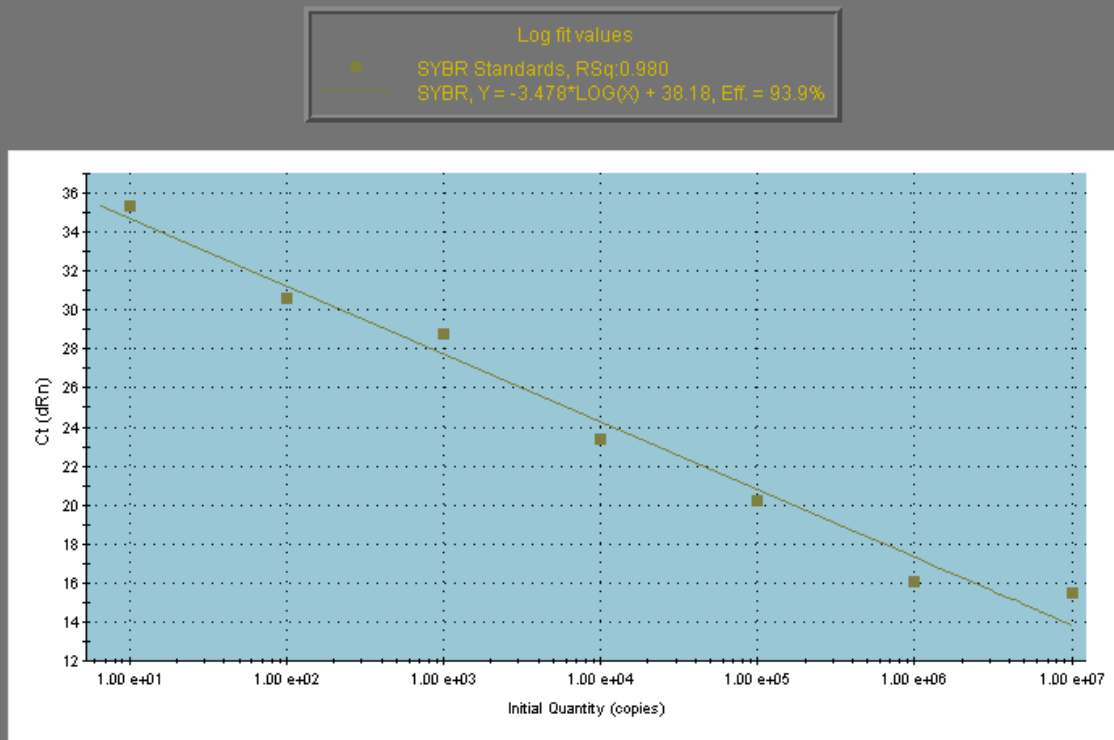


**Figure 6** Example of q-PCR Standard curve. Ten-fold dilutions of gene copies (*nirS*) from anammox bacteria, ranging from 1 to  $10^7$  copies were plotted against their Threshold cycles ( $C_t$ ) and the linear regression for this data was calculated.



## Dissociation Curve

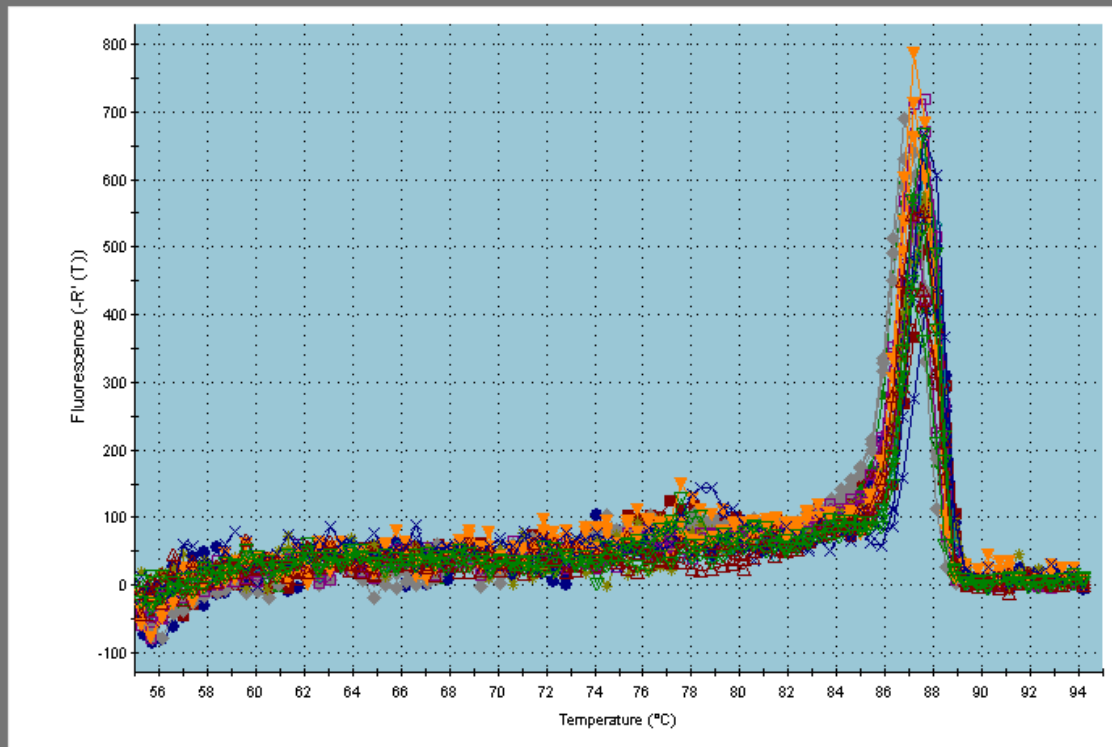


**Figure 7** Example of dissociation curve where the products of the PCR reaction went through a heating-cooling-heating cycle where the DNA products of the PCR reaction dissociate and later annealed again, the temperature at which DNA denatures reveals their the molecular weight.

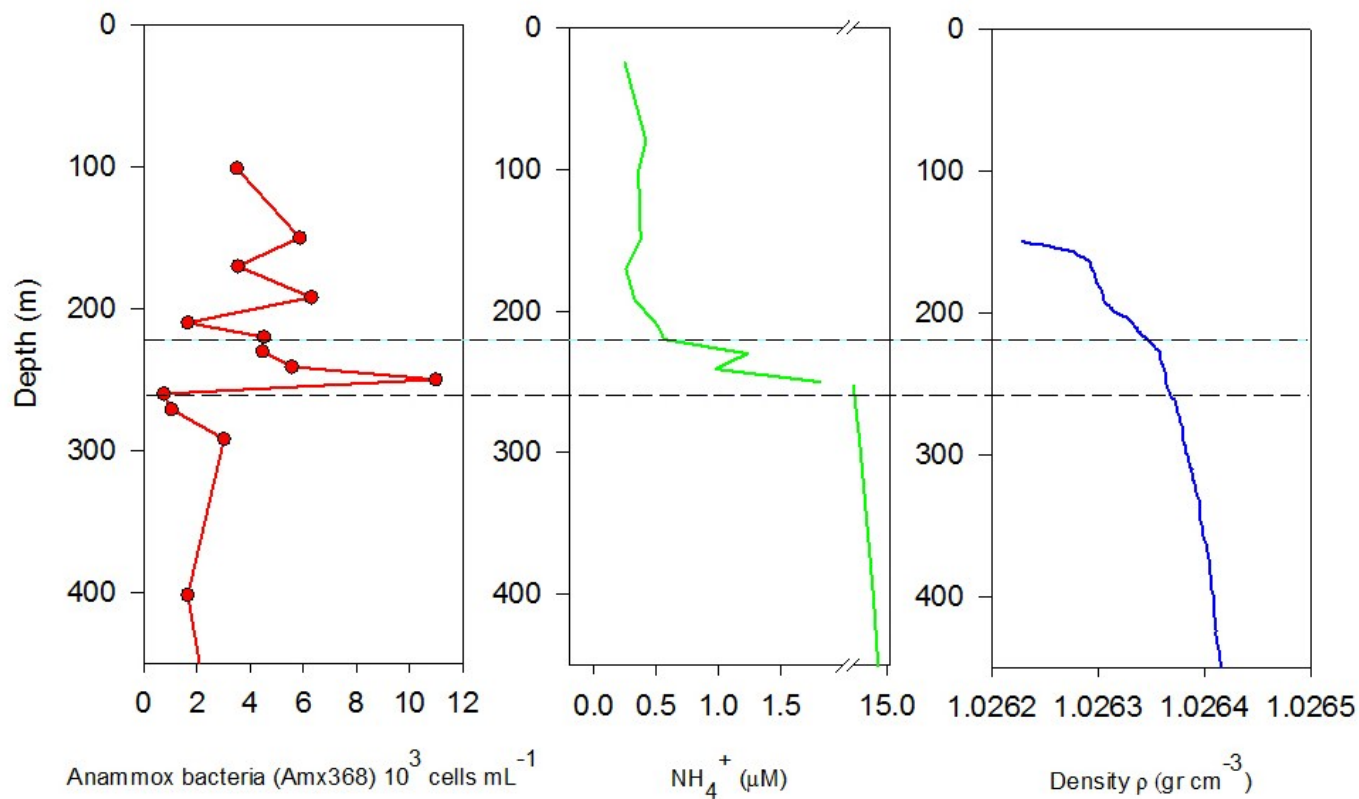


**Figure 8** Example of data used to calculate the upward vertical flux of ammonium in C-175. Dashed lines mark the depth interval used in the calculations. Nutrient gradient and density gradient were estimated from the slope of the regression line of the data points within the dashed lines.

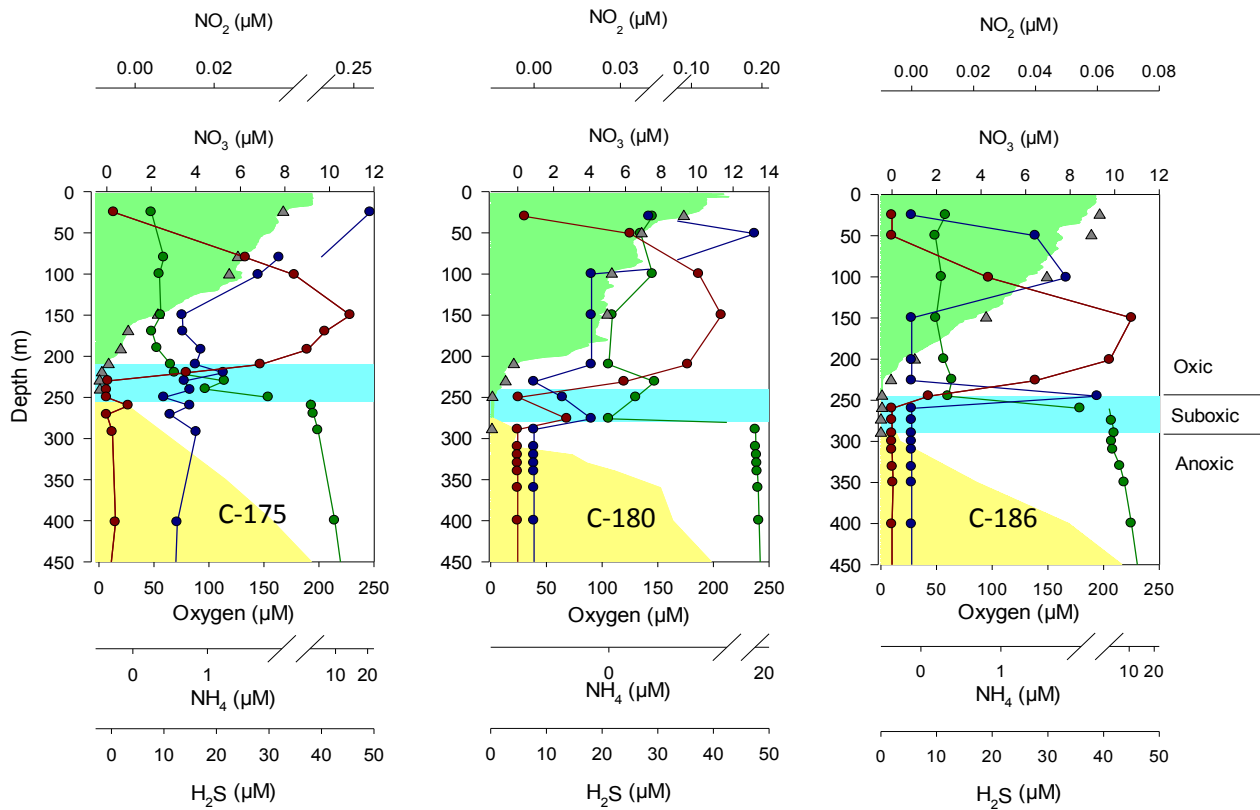


**Figure 9** Nutrient profiles for C-175, C-180 and C-186. The continuous lines represent the vertical profiles for  $\text{NH}_4^+$  concentration (●),  $\text{NO}_2^-$  concentration (●) and  $\text{NO}_3^-$  concentration (●). The green area represents the CTD profile for oxygen concentration (■) and the triangles the Oxygen measured in the lab from water samples (▲). The yellow area corresponds to  $\text{H}_2\text{S}$  concentration (■). The blue area represents the suboxic zone, separating the oxic zone from the anoxic zone (■).  $\text{NH}_4^+$ ,  $\text{NO}_2^-$  and  $\text{NO}_3^-$  data courtesy of Dr. Kent Fanning from University of South Florida.  $\text{H}_2\text{S}$  data courtesy of Lan T. Tong and Yrene Astor.

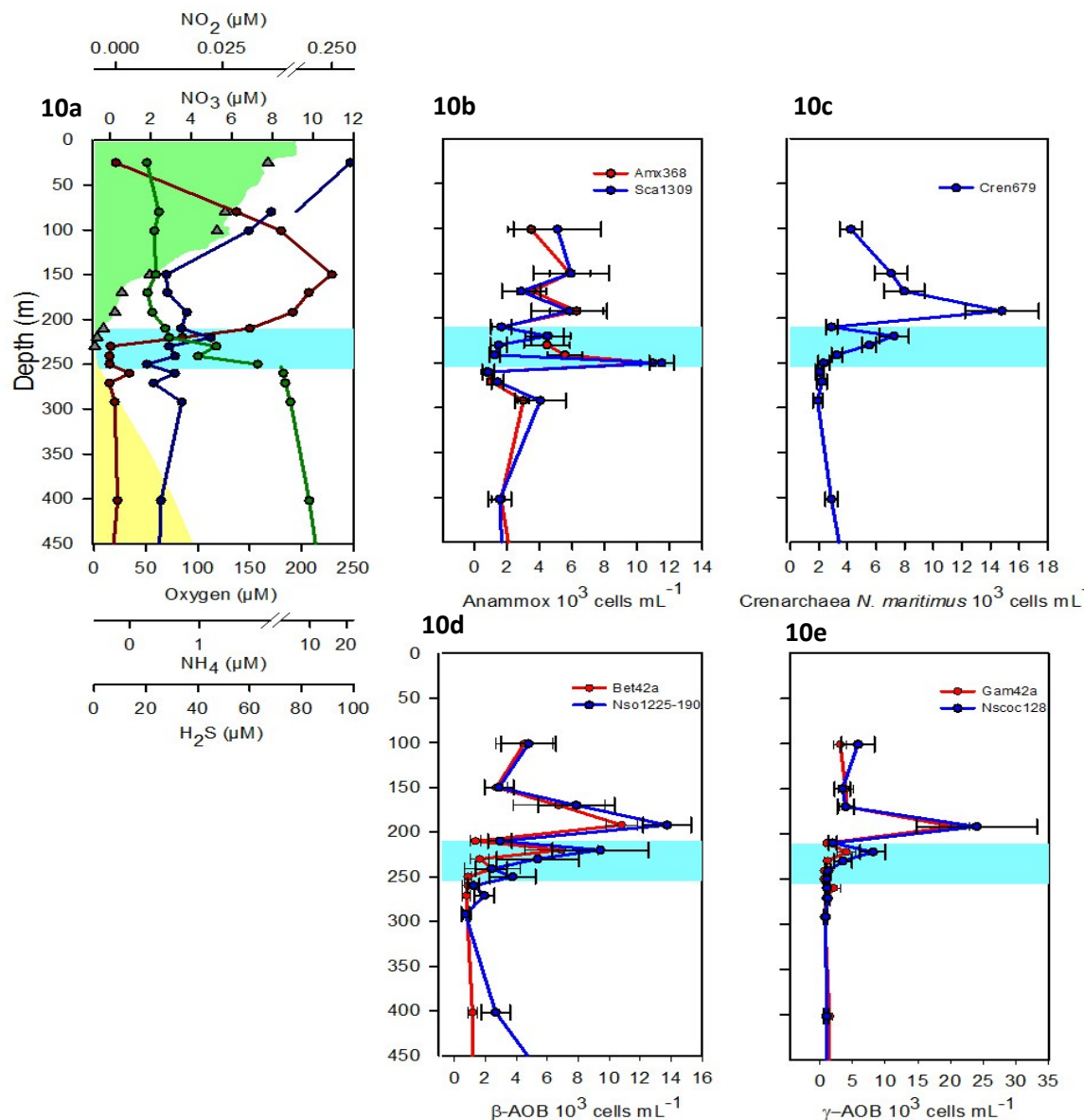


**Figure 10a** Nutrient profile C-175; the continuous lines represent the vertical profiles for  $\text{NH}_4^+$  concentration (●),  $\text{NO}_2^-$  concentration (●) and  $\text{NO}_3^-$  concentration (●). The green area represents the CTD profile for oxygen concentration (■) and the triangles the oxygen measured in the lab from water samples (▲). The yellow area corresponds to  $\text{H}_2\text{S}$  concentration (■). The blue area represents the suboxic zone, separating the oxic zone from the anoxic zone (■).

**Figure 10b** FISH depth profile for anammox bacteria (Amx368) and *Scalindua* sp. (Sca1309) positive cells.

**Figure 10c** FISH depth profile for AOA, *N. maritimus* (Cren67) positive cells.

**Figure 10d** FISH depth profile for  $\beta$ -Proteobacteria (Bet42a) and  $\beta$ -AOB (Nso1225-190) positive cells.

**Figure 10e** FISH depth profile for  $\gamma$ -Proteobacteria (Gam42a) and  $\gamma$ -AOB (Nscoc128) positive cells.

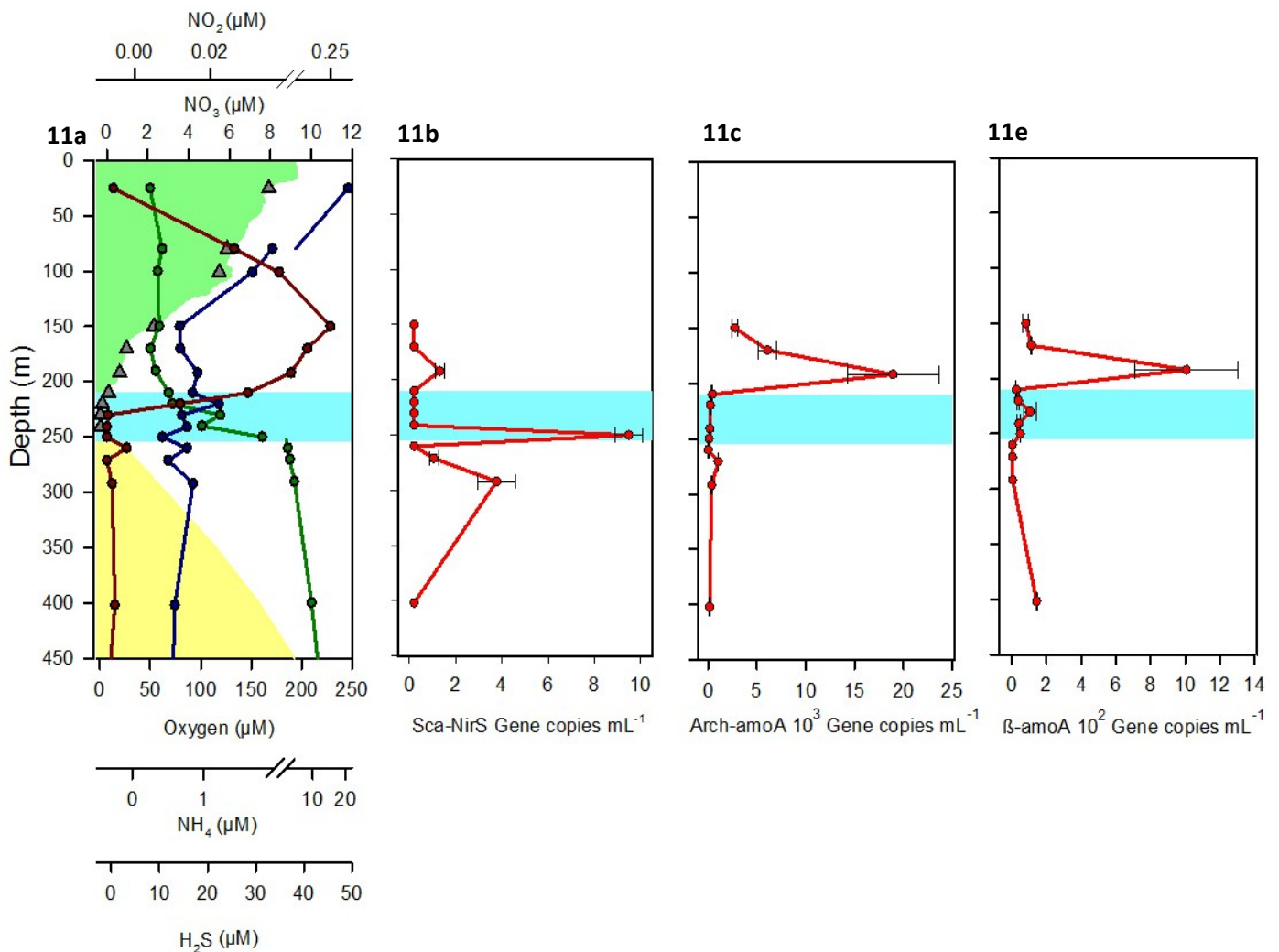


**Figure 11** Nutrient profile and DNA profiles obtained from the q-PCR analyses for C-175

**Figure 11a** Nutrient profiles for C-175. The continuous lines represent the vertical profile for  $\text{NH}_4^+$  concentration (●),  $\text{NO}_2^-$  concentration (●) and  $\text{NO}_3^-$  concentration (●). The green area represents the CTD profile for oxygen concentration (■) and the triangles the oxygen measured in the lab from water samples (▲). The yellow area corresponds to  $\text{H}_2\text{S}$  concentration (■). The blue area represents the suboxic zone, separating the oxic zone from the anoxic zone (■).

**Figure 11b** Vertical profile of gene copies per mL of the gene *nirS*, specific for anammox bacteria of the genus *Scalindua*. Two peaks are observed at 250 and 292 meters.

**Figure 11c** Vertical profile of gene copies per mL of the gene *Arch-amoA*, specific for Archaeal aerobic ammonia oxidizers. One peak is observed at 192 meters.

**Figure 11d** Vertical profile of copies per mL of the gene *amoA* specific for  $\beta$ -bacterial ammonia oxidizers. One peak is observed at 192 meters.

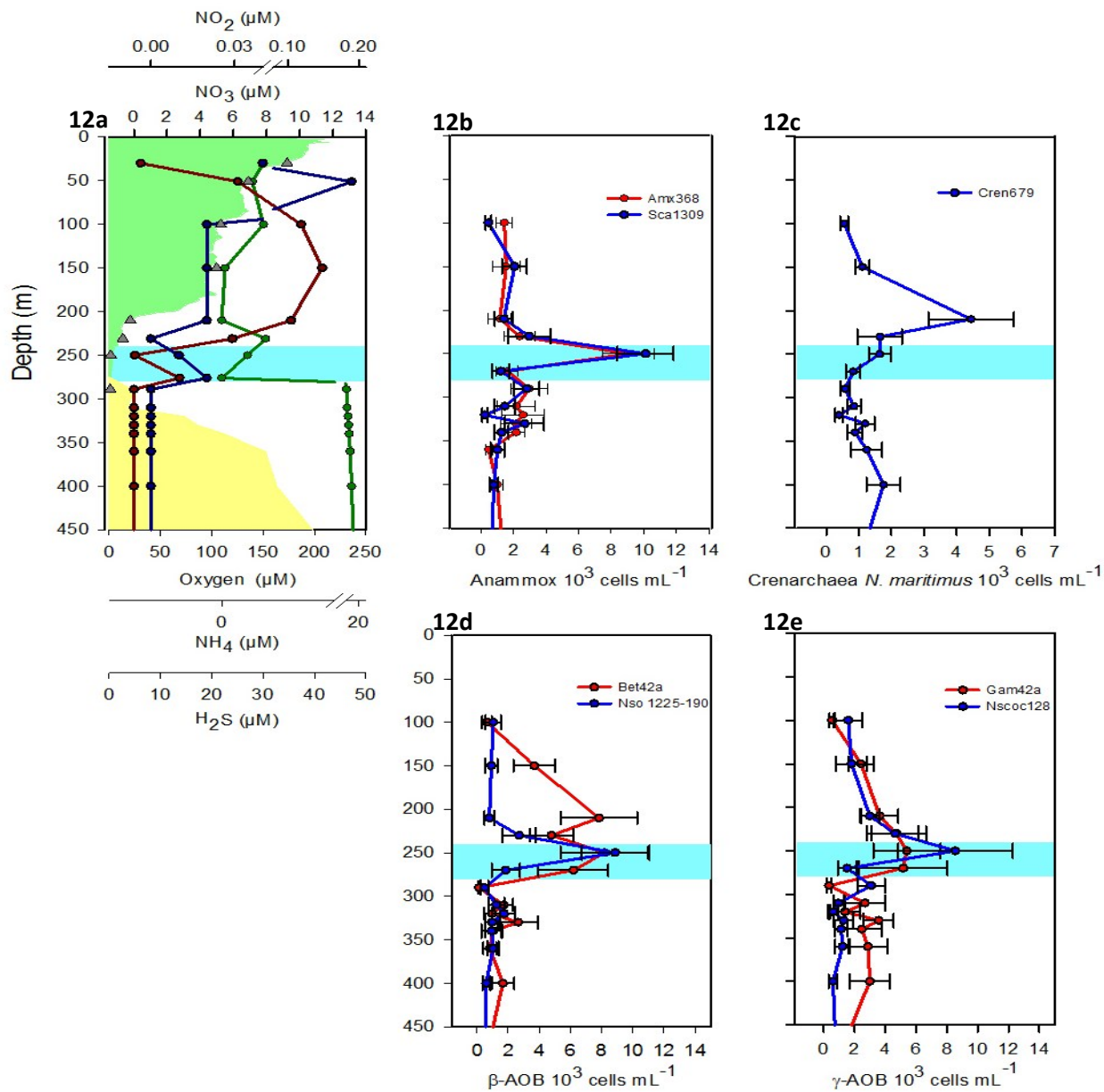


**Figure 12a** Nutrient profile C-180; the continuous lines represent the vertical profiles for  $\text{NH}_4^+$  concentration (●),  $\text{NO}_2^-$  concentration (●) and  $\text{NO}_3^-$  concentration (●). The green area represents the CTD profile for oxygen concentration (■) and the triangles the oxygen measured in the lab from water samples (▲). The yellow area corresponds to  $\text{H}_2\text{S}$  concentration (■). The blue area represents the suboxic zone, separating the oxic zone from the anoxic zone (■).

**Figure 12b** FISH depth profile for anammox bacteria (Amx368) and *Scalindua* (Sca1309)

**Figure 12c** FISH depth profile for AOA, *N. maritimus* (Cren67) positive cells.

**Figure 12d** FISH depth profile for  $\beta$ -Proteobacteria (Bet42a) and  $\beta$ -AOB (Nso1225-190) positive cells.

**Figure 12e** FISH depth profile for  $\gamma$ -Proteobacteria (Gam42a) and  $\gamma$ -AOB (Nscoc128) positive cells.



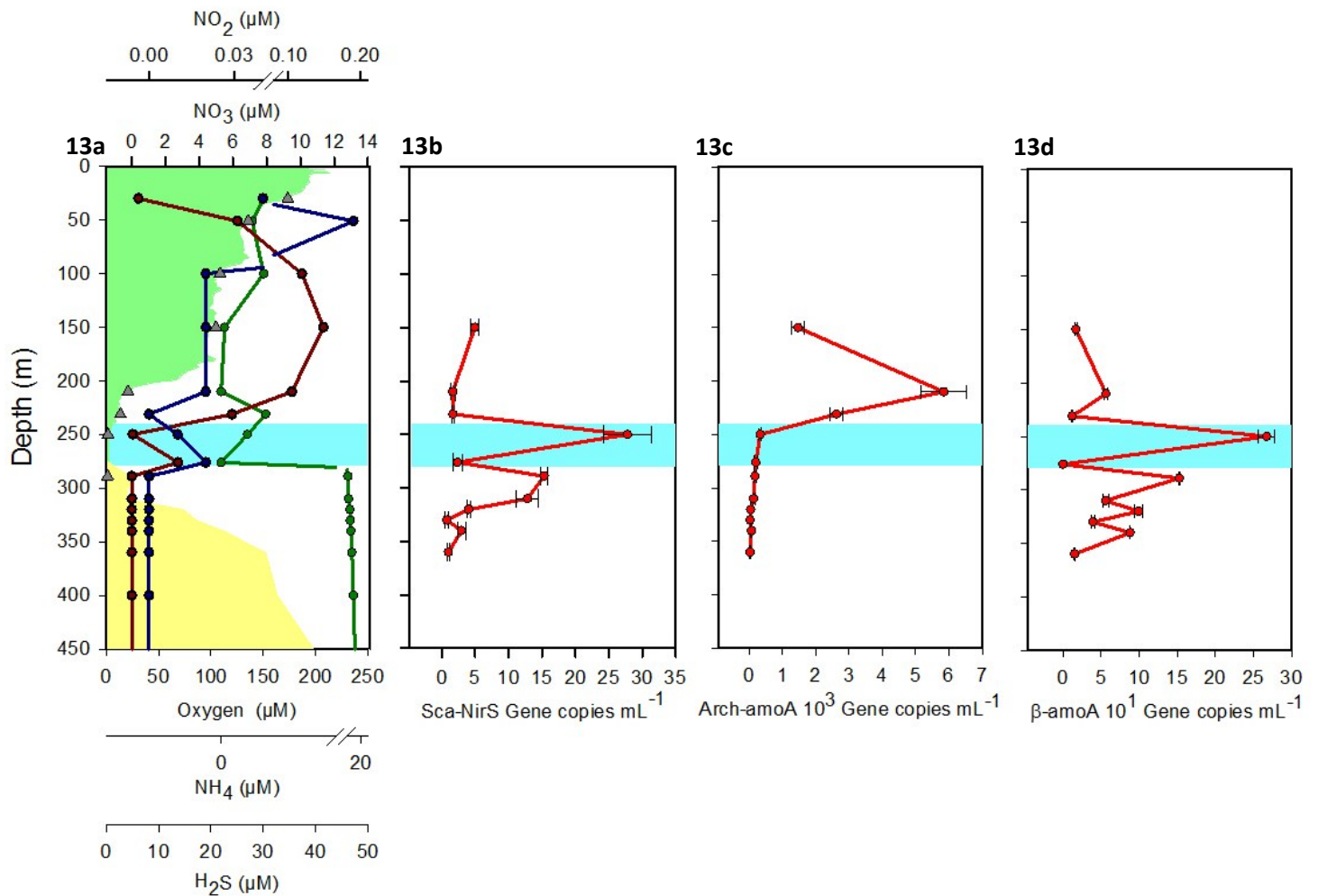


**Figure 13** Nutrient and DNA profiles obtained from the q-PCR analyses for C-180;

**Figure 13a** Nutrient profile; the continuous lines represent the vertical profiles for  $\text{NH}_4^+$  concentration (●),  $\text{NO}_2^-$  concentration (●) and  $\text{NO}_3^-$  concentration (●). The green area represents the CTD profile for oxygen concentration (■) and the triangles the oxygen measured in the lab from water samples (▲). The yellow area corresponds to  $\text{H}_2\text{S}$  concentration (■). The blue area represents the suboxic zone, separating the oxic zone from the anoxic zone (■).

**Figure 13b** Vertical profile of gene copies per mL of the gene *nirS*, specific for anammox bacteria of the genus *Scalindua*. Two peaks are observed at 250 and 289 meters.

**Figure 13c** Vertical profile of gene copies per mL of the gene *Arch-amoA*, specific for Archaeal aerobic ammonia oxidizers. One peak is observed at 210 meters.

**Figure 13d** Vertical profile of gene copies per mL of the gene *amoA* specific for  $\beta$ -bacterial ammonia oxidizers. One peak is observed at 250 meters.

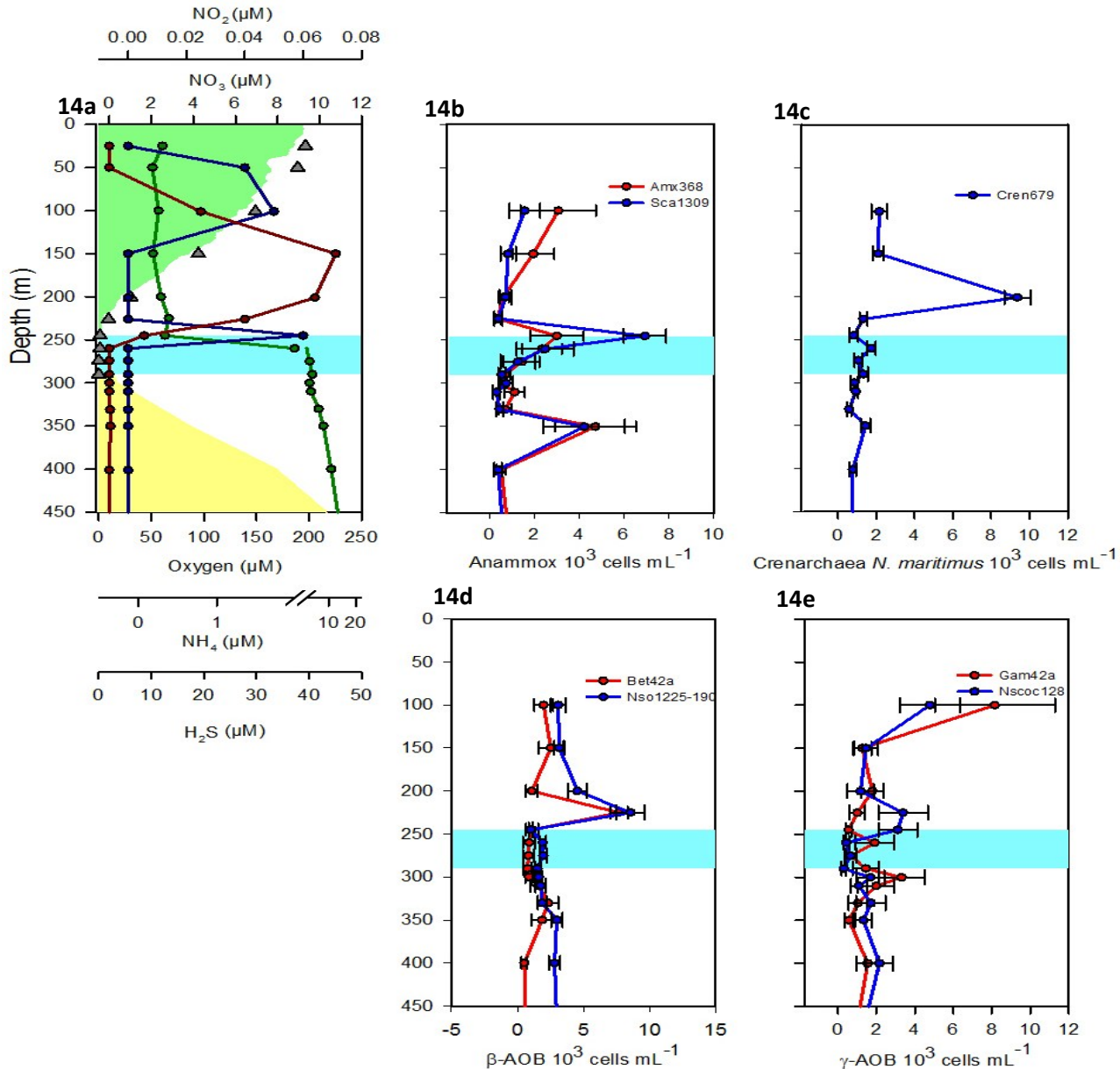


**Figure 14a** Nutrient profile C-186; the continuous lines represent the vertical profiles for  $\text{NH}_4^+$  concentration (●),  $\text{NO}_2^-$  concentration (●) and  $\text{NO}_3^-$  concentration (●). The green area represents the CTD profile for oxygen concentration (■) and the triangles the oxygen measured in the lab from water samples (▲). The yellow area corresponds to  $\text{H}_2\text{S}$  concentration (■). The blue area represents the suboxic zone, separating the oxic zone from the anoxic zone (■).

**Figure 14b** FISH depth profile for anammox bacteria (*Amx368*) and *Scalindua* (*Sca1309*) positive cells.

**Figure 14c** FISH depth profile for AOA, *N. maritimus* (*Cren67*) positive cells.

**Figure 14d** FISH depth profile for  $\beta$ -Proteobacteria (*Bet42a*) and  $\beta$ -AOB (*Nso1225-190*) positive cells.

**Figure 14e** FISH depth profile for  $\gamma$ -Proteobacteria (*Gam42a*) and  $\gamma$ -AOB (*Nscoc128*) positive cells.



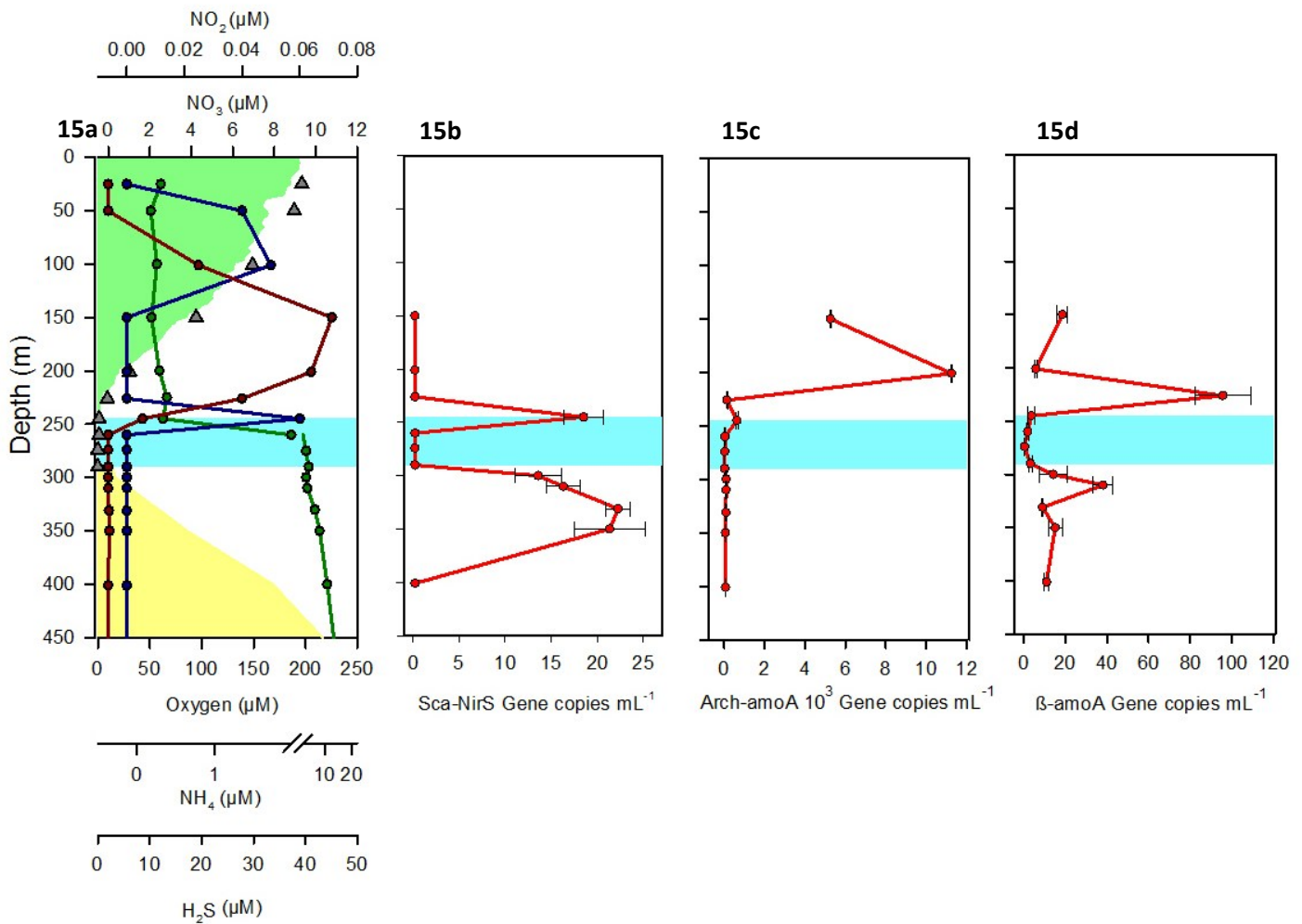


**Figure 15** Nutrient and DNA profiles obtained from the q-PCR analyses for C-186; **Figure 15a** Nutrient profile; the continuous lines represent the vertical profiles for  $\text{NH}_4^+$  concentration (●),  $\text{NO}_2^-$  concentration (●) and  $\text{NO}_3^-$  concentration (●). The green area represents the CTD profile for oxygen concentration (■) and the triangles the oxygen measured in the lab from water samples (▲). The yellow area corresponds to  $\text{H}_2\text{S}$  concentration (■). The blue area represents the suboxic zone, separating the oxic zone from the anoxic zone (■).

**Figure 15b** Vertical profile of gene copies per mL of the gene *nirS*, specific for anammox bacteria of the genus *Scalindua*. Two peaks are observed at 245 and 330 meters.

**Figure 15c** Vertical profile of gene copies per mL of the gene *Arch-amoA*, specific for Archaeal aerobic ammonia oxidizers. One peak is observed at 201 meters.

**Figure 15d** Vertical profile of gene copies per mL of the gene *amoA* specific for  $\beta$ -bacterial ammonia oxidizers. One major peak is observed at 226 meters.

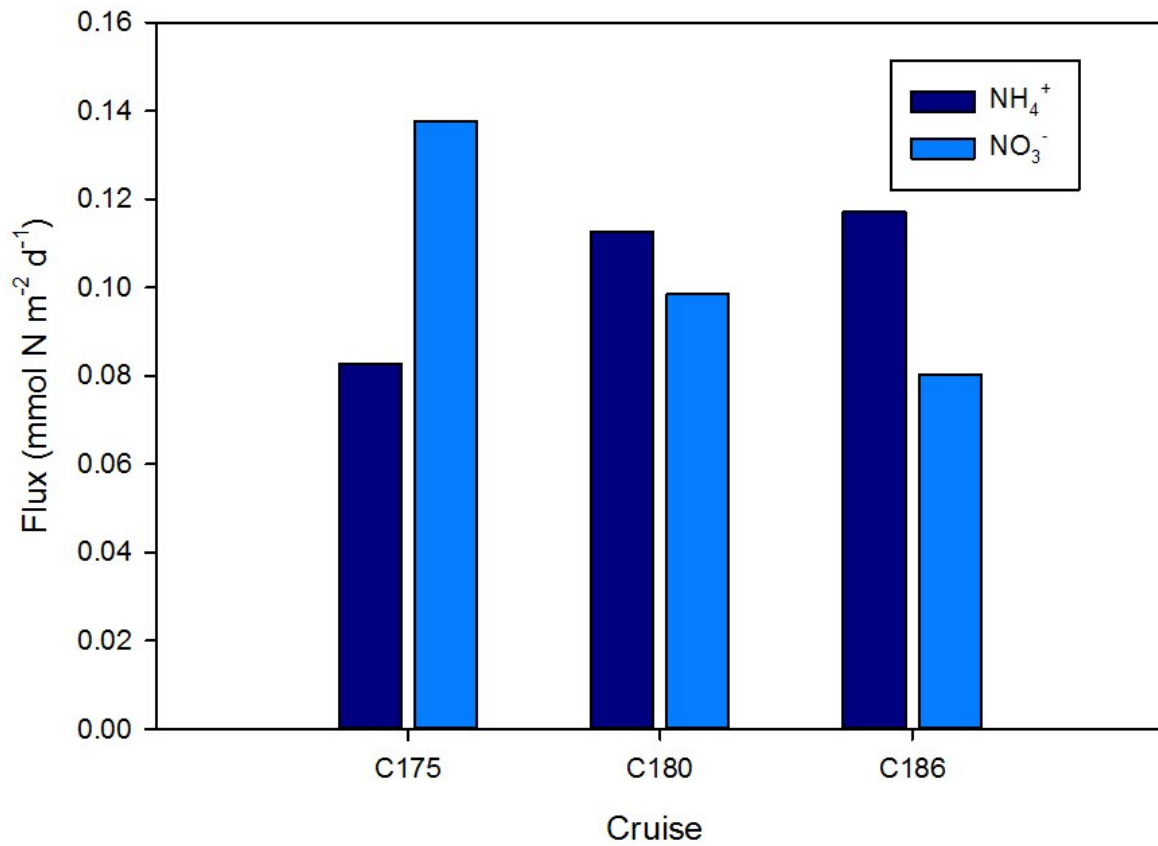


**Figure 16** Upward flux of ammonium to the suboxic zone and downward flux of nitrate to the suboxic zone for the three cruises studied, where cruise to cruise variations can be observed.

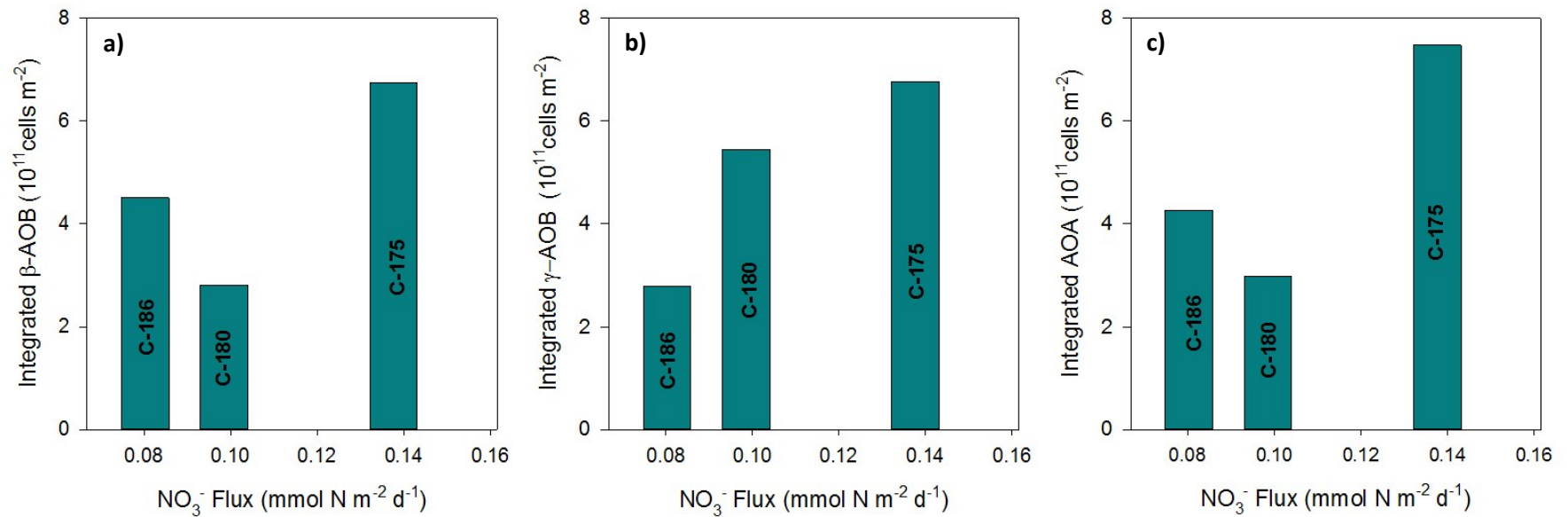


**Figure 17** Inventories of  $\beta$ -ammonia oxidizers (a),  $\gamma$ -ammonia oxidizers (b) and Archaeal ammonia oxidizers and (c) compared to downward flux of nitrate from the lower oxic zone to the suboxic zone the, where higher bacterial concentrations coincide with higher nitrate fluxes.

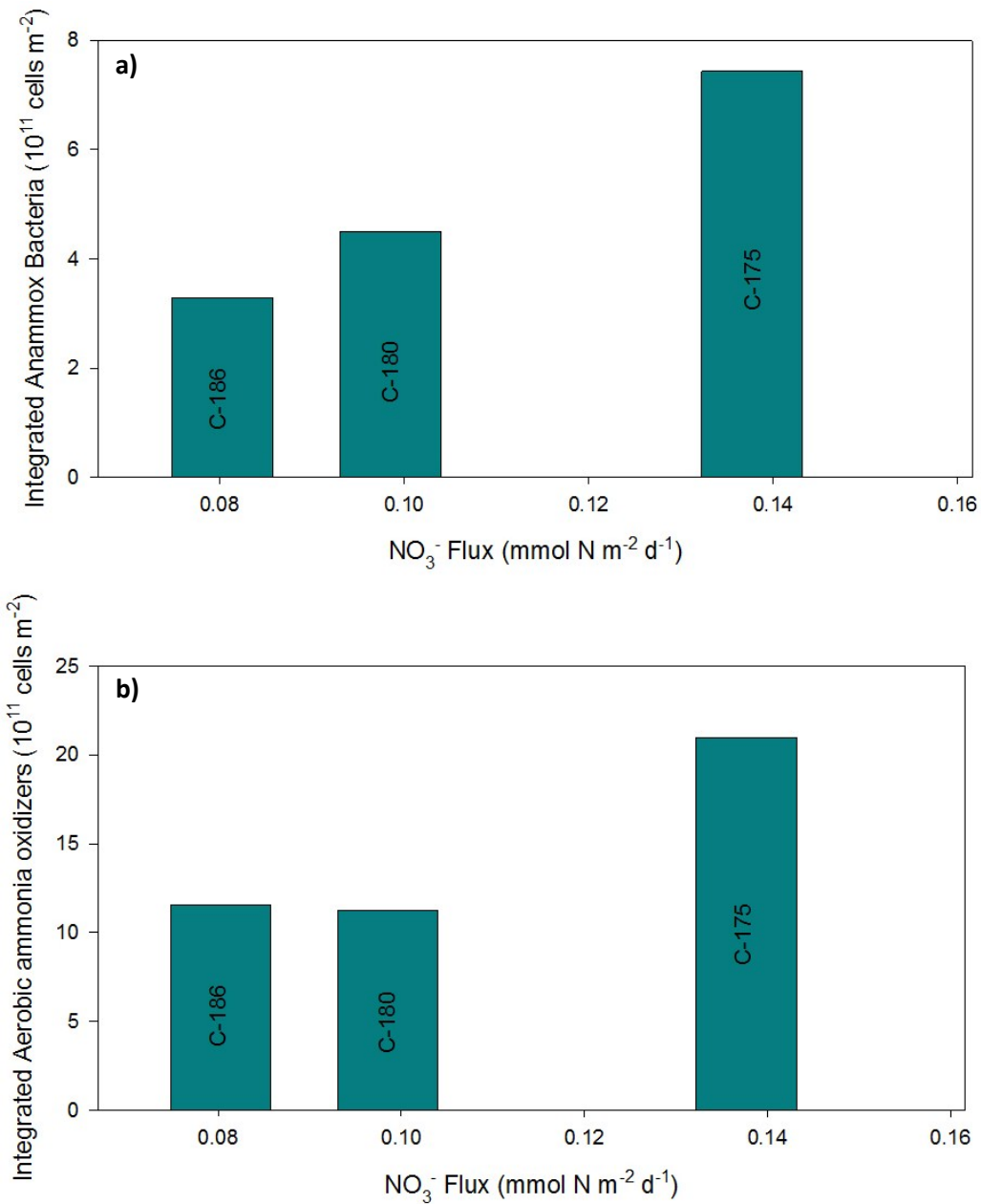


**Figure 18** Inventories of anammox bacteria (a) and Total aerobic ammonia oxidizers (b) compared to downward flux of nitrate from the lower oxic zone to the suboxic zone, where higher bacterial concentrations coincide with higher nitrate fluxes.

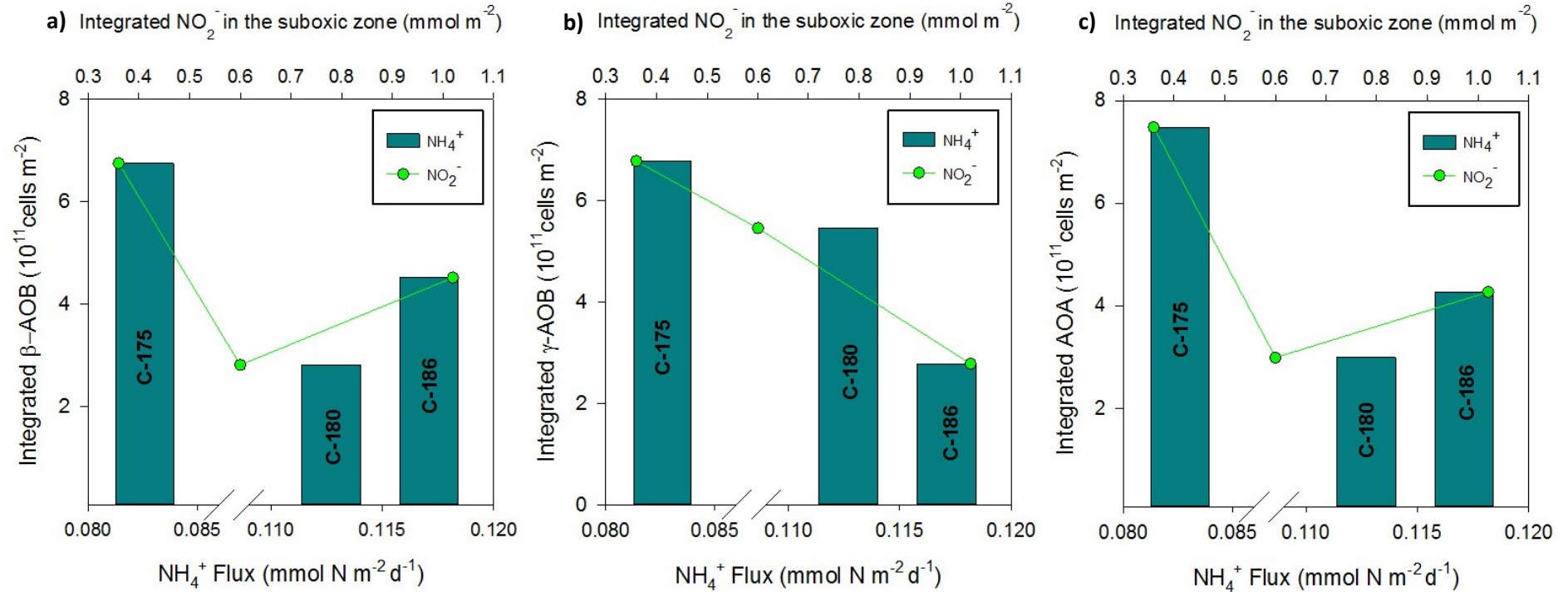


**Figure 19** Inventories of  $\beta$ -ammonia oxidizers (a),  $\gamma$ -ammonia oxidizers (b) and Archaeal ammonia oxidizers (c) compared to upward flux of ammonium from the anoxic zone to the suboxic zone and integrated nitrite, where higher bacterial concentrations coincide with lower ammonium fluxes and, in the case of  $\gamma$ -AOB, also with lower nitrite inventories.

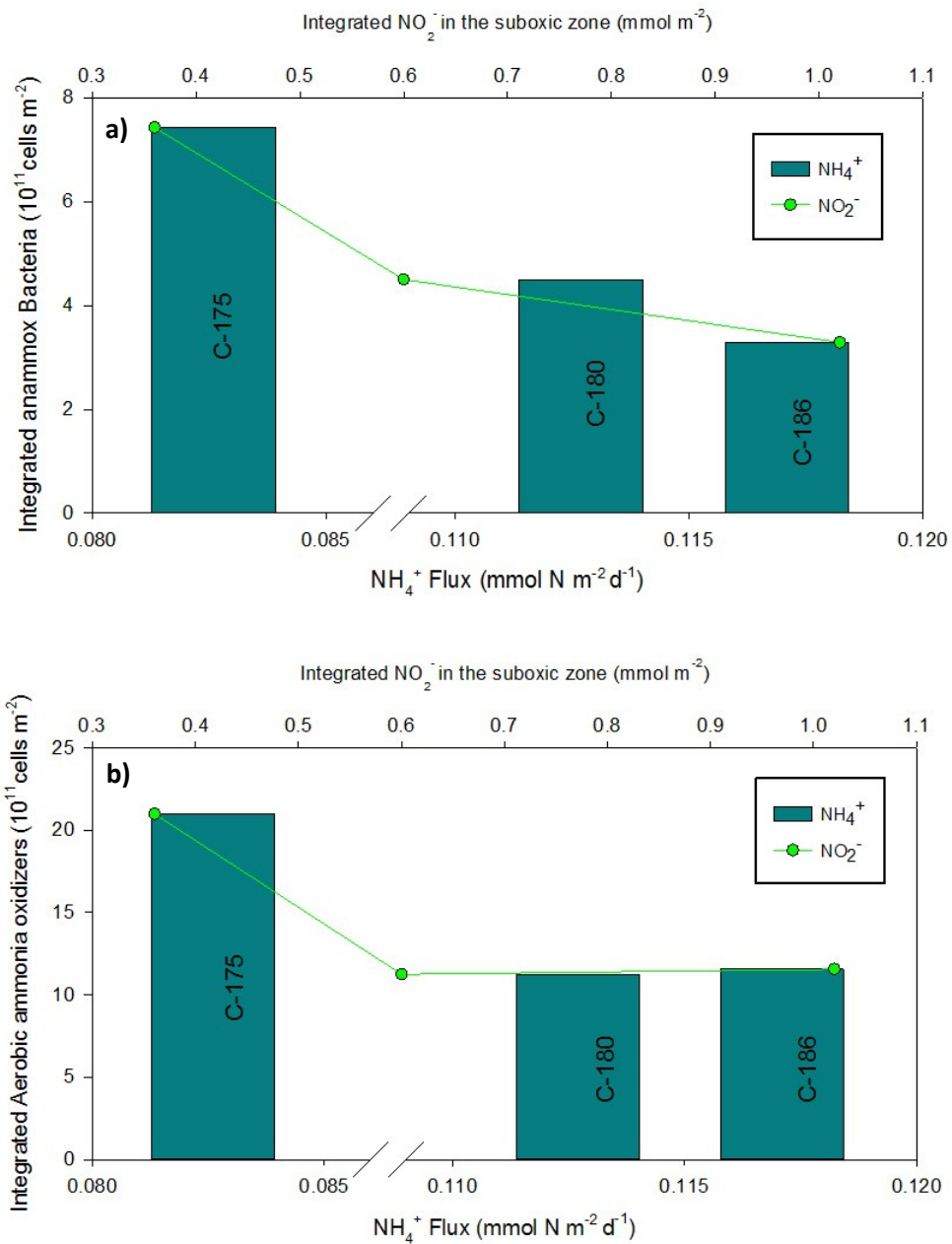


**Figure 20** Inventories of anammox bacteria (a) and total aerobic ammonia oxidizers (b) compared to integrated nitrite and upward flux of ammonium from the anoxic zone to the suboxic zone and where higher bacterial concentrations coincide with lower ammonium fluxes and lower nitrite inventories.

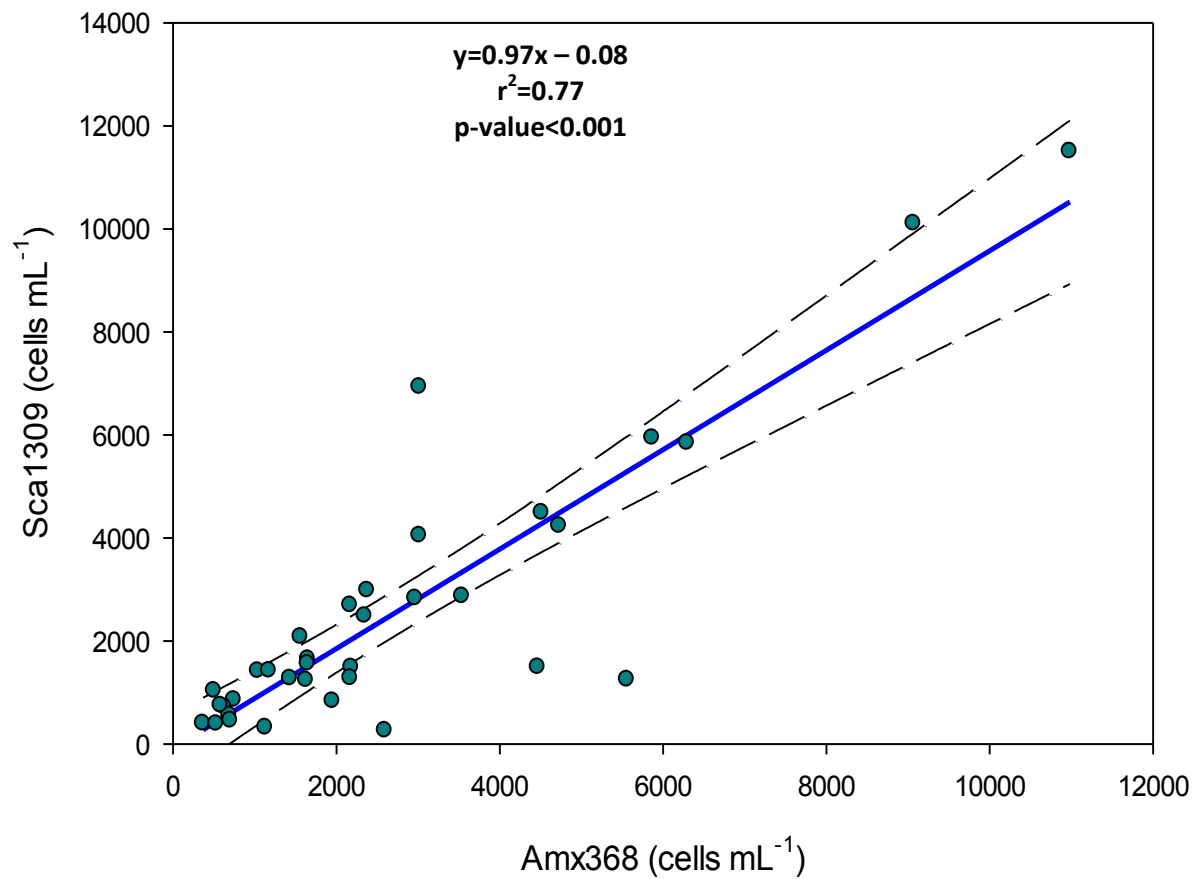


**Figure 21** Comparison of FISH data for anammox bacteria from the g. *Scalindua* (Sca1309) and all known anammox bacteria (Amx368) for all cruises. There is a significant linear relation where 77% of the variance in the Sca1309 probe-positive cells is explained by variance in Amx368 abundances. Dashed lines represent 95% confidence interval.

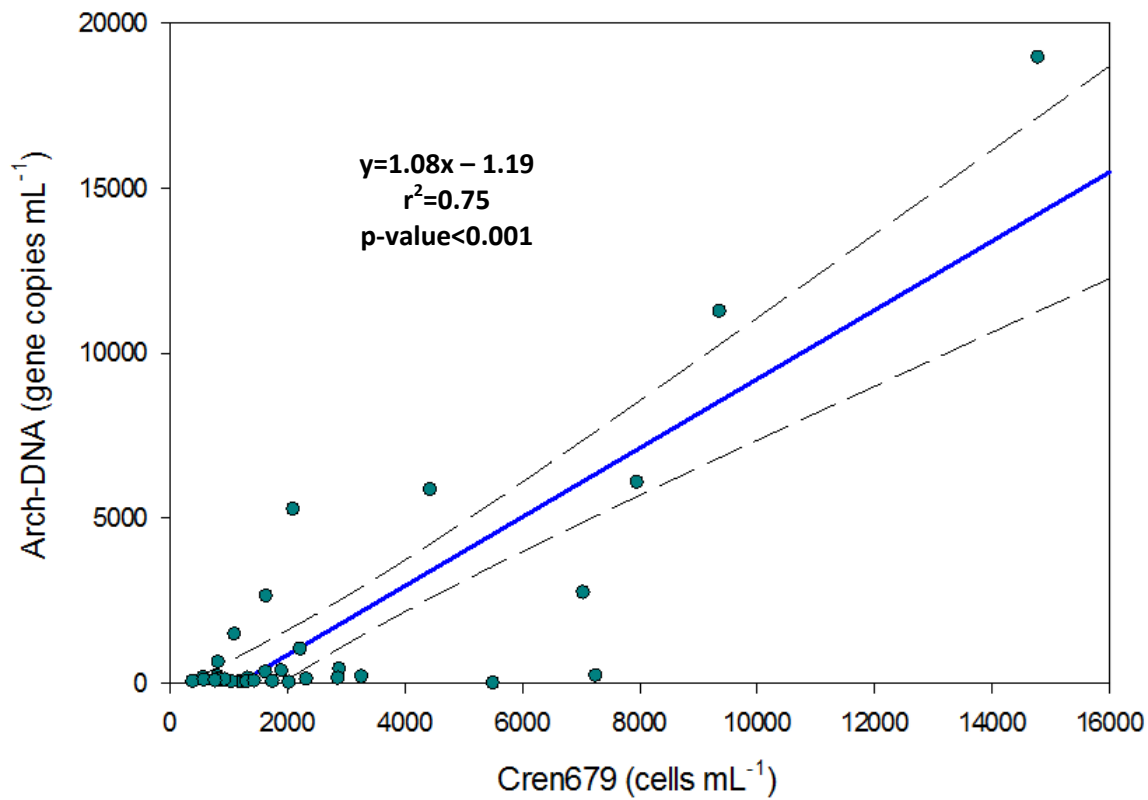


**Figure 22** Comparison of the q-PCR DNA data for archaeal ammonia-oxidizing bacteria to FISH data for Crenarchaeal *N. maritimus* (Cren679) for all cruises. There is a significant linear relation where 75% of the variance in the q-PCR profile is explained by variance in Cren679 abundances. Dashed lines represent 95% confidence interval.



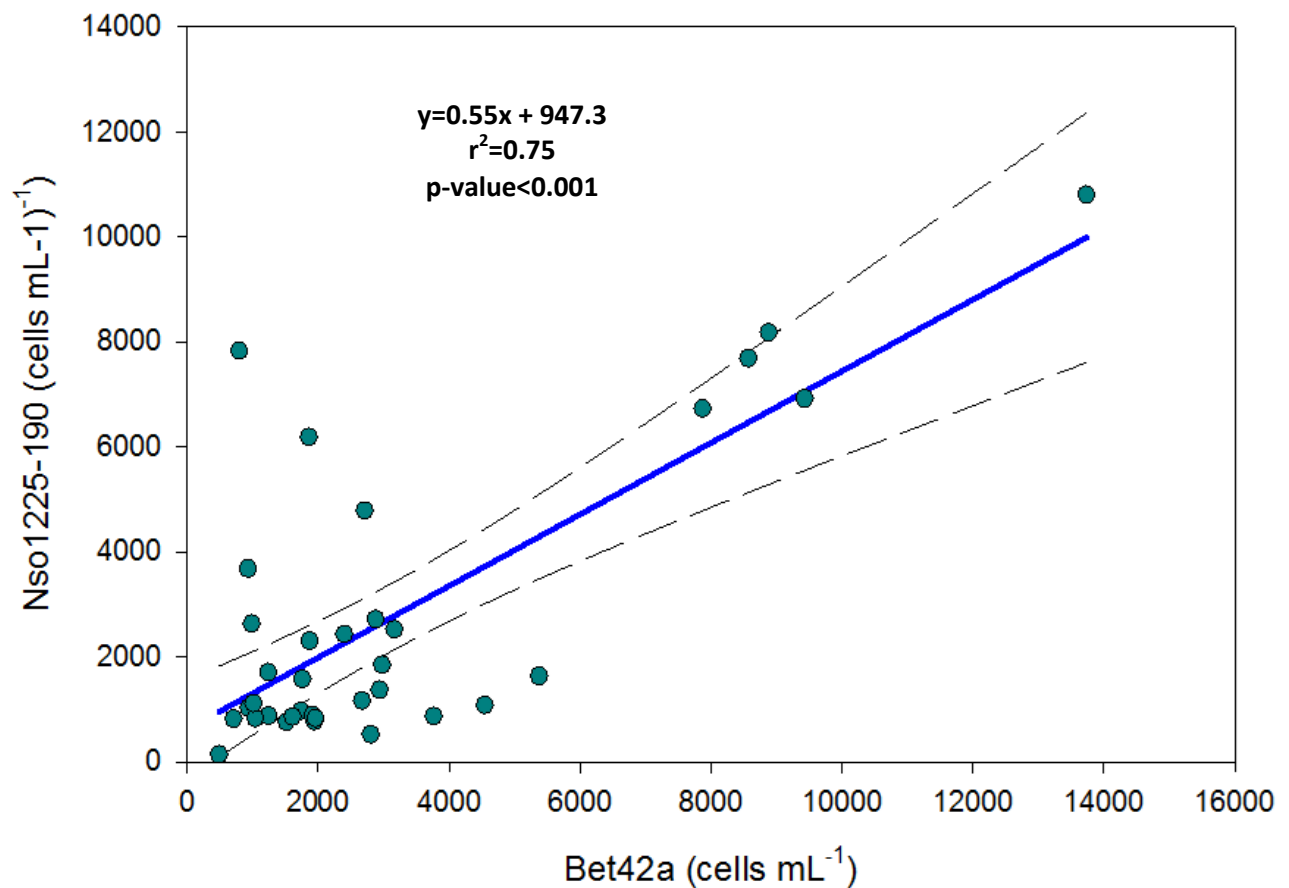


**Figure 23** Comparison of FISH data for  $\beta$ -ammonia-oxidizing bacteria (Nso1225-190) and all  $\beta$ -Proteobacteria (Bet42a) for all cruises. There is a significant linear relation where 75% of the variance in the Nso1225-190 probe-positive cells is explained by variance in Bet42a abundances. Dashed lines represent 95% confidence interval.

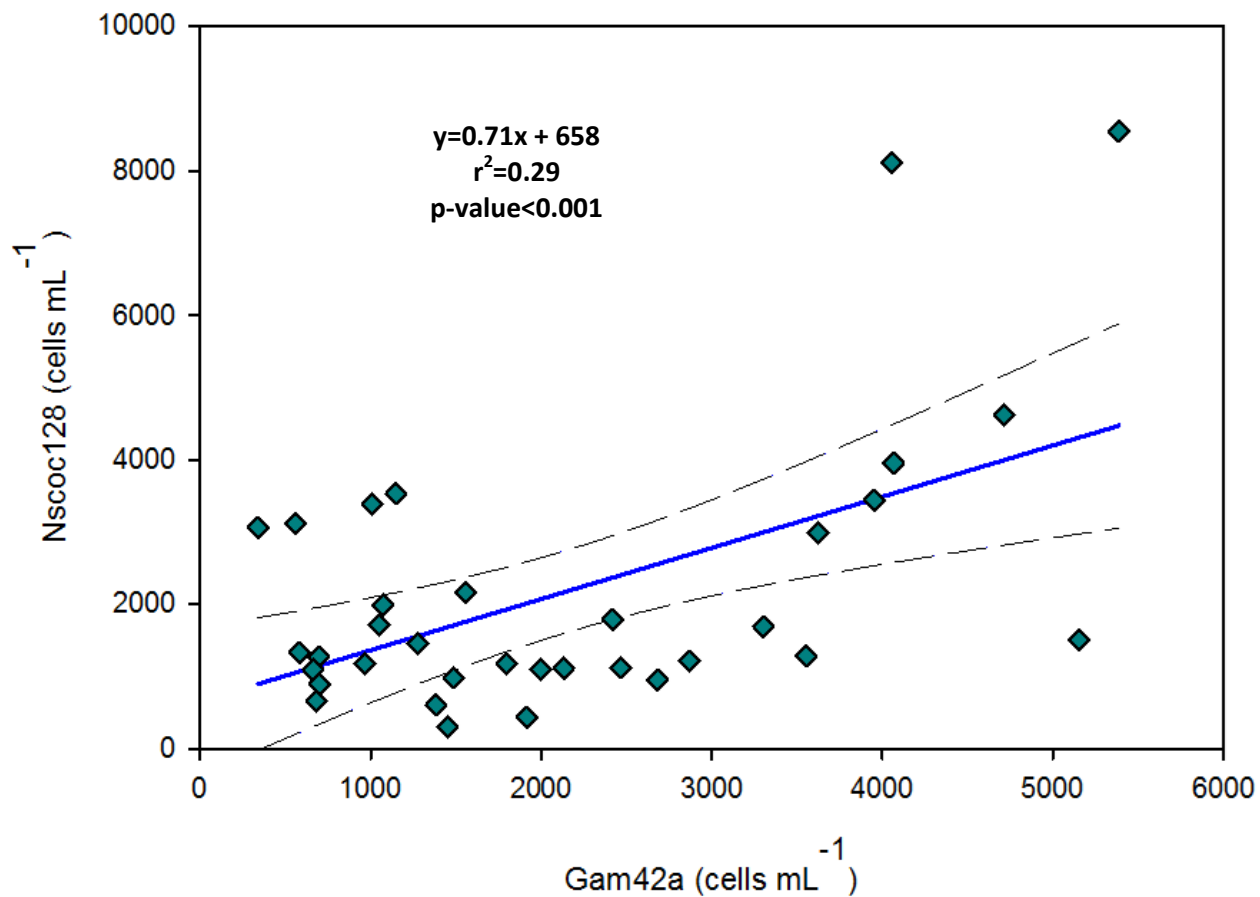


**Figure 24** Comparison of FISH data for  $\gamma$ -ammonia-oxidizing bacteria (Nscoc128) and all  $\gamma$ -Proteobacteria (Gam42a) for all cruises. There is a significant linear relation but only 29% of the variance in the Nscoc128 probe-positive cells is represented by variance in Gam42a abundances. Dashed lines represent 95% confidence interval.

## Appendix II: Tables

Specificity	Name	Sequence 5'-3'	Formamide	Reference
All anammox bacteria	Amx368 <sup>a</sup>	CCT-TTC-GGG-CAT-TGC-GAA	15%	Schmid, M., Walsh, K., Webb, R., Rijpstra, I.C.W., Schonen van de pas K., Verbruggen, J.M., Hill, T., Moffet, B., Fuerst, J., Schouten, S., Damstè, S.S.J., Harris, J., Shaw P., Jetten, M. and Strous, M., 2003.
Genus <i>Scalindua</i>	Sca1309 <sup>a</sup>	TGG-AGG-CGA-ATT-TCA-GCC-TCC	5%	
$\beta$ -Proteobacteria	Bet42a <sup>a</sup>	GCC-TTC-CCA-CTT-CGT-TT	35%	Manz, W., Amann, R., Ludwig, W., Wagner, M. and Schleifer, K.H., 1992.
$\beta$ -Proteobacterial ammonia-oxidizing bacteria	Nso190 <sup>ac</sup>	CGATCCCCTGCTTTTCTCC	55%	Mobarry, B.K., Wagner, M., Urbain, V., Rittmann, B.E. and Stahl, D.A, 1996.
	Nso1225 <sup>ac</sup>	CGCGATTGTATTACGTGTGA	35%	
$\gamma$ -Proteobacteria	Gam42a <sup>a</sup>	GCC-TTC-CCA-CAT-CGT-TT	35%	Manz, W., Amann, R., Ludwig, W., Wagner, M. and Schleifer, K.H., 1992.
<i><math>\gamma</math>-Proteobacteria Nitrosococcus oceanii, N.halophilus</i>	Nscoc128 <sup>a</sup>	CCC-CTC-TAG-AGG-CCA-GAT	35%	Juretschko, S., 2000.
Crenarchaea, <i>Nitrosopumilus maritimus</i> , MGI c.	Cren679 <sup>b</sup>	TTT-TAC-CCC-TTC-CTT-CCG	35%	Labrenz, M., Sintes, E., Toetzke, F., Zumsteg, A., Herndl, G.J., Seidler, M. and Jürgens, K., 2010.

<sup>a</sup> Probe labeled with Cy3

<sup>b</sup> Probe used in Catalyzed Reporter Deposition FISH (CARD-FISH) analysis. Labelled with Horseradish Peroxidase (HRP)

<sup>c</sup> Probes used in successive hybridization

**Table 1** Probes used for FISH analyses

Target organism	Functional gene	Primer name	Sequence (5'-3')	Tm (°C)	Reference
Anammox bacteria <i>g. Scalindua</i>	<i>nirS</i>	Scnir372F	TGTAGCCAGCATTGTAGCGT	56.8	Lam, P., Lavik, G., Jensen, M.M., van de Vossenberg, J., Schmid, M., Woebken, D., Gutiérrez, D., Amann, R., Jetten, M.S.M. and Kuypers, M.M.M. (2009), Revising the nitrogen cycle in the Peruvian oxygen minimum zone, 4752-4757, PNAS, March 24, 2009, vol. 106 no. 12.
		Scnir845R	TCAAGCCAGACCCATTTGCT	57.2	
$\beta$ -ammonia-oxidizing bacteria	<i>amoA</i>	<i>amoA1F</i>	GGGGTTTCTACTGGTGGT	54.1	Rotthauwe, J.H., Witzel, K.P. and Liesack, W. (1997) The ammonia monooxygenase structural gene <i>amoA</i> as a functional marker: Molecular fine-scale analysis of natural ammonia-oxidizing populations. Appl Environ Microbiol 63:4704–4712.
		<i>amoA2R</i>	CCCCTCKGSAAAGCCTTCTTC	59.2	
Archaeal ammonia oxidizers	<i>Arch-amoA</i>	Arch- <i>amoAF</i>	STAATGGTCTGGCTTAGACG	52.6	Francis, C.A., Roberts, K.J., Beman, J.M., Santoro, A.E. and Oakley, B.B. (2005), Ubiquity and diversity of ammonia-oxidizing archaea in water columns and sediments of the ocean, Proc. Natl Acad. Sci. USA 102, 14683–14688
		Arch- <i>amoAR</i>	GCGGCCATCCATCTGTATGT	57.5	

**Table 2** Primer sets used for the PCR and q-PCR reactions. (Tm = Melting temperature)

Target Gene	First stage – 1 cycle	Second stage – 30 cycles			Third stage- 1 cycle
	Activation	Denaturation	Annealing	Extension	Final Elongation
<i>nirS</i>	5 min – 95 °C	45 sec – 95 °C	1 min – 55 °C	1 min – 72 °C	15 min – 72 °C
<i>β-amoA</i>	4 min – 94 °C	30 sec – 94 °C	1 min – 53 °C	1 min – 72 °C	10 min – 72 °C
<i>Arch-amoA</i>	5 min – 95 °C	45 sec – 94 °C	1 min – 53 °C	1 min – 72 °C	15 min – 72 °C

**Table 3** PCR thermal profiles for each of the three functional groups studied; Anammox (*nirS*),  $\beta$ -ammonia-oxidizing bacteria ( $\beta$ -AOB) and Archaeal ammonia oxidizers (AOA).

Target	Primers (10 $\mu$ M)	Environmental DNA	Spiked DNA (10 <sup>2</sup> copies/ $\mu$ L)	SyBr Green I	Reference dye ROX	Failsafe Enzyme Mix	Failsafe Premix 2X	PCR grade H <sub>2</sub> O
Anammox	1.25 $\mu$ L	2 $\mu$ L	1 $\mu$ L	0.5 $\mu$ L	0.4 $\mu$ L	0.25 $\mu$ L	12.5 $\mu$ L <sup>a</sup>	5.85 $\mu$ L
$\beta$ -AOB	1.25 $\mu$ L	2 $\mu$ L	1 $\mu$ L	0.625 $\mu$ L	0.4 $\mu$ L	0.25 $\mu$ L	12.5 $\mu$ L <sup>a</sup>	5.73 $\mu$ L
AOA	1.25 $\mu$ L	2 $\mu$ L	1 $\mu$ L	0.5 $\mu$ L	0.4 $\mu$ L	0.25 $\mu$ L	12.5 $\mu$ L <sup>b</sup>	5.85 $\mu$ L

<sup>a</sup> Failsafe Premix 2X D

<sup>b</sup> Failsafe Premix 2x F

**Table 4** Quantitative PCR detailed reaction chemistry for the three groups of ammonia oxidizers

### Appendix III: Creating a Standard Curve with Plasmid DNA

1- For creating a standard curve from plasmid DNA, the first thing you have to know is your plasmid and inserts length in base pairs (bp). My standard curves were created from the Plasmid pCR<sup>®</sup> 2.1-TOPO<sup>®</sup> (Invitrogen<sup>™</sup> Life Technologies<sup>™</sup>) which is 3931 nucleotides long (=3.9 Kb). The inserts used for the gene ligation were the targeted functional genes for each group of Bacteria and Archaea studied plus the length of the primers used;

- Ammonia-oxidizing Archaea → Arch-amoA = 635 bp
- Anammox bacteria → nirS = 473 bp
- β-ammonia-oxidizing bacteria → 492 bp

2- Calculate the mass of the plasmid plus the insert using the following formula:

$$m = n \times \frac{1}{A} \times w$$

Where  $m$  is the mass of the plasmid plus the insert per one gene copy,  $n$  is the number of base pairs of your plasmid plus the insert,  $A$  is Avogadro's number ( $6.023 \times 10^{23}$  molecules/mol) and  $w$  is the average molecular weight of a double-stranded DNA molecule (660 g/mole).

3- After calculating the mass per one gene copy you need to know what is your target mass per each copy number in your curve:

$$m_s = S \times m$$

Where  $m_s$  is the mass of your plasmid and insert per each  $S$  and  $S$  is the number of copies in each point of your Standard curve (1 to  $10^7$  gene copies).

4- Once you know what is your target mass for each of your Standard dilutions you need to find what will be your target concentration.

$$C = m_s \times v$$

Where  $C$  is the target concentration and  $v$  is the volume of Standard DNA you will be adding to the PCR reaction (2  $\mu$ L).

5- Finally calculate the concentration of your plasmid extracts (see “Gene ligation, cell transformation and plasmid extraction” from the Methods section) with a ND-1000 Spectrophotometer (Nanodrop®) and prepare a serial dilution of those plasmids until reaching a workable concentration ( $10^{-11}$  g/ $\mu$ L). From there you can create the stock Plasmid solutions for your highest point in your Standard Curve ( $10^7$  gene copies) and, by a ten-fold serial dilution, the rest of the points of the Standard Curve.



#### Appendix IV: Quantitative PCR for $\gamma$ -AOB

Quantitative PCR analyses for the  $\gamma$ -AOB functional group were not possible due to the combination of two factors: scarce information in the scientific literature about PCR primers targeting the ammonia monooxygenase gene (subunits A and B) specific for  $\gamma$ -AOB and second, the impossibility to extract the Plasmid with the amplified genenligated.

*Nitrosococcus oceani*, was chosen as the representative species for the group of  $\gamma$ -AOB. DNA extracted from axenic cultures of this species (ATCC<sup>®</sup>19707<sup>™</sup>) was amplified using the primer set *amoA-3F* (5'- GGT GAG TGG GYT AAC MG-3') and *amoB-4F* (5'-GCT AGC CAC TTT CTG G-3') designed by Purkhold et al. (2000). Those primers were designed as a multigene approach, targeting the subunits A and B of the gene ammonia monooxygenase (*amoA* and *amoB*, respectively). The primer *amoA-3F* corresponds to positions 295 to 310 of the *amoA* gene of *Nitrosomonas europaea* ( $\beta$ -AOB) and the primer *amoB-4R* corresponds to the positions 30 to 44 of the *amoB* gene of *Nitrosococcus oceani*, which are complementary to target regions in the *amoA* and *amoB* genes of *Nitrosococcus oceani* and *Nitrosococcus sp.* In his paper, Purkhold used those primers for amplifying *Nitrosococcus halophilus* ( $\gamma$ -AOB) and obtained a 507 bp *amoA-amoB* gene fragment. In my research those same primers were used in *N. oceani* and produced a gene fragment of approximately 1000 bp.

For the DNA Standard preparation an exact length of the amplified fragment is needed, but nothing was found on the published literature to confirm the accuracy of my

amplification products and the exact length of those, even though these primer set is commonly used for q-PCR amplification of  $\gamma$ -AOB.

After personally contacting other scientists who were using the same primer set, I was able to confirm that a fragment length of approximately 1000 bp was correct, but still needed to find the exact length. The approach I planned was to insert the gene fragment into a Plasmid pCR<sup>®</sup> 2.1-TOPO<sup>®</sup> (Invitrogen<sup>™</sup> Life Technologies<sup>™</sup>) and, after plasmid extraction, re-amplify that gene using the primer set M13 Forward/ M13 Reverse (Invitrogen<sup>™</sup> Life Technologies<sup>™</sup>) which targets a fragment from the position 221 to the position 391. Within that region is where the target gene ( $\gamma$ -*amoA-B*) is ligated. After PCR amplification the resulting amplicons would be sequenced and, after using the map for the pCR<sup>®</sup> 2.1-TOPO<sup>®</sup> sequence (Invitrogen<sup>™</sup> Life Technologies<sup>™</sup>) the inserted gene fragment would be located and its base pairs counted. Unfortunately, after the gene ligation and cell transformation procedures I was never able to extract the Plasmids containing the target gene fragment. The kit used for the plasmid extraction was the same used with all the other functional genes (*Arch-amoA*, *nirS* and  $\beta$ -*amoA*) and no results were obtained. Different volumes, centrifugation and incubation times, extra cleaning centrifugations were tried in all possible combinations, but still no extraction was successful.

## Appendix V: Numeric Data

		Arch-amoA Gene		Sca-NirS Gene		β-amoA Gene	
	Depth	Gene copies/mL	Standard Error	Gene copies/mL	Standard Error	Gene copies/mL	Standard Error
C-175	150	2.73E+03	3.11E+02	2.00E-01	0.00E+00	8.02E+01	1.61E+01
	170	6.06E+03	9.01E+02	2.00E-01	0.00E+00	1.11E+02	8.73E-01
	192	1.89E+04	4.68E+03	1.32E+00	1.98E-01	1.01E+03	3.00E+02
	210	4.20E+02	7.07E+01	2.00E-01	0.00E+00	2.45E+01	4.19E-01
	220	2.18E+02	7.23E+01	2.00E-01	0.00E+00	3.60E+01	4.07E+00
	230	0.00E+00	0.00E+00	2.00E-01	0.00E+00	1.04E+02	3.74E+01
	241	1.91E+02	1.29E+01	2.00E-01	0.00E+00	3.93E+01	1.07E+01
	250	1.18E+02	1.91E+01	9.49E+00	5.72E-01	4.86E+01	1.22E+00
	260	1.48E+01	6.27E+00	2.00E-01	0.00E+00	4.00E+00	0.00E+00
	271	1.03E+03	2.89E+01	1.05E+00	2.09E-01	4.00E+00	0.00E+00
	292	3.70E+02	5.45E+01	3.78E+00	8.21E-01	4.00E+00	0.00E+00
402	1.38E+02	2.33E+01	2.00E-01	0.00E+00	1.42E+02	3.39E+00	
C-180	150	1.47E+03	1.91E+02	4.95E+00	5.33E-01	1.74E+02	1.49E+01
	210	5.84E+03	6.79E+02	1.66E+00	3.73E-01	5.66E+02	2.80E+01
	231	2.62E+03	1.82E+02	1.70E+00	2.46E-01	1.22E+02	1.30E+01
	250	3.31E+02	2.77E+01	2.78E+01	3.62E+00	2.68E+03	1.10E+02
	276	1.96E+02	6.58E+01	2.33E+00	6.86E-01	7.96E+01	2.53E+01
	289	1.76E+02	3.10E+01	1.53E+01	5.06E-01	1.53E+03	5.84E+00
	310	1.35E+02	3.61E+01	1.28E+01	1.65E+00	5.63E+02	4.09E+01
	320	4.03E+01	6.53E+00	4.02E+00	2.45E-01	9.94E+02	5.22E+01
330	2.88E+01	1.86E+00	7.78E-01	2.05E-01	3.97E+02	2.78E+01	

	340	6.86E+01	1.30E+01	2.97E+00	6.28E-01	8.84E+02	3.28E+00
	360	2.71E+01	3.34E+00	1.00E+00	2.18E-01	1.57E+02	6.12E+00
C-186	150	5.25E+03	4.01E+01	2.00E-01	0.00E+00	1.87E+01	2.57E+00
	201	1.12E+04	3.63E+01	2.00E-01	0.00E+00	5.89E+00	5.73E-01
	226	1.39E+02	3.21E+01	2.00E-01	0.00E+00	9.55E+01	1.34E+01
	245	6.32E+02	6.76E+01	1.85E+01	2.18E+00	3.77E+00	1.60E+00
	260	4.39E+01	5.67E+00	2.00E-01	0.00E+00	1.95E+00	5.63E-01
	274	3.78E+01	3.95E+00	2.00E-01	0.00E+00	4.72E-01	1.48E-02
	290	3.13E+01	1.12E+00	2.00E-01	0.00E+00	3.32E+00	6.59E-01
	300	1.02E+02	9.06E+00	1.36E+01	2.51E+00	1.42E+01	6.66E+00
	310	1.01E+02	1.27E+01	1.63E+01	1.87E+00	3.80E+01	4.59E+00
	331	8.63E+01	1.17E+01	2.22E+01	1.31E+00	9.06E+00	3.34E-01
	350	6.08E+01	3.19E+00	2.13E+01	3.80E+00	1.52E+01	3.40E+00
	401	6.99E+01	6.14E+00	1.43E+01	1.49E+00	1.10E+01	1.28E+00

**Table 5** Results and standard errors from the q-PCR analyses for C-175, C-180 and C-186. Values in red were below limits of detection and should be considered as zeros.

		All Anammox		Scalindua		N. maritimus	
		Amx368		Sca1309		Cren769	
	Depth	10 <sup>3</sup> cells/mL	Standard Error	10 <sup>3</sup> cells/mL	Standard Error	10 <sup>3</sup> cells/mL	Standard Error
C-175	25	6.24	1.93	2.45	0.95	8.13	0.77
	80	6.28	1.43	8.88	3.12	5.14	0.52
	101	3.50	1.46	5.10	2.70	4.23	0.79
	150	5.87	1.24	5.94	2.33	7.05	1.17
	170	3.54	0.88	2.87	1.19	7.96	1.41
	192	6.30	1.63	5.84	2.33	14.80	2.58
	210	1.65	0.58	1.65	0.62	2.90	0.40
	220	4.51	1.40	4.49	1.01	7.26	1.04
	230	4.46	1.40	1.49	0.52	5.51	0.47
	241	5.56	1.08	1.25	0.32	3.27	0.40
	250	10.98	0.76	11.51	0.74	2.33	0.37
	260	0.75	0.28	0.86	0.36	2.04	0.29
	271	1.04	0.28	1.42	0.38	2.23	0.34
	292	3.02	0.35	4.05	1.56	1.91	0.32
	402	1.65	0.60	1.56	0.69	2.87	0.42
	502	2.58	0.57	1.80	0.79	4.00	0.54
	900	3.01	0.83	1.42	0.70	3.56	0.63
1295	2.40	0.62	0.85	0.42	4.34	0.69	

**Table 6** C-175 FISH results for anammox bacteria (Amx368), anammox bacteria from the genus *Scalindua* (Sca1309) and Archaeal ammonia oxidizers from the species *Nitrosopumilus maritimus* (Cren679) with their respective standard errors.

		$\beta$ -Proteobacteria		$\beta$ -AOB		$\gamma$ -Proteobacteria		$\gamma$ -AOB	
		Bet42a		Nso1225-190		Gam42a		Nscoc128	
Depth		10 <sup>3</sup> cells/mL	Standard Error	10 <sup>3</sup> cells/mL	Standard Error	10 <sup>3</sup> cells/mL	Standard Error	10 <sup>3</sup> cells/mL	Standard Error
<b>C-175</b>	25	3.21	1.07	6.19	2.08	3.11	0.97	7.46	3.29
	80	2.83	0.87	7.94	5.07	2.07	0.90	5.88	2.51
	101	4.50	1.81	4.79	1.77	3.10	1.00	5.82	2.57
	150	2.72	0.73	2.88	0.94	3.95	1.16	3.44	1.16
	170	6.73	2.96	7.87	2.49	4.07	1.15	3.95	1.28
	192	10.81	0.98	13.73	1.56	20.60	2.37	24.01	9.25
	210	1.37	0.35	2.93	0.78	1.07	0.27	1.99	0.64
	220	6.92	2.33	9.43	3.09	4.06	1.35	8.12	1.95
	230	1.63	0.62	5.37	2.64	1.15	0.42	3.53	1.39
	241	2.43	1.78	2.39	1.03	0.70	0.23	1.27	0.33
	250	0.87	0.25	3.76	1.46	0.66	0.28	1.10	0.41
	260	0.88	0.39	1.24	0.39	2.13	1.00	1.12	0.38
	271	0.78	0.28	1.94	0.65	0.97	0.32	1.18	0.36
	292	0.82	0.27	0.71	0.26	0.70	0.24	0.90	0.33
	402	1.16	0.30	2.67	0.92	1.49	0.44	0.99	0.37
	502	1.14	0.51	6.95	3.32	1.38	0.41	0.91	0.33
900	1.78	0.49	3.49	1.43	1.84	0.64	10.26	7.34	
1295	1.15	0.42	2.16	0.54	1.00	0.34	0.91	0.33	

**Table 7** C-175 FISH results for  $\beta$ -Proteobacteria (Bet42a),  $\beta$ -ammonia-oxidizing bacteria (Nso1225-190),  $\gamma$ -Proteobacteria (Gam42a) and  $\gamma$ -ammonia-oxidizing bacteria (Nscoc128) with their respective standard errors.

		All Anammox		Scalindua		N. maritimus	
		Amx368		Sca1309		Cren769	
	Depth	10 <sup>3</sup> cells/mL	Standard Error	10 <sup>3</sup> cells/mL	Standard Error	10 <sup>3</sup> cells/mL	Standard Error
C-180	30	2.10	0.76	0.64	0.13	1.18	0.19
	50	0.58	0.34	1.11	0.56	1.81	0.26
	100	1.44	0.51	0.48	0.18	0.55	0.13
	150	1.56	0.86	2.08	0.76	1.11	0.22
	210	1.18	0.70	1.42	0.56	4.44	1.31
	230	2.38	0.92	2.98	1.31	1.64	0.68
	250	9.07	1.56	10.11	1.72	1.64	0.34
	270	1.63	0.66	1.24	0.52	0.82	0.22
	290	2.97	1.12	2.83	0.78	0.58	0.14
	310	2.18	1.17	1.49	0.62	0.85	0.21
	320	2.59	1.28	0.26	0.16	0.39	0.12
	330	2.17	0.98	2.69	1.19	1.20	0.28
	340	2.17	0.56	1.28	0.43	0.88	0.24
	360	0.50	0.20	1.03	0.41	1.24	0.48
	400	1.01	0.33	0.80	0.28	1.76	0.52
	500	1.46	0.63	0.62	0.22	0.92	0.21
900	0.09	0.06	0.09	0.05	0.15	0.09	
1300	1.46	0.56	0.58	0.20	1.21	0.23	

**Table 8** C-180 FISH results for anammox bacteria (Amx368), anammox bacteria from the genus *Scalindua* (Sca1309) and Archaeal ammonia oxidizers from the species *Nitrosopumilus maritimus* (Cren679) with their respective standard errors.

	<b>β-Proteobacteria</b>		<b>β-AOB</b>		<b>γ-Proteobacteria</b>		<b>γ-AOB</b>		
	<b>Bet42a</b>		<b>Nso1225-190</b>		<b>Gam42a</b>		<b>Nscoc128</b>		
	Dep th	10 <sup>3</sup> cells/mL	Standard Error	10 <sup>3</sup> cells/mL	Standard Error	10 <sup>3</sup> cells/mL	Standard Error	10 <sup>3</sup> cells/mL	Standard Error
<b>C-180</b>	30	1.21	0.32	0.90	0.21	1.39	0.55	0.73	0.19
	50	0.56	0.21	0.38	0.11	7.64	3.38	0.89	0.22
	100	0.65	0.31	1.04	0.49	0.54	0.18	1.58	0.92
	150	3.68	1.35	0.93	0.38	2.42	0.82	1.79	0.99
	210	7.83	2.46	0.79	0.31	3.62	1.22	2.99	0.62
	230	4.78	1.40	2.71	1.06	4.71	1.93	4.62	1.52
	250	8.18	2.82	8.88	2.17	5.39	2.18	8.55	3.72
	270	6.19	2.24	1.86	0.92	5.15	2.88	1.51	0.59
	290	0.14	0.05	0.48	0.25	0.34	0.16	3.07	0.90
	310	1.71	0.60	1.24	0.50	2.68	1.31	0.96	0.32
	320	0.97	0.51	1.73	0.73	1.38	0.98	0.61	0.32
	330	2.63	1.27	0.98	0.47	3.56	0.99	1.29	0.62
	340	1.03	0.50	0.94	0.66	2.47	1.30	1.13	0.40
	360	0.83	0.42	1.03	0.34	2.87	1.27	1.21	0.48
	400	1.67	0.72	0.60	0.25	2.99	1.30	0.59	0.28
	500	0.38	0.16	0.56	0.27	0.63	0.21	0.86	0.29
	900	0.05	0.03	0.07	0.04	0.11	0.07	0.16	0.11
1300	0.77	0.31	0.81	0.31	0.53	0.20	0.55	0.17	

**Table 9** C-180 FISH results for β-Proteobacteria (Bet42a), β-ammonia-oxidizing bacteria (Nso1225-190), γ-Proteobacteria (Gam42a) and γ-ammonia-oxidizing bacteria (Nscoc128) with their respective standard errors.



		All Anammox		Scalindua		N. maritimus	
		Amx368		Sca1309		Cren769	
	Depth	10 <sup>3</sup> cells/mL	Standard Error	10 <sup>3</sup> cells/mL	Standard Error	10 <sup>3</sup> cells/mL	Standard Error
C-186	25	4.42	1.54	3.74	1.55	0.85	0.32
	50	6.19	1.91	2.86	0.98	15.27	2.94
	100	3.07	1.67	1.58	0.69	2.16	0.41
	150	1.95	0.94	0.84	0.33	2.11	0.28
	200	0.63	0.24	0.71	0.27	9.37	0.68
	225	0.37	0.13	0.40	0.19	1.33	0.21
	245	3.01	1.19	6.93	0.95	0.83	0.23
	260	2.35	0.87	2.49	1.27	1.76	0.23
	275	1.43	0.80	1.27	0.77	1.06	0.20
	290	0.69	0.26	0.56	0.17	1.32	0.25
	300	0.58	0.20	0.75	0.31	0.86	0.21
	310	1.13	0.45	0.32	0.16	0.93	0.11
	330	0.70	0.28	0.45	0.15	0.59	0.11
	350	4.73	1.82	4.23	1.82	1.44	0.25
	400	0.53	0.21	0.39	0.17	0.78	0.17
	500	0.97	0.49	0.70	0.34	0.76	0.13
900	0.45	0.22	0.27	0.12	0.73	0.17	
1300	0.28	0.14	0.13	0.07	0.45	0.11	

**Table 10** C-186 FISH results for anammox bacteria (Amx368), anammox bacteria from the genus *Scalindua* (Sca1309) and Archaeal ammonia oxidizers from the species *Nitrosopumilus maritimus* (Cren679) with their respective standard errors.

Dep th	$\beta$ -Proteobacteria		$\beta$ -AOB		$\gamma$ -Proteobacteria		$\gamma$ -AOB		
	Bet42a		Nso1225-190		Gam42a		Nscoc128		
	10 <sup>3</sup> cells/mL	Standard Error	10 <sup>3</sup> cells/mL	Standard Error	10 <sup>3</sup> cells/mL	Standard Error	10 <sup>3</sup> cells/mL	Standard Error	
C-186	25	7.00	2.53	19.33	2.65	9.87	3.65	15.28	5.76
	50	4.04	1.10	8.51	1.26	3.14	1.23	3.62	0.90
	100	1.98	0.72	3.08	0.56	8.16	3.12	4.78	1.55
	150	2.53	0.93	3.16	0.37	1.27	0.47	1.46	0.64
	200	1.08	0.44	4.54	0.71	1.80	0.58	1.18	0.68
	225	7.69	0.67	8.57	1.07	1.01	0.40	3.39	1.28
	245	1.11	0.48	1.01	0.14	0.56	0.14	3.11	1.00
	260	0.89	0.49	1.91	0.25	1.91	1.01	0.44	0.15
	275	0.83	0.42	1.95	0.27	0.68	0.28	0.66	0.31
	290	0.76	0.32	1.51	0.22	1.45	0.68	0.30	0.12
	300	0.86	0.27	1.61	0.22	3.30	1.20	1.69	0.73
	310	1.58	0.59	1.76	0.39	2.00	0.95	1.10	0.42
	330	2.31	0.78	1.87	0.32	1.05	0.49	1.72	0.76
	350	1.85	0.74	2.97	0.44	0.58	0.22	1.33	0.44
	400	0.52	0.22	2.80	0.44	1.56	0.59	2.16	0.70
	500	0.59	0.22	3.08	0.55	0.76	0.38	1.06	0.48
	900	0.55	0.18	1.50	0.28	0.53	0.17	0.44	0.14
1300	0.79	0.23	1.11	0.18	0.54	0.19	1.15	0.31	

**Table 11** C-186 FISH results for  $\beta$ -Proteobacteria (Bet42a),  $\beta$ -ammonia-oxidizing bacteria (Nso1225-190),  $\gamma$ -Proteobacteria (Gam42a) and  $\gamma$ -ammonia-oxidizing bacteria (Nscoc128) with their respective standard errors.

	<b>AMX</b>	<b>SCA</b>	<b>Sca-dna</b>	<b>AOA</b>	<b>Arch-dna</b>
[NH4] (μM)	-0.239 0.165 35	-0.292 0.0884 35	0.114 0.513 35	-0.422 0.0119 35	-0.701 0.000000200 35
[NO2] (μM)		0.475 0.00412 35	-0.0752 0.666 35	0.446 0.00750 35	0.453 0.00652 35
[NO3] (μM)			-0.245 0.154 35	0.536 0.000984 35	0.711 0.000000200 35
AMX				0.345 0.0424 35	0.240 0.163 35
SCA					0.358 0.0347 35
Sca-dna					0.00700 0.967 35
AOA					0.462 0.00540 35

	<b>BET</b>	<b>NSO</b>	<b>β-dna</b>	<b>GAM</b>	<b>NSCOC</b>
[NH4] (μM)	-0.616 0.0000849 35	-0.301 0.0790 35	-0.0919 0.597 35	-0.329 0.0539 35	-0.528 0.00119 35
[NO2] (μM)	0.387 0.0217 35	0.0666 0.701 35	0.0607 0.727 35	0.165 0.341 35	0.389 0.0210 35
[NO3] (μM)	0.640 0.0000337 35	0.351 0.0389 35	0.133 0.444 35	0.311 0.0685 35	0.559 0.000534 35
AMX	0.332 0.0513 35	0.305 0.0744 35	0.439 0.00855 35	0.0277 0.873 35	0.283 0.0986 35
SCA	0.292 0.0877 35	0.178 0.304 35	0.251 0.144 35	0.113 0.516 35	0.395 0.0190 35

Sca-dna	0.0201	-0.365	0.0753	-0.0595	0.0441
	0.907	0.0314	0.665	0.732	0.800
	35	35	35	35	35
AOA	0.366	0.572	0.243	0.209	0.268
	0.0306	0.000359	0.158	0.226	0.119
	35	35	35	35	35
Arch-dna	0.485	0.266	0.172	0.245	0.497
	0.00333	0.122	0.321	0.154	0.00254
	35	35	35	35	35
BET		0.424	0.420	0.559	0.628
		0.0113	0.0124	0.000521	0.0000536
		35	35	35	35
NSO			0.270	0.135	0.433
			0.117	0.438	0.00962
			35	35	35
β-dna				0.218	0.405
				0.206	0.0160
				35	35
GAM					0.367
					0.0304
					35

**Table 12** Spearman Rank Order Correlation. Cell content (Top to bottom): correlation coefficient, p-value and number of samples. The pairs of variables with P-values below 0.05 are considered significant. In pairs with P-values greater than 0.050 there is no significant relationship between the two variables.